KU70 BINDING PROTEIN 5 (KUB5), A NOVEL FACTOR IN DNA DOUBLE STRAND BREAK REPAIR AND RADIO-RESISTANCE IN HUMAN BREAST CANCER

APPROVED BY SUPERVISORY COMMITTEE

_____
David A. Boothman, Ph.D. (Mentor)

_____
Matthew H. Porteus, M.D., Ph.D. (Chairman)

_____
Sandeep Burma, Ph.D.

_____
David J. Chen, Ph.D.

DEDICATION

Growing up my parents instilled in me a belief that I could do anything I wanted. My journey to becoming a researcher began with Science Fair Projects. My parents would spend hours with me, teaching me how to write up my ideas, helping me get the parts I needed and my brothers would help me build everything from weather instruments to rubber band heat engines. I learned valuable lessons on the importance of teamwork, carefully forming testable hypotheses and time management. Without the support of my parents, Faye and Gary Rommel, and my brothers, David, Ken and Keith, I would never had grown up with these important lessons. I owe my original inspiration to pursue the unknown to them.

I have been lucky in my formal education to choose two fantastic examples of driven, inspirational mentors: Dr. Kent Chapman for my Master's and Dr. David Boothman for my Doctorate. With their guidance I learned to think independently, write clearly, and become a confident researcher and public speaker. I also have supportive friends who have guided me and kept me focused. Many of these friends are coworkers and fellow researchers, and I will continue to foster collaborations with them as I move forward in my career. Finally, my husband Vic Hernandez has been standing by me and supporting me in my dreams everyday. He is always the one I can rely on to remind me why I do what I do when times get tough, and things don't always work out the way I planned. I couldn't have chosen a better partner in life. I dedicate this dissertation to my solid foundation of family, mentors and friends.

KU70 BINDING PROTEIN 5 (KUB5), A NOVEL FACTOR IN DNA DOUBLE STRAND BREAK REPAIR AND RADIO-RESISTANCE IN HUMAN BREAST CANCER

by

Amy Ann Rommel

DISSERTATION

Presented to the Faculty of the Graduate School of Biomedical Sciences

The University of Texas Southwestern Medical Center at Dallas

In Partial Fulfillment of the Requirements

For the Degree of

DOCTOR OF PHILOSOPHY

The University of Texas Southwestern Medical Center at Dallas

Dallas, Texas

November, 2010

KU70 BINDING PROTEIN 5 (KUB5), A NOVEL FACTOR IN DNA DOUBLE STRAND BREAK REPAIR AND RADIO-RESISTANCE IN HUMAN BREAST CANCER

Amy Ann Rommel

The University of Texas Southwestern Medical Center at Dallas, 2010

David Allen Boothman, Ph.D.

DNA double strand breaks (DSBs) are considered both mutagenic and carcinogenic if left un-repaired resulting in genomic instability and ultimately cancer. There are two main pathways for DSB repair: homologous recombination (HR) and non-homologous end joining (NHEJ). Defects in DSB repair have already been associated with breast cancer formation and increased breast cancer risk. Breast cancer susceptibility genes, BRCA1 and BRCA2 are largely thought to be involved with HR while LIG4, XRCC4, and Ku70 are linked to NHEJ. Deficiencies in any one of these genes can predispose individuals to breast cancer. In addition to predisposition to breast cancer, altered DNA repair processes can influence chemo- and radiotherapy efficacy by creating resistance to therapy. To study NHEJ further, our laboratory has identified a novel Ku70 binding protein #5 (KUB5) by a yeast two-hybrid screen using Ku70 as bait. Loss of RTT103, a putative yeast homolog of KUB5, resulted in increased sensitivity to IR, similar to

that observed in hdf1-deletion yeast, the yeast homolog of Ku70. Results also show that RTT103-deletion yeast are deficient in repairing blunt and non-compatible DNA ends and re-expression of hKub5 can correct the IR-sensitivity and DNA repair deficiency of these deficient yeast demonstrating a strong functional model for human KUB5 function in yeast.

Analyses of breast cancer cell lines for their KUB5 protein expression yielded a strong correlation between KUB5 protein level and sensitivity to DNA damage. These data strongly suggests that KUB5 is a novel repair factor involved in NHEJ and endogenous over-expression of KUB5 plays a role in chemotherapeutic and/or radio-therapeutic resistance via increasing the capacity to facilitate NHEJ repair of DSBs in breast cancer cells.

TABLE OF CONTENTS

LIST OF FIGURES……..viii

LIST OF ABBREVIATIONS……xi

CHAPTER I: Introduction……..1

DNA Damage Response……..2

Types of DNA Damage and Repair Pathways……...….3

DNA Double Strand Break Repair…….……5

Homologous Recombination…….…….6

Non-Homologous End Joining (NHEJ)……....…….……..7

Identification of Novel Factors in NHEJ……..……..8

Hypothesis and Specific Aims……..…….9

CHAPTER II: RTT103, yeast homolog of KUB5/HERA involvement in DNA DSB Repair….12

Introduction……13

Materials and Methods…….……..16

Results……...……...……20

Discussion……..……26

CHAPTER III: Biochemical Analysis of KUB5/HERA……..……38

Introduction……..…..39

Materials and Methods……..…..41

Results……...….52

Discussion……..….60

CHAPTER IV: Cells Survive KUB5 Loss When p53 is Mutant……...…79

Introduction……..…..80

Results……..……..82

Discussion……...85

CHAPTER V: KUB5/HERA Involvement in Breast Cancer Chemo and Radio-Resistance..93

Introduction……...…..94

Materials and Methods……..…….98

Results……..……..104

Discussion……..……118

CHAPTER VI: Conclusions and Future Directions……..……..141

REFERENCES……...……..151

LIST OF FIGURES

Figure 1.1: Model for proposed KUB5/HERA involvement in NHEJ……..11

Figure 2.1: Alpha factor arrests cells in G_1……..…29

Figure 2.2: Responses of asynchronous vs. synchronous *rtt103-/-* yeast……..31

Figure 2.3: Survival analysis of wt, *rtt103-/-* and *hdf1-/-* yeast after chemotherapeutic and radiation treatment……....……32

Figure 2.4: *rtt103-/-* and *hdf1-/-* yeast have an inability to repair several types of DNA breaks…….34

Figure 2.5: hKUB5 rescues both IR sensitivity and DNA repair defect in *rtt103-/-* yeast……35

Table 2.1: Comparison of yeast DNA repair proteins and pathways to that of human……37

Figure 3.1: Endogenous KUB5 protein levels appear tightly regulated across cell lines and levels do not change after DNA damage……62

Figure 3.2: KUB5 protein expression is localized to the nucleus……63

Figure 3.3: Whole cell protein lysate Co-IPs reveal KUB5 interaction with Ku70…….64

Figure 3.4: hKUB5 protein can be purified by Ni-NTA after expression in BL21 cells with high yield and purity……65

Figure 3.5: KUB5 purification by FPLC successfully purified and concentrated KUB5 protein..66

Figure 3.6: Gel shift analysis confirms interaction of KUB5 and Ku70 in the presence of DNA..67

Figure 3.7: Pure protein Co-IPs reveal KUB5 interaction with Ku70…….68

Figure 3.8: GST fusion proteins of Ku70 and Ku80 protein binding reactions with purified KUB5 revealed a dependence on Ku70 C-terminal domain for interaction with Ku70 and KUB5……69

Figure 3.9: Yeast Two Hybrid Experimental Design……..71

Figure 3.10: KUB5/HERA protein motifs of interest…….72

Table 3.1: KUB5/HERA C-terminal domain deletion and point mutation L276A was sufficient to abrogate binding with Ku70…….73

Figure 3.11: C-terminal domain deletion in hKUB5/HERA also affects IR sensitivity…….75

Figure 3.12: Whole cell lysate fractionation reveals KUB5 existence in several molecular weight fractions……77

Figure 4.1: siRNA to KUB5 successfully knocked down KUB5 protein levels……..…88

Figure 4.2: Transient knockdown of KUB5/HERA resulted in death in cells with functional p53 ……89

Figure 4.3: Transient KUB5 knockdown resulted in phosphorylation of p53 (Ser15) at 72 hours……90

Figure 4.4: KUB5 knockdown in MEFs lacking Ku70 or ATM results in changes in cell Survival……91

Figure 5.1: Single copy number loss in MEF cells results in significantly decreased protein expression and increased radiation sensitivity……121

Figure 5.2: Stable knockdown of KUB5 protein by shRNA resulted in increased sensitivity to IR…….122

Figure 5.3: KUB5 shRNA treatment results in increased basal H2AX phosphorylation and persistence of foci compared to untreated…….124

Figure 5.4: Comet assay shows KUB5 knockdown cells have more DNA damage 30 minutes after treatment with either H_20_2, Etoposide or IR……..…126

Figure 5.5: Comet assay shows repair of DNA damage over time, with loss of KUB5 resulting in persistent DNA damage……128

Figure 5.6: KUB5 loss affects the survival of cells upon treatment with several different types of DNA damage agents…….130

Figure 5.7: KUB5 deficient cells are sensitive to some common chemotherapeutic agents..132

Figure 5.8: hKUB5 transfected into shKUB5 231 cells resulted in rescue of IR sensitivity…..133

Figure 5.9: Comparative Genomic Hybridization Analysis and western blot protein analysis illustrate endogenous KUB5 levels in breast cancer cell lines……..….134

Figure 5.10: A strong correlation exists between relative protein level in breast cancer cell lines and radiation sensitivity……..136

Table 5.1: KUB5 loss and radiation sensitivity does not seem to correlate with HER2, ER, PR or BRCA1 status of cells……..…137

Figure 5.11: Un-immortalized and immortalized primary HMECs show low basal KUB5 expression level……..138

Figure 5.12: Immunohistochemical analysis of 231 subcutaneous tumor specimens showed decreased KUB5 expression in knockdown cells…….140

Figure 6.1: Published model of transcription termination in yeast……150

LIST OF ABBREVIATIONS

4NQO: 4-nitroquinolone 1-oxide

AP: apurinic/apyrimidinic

APE: apurinic/apyrimidinic endonuclease

ATM: *Ataxia telangiectasia mutated*

ATR: ATM and/or RAD3 related

BME: beta-mercaptoethanol

BER: base excision repair

CGH: comparative genomic hybridization

CHO: Chinese hamster ovary

CLU: Clusterin

CoIP: co-immunoprecipitation

DBD: DNA binding domain

DDB: DNA-damage binding

DNA-PK: DNA-dependent protein kinase

DNA-PKcs: DNA dependent protein kinase catalytic subunit

DSB: double strand break

DTT: dithiothreitol

ECL: enhanced chemiluminescence

ER: estrogen receptor

FBS: fetal bovine serum

FPLC: fast protein liquid chromatography

GGR: global genome repair

GST: glutathione S-transferase

H2AX: histone variant 2AX

HMEC: human mammary epithelial cell

HER2: human epidermal growth factor - 2

HR: homologous recombination

IGF-1: insulin-like growth factor-1

IHC: immunohistochemistry

IPTG: isopropyl-β-D-thio-galactoside

IR: ionizing radiation

KUB5: Ku70 binding protein 5

LUC: luciferase

MEF: mouse embryonic fibroblast

MMR: mismatch repair

MNNG: N-methyl-N-nitro-N-nitrosoguanidine

MRN: Mre11, Rad50, NBS1

NER: nucleotide excision repair

NHEJ: non-homologous end joining

NLS: nuclear localization sequence

PARP1: poly(ADP) ribosylating protein

PI3K: phosphoinositide-3-kinase

PR: progesterone receptor

SCR: scrambled

SDS-PAGE: sodium dodecyl sulfate polyacrylamide gel electrophoresis

SEM: standard error of mean

shKUB5: small hairpin targeted to KUB5

SPORE: specialized program of research excellence

SSB: single strand break

TCR: transcription coupled repair

TOPOI: topoisomerase I

TPT: topotecan

UT: untreated

UV: ultraviolet

WT: wild-type

CHAPTER I

GENERAL INTRODUCTION

DNA Damage Response. Cells can accrue DNA damage by endogenous means through normal cellular processes, and also by exogenous means, through industrial chemicals or radiation. Though a cell can accrue all types of DNA damage ranging from DNA mismatches, double strand breaks (DSBs), single strand breaks (SSBs), base modifications, and crosslinks, usually the cell can maintain genomic stability through proper repair of this damage. To do this, the cell, upon DNA damage, must undergo a cell-signaling cascade to control cell cycle progression to give time for repair to be accurately completed(1). The main DNA DSB damage kinases belong to the PIKK (phosphatidylinositol 3-like kinases) (2, 3) family and include, ATM (mutated in *ataxia telengiectasia(4)*)(5), ATR (*ataxia and Rad3 related*)(6), and DNA-PK (DNA dependent protein kinase). These kinases have the ability to phosphorylate p53 as well as many other proteins involved in DNA repair and damage signaling, such as histone variant H2AX and 53BP1 (BRCT protein p53 binding protein-1). ATR is important in sensing UV and bulky DNA damage, mainly repaired by NER(7, 8). ATR is also implicated in replicative DNA damage repair such as that resulting from stalled replication forks, or any other DNA modification arising from inhibition of DNA synthesis. ATM, is known to regulate G_1 checkpoint by phosphorylating and transcriptionally activating p53 and CHK2 (cell cycle checkpoint protein)(9, 10). Both ATM and ATR phosphorylate MDM2, an

endogenous ubiquitin ligase that inhibits and degrades p53(10, 11). Phosphorylation of MDM2 leads to its degradation, resulting in p53 stabilization and transcriptional activation of p21, a CDK inhibitor(12). ATM also controls G_2/M check point by phosphorylating CHK2, thus inhibiting CDC25 and preventing G_2/M transition(13).

Types of DNA Damage and Repair Pathways. Exogenous or environmental sources of DNA damage include damage from UV radiation. Exposure to UV radiation creates two types of DNA lesions, cyclobutane-pyrimidine dimers and 6-4 photoproducts (6-4 PPs, which are pyrimidine adducts). Other DNA damaging agents include industrial chemicals, such as benzopyrene that can induce DNA damage by intercalating into DNA or covalently bond to nucleophilic guanine, creating DNA adducts or bulky bases. These types of DNA lesions are usually repaired by nucleotide excision repair (NER)(14-18). Two types of NER exist, including Global Genome Repair (GGR) and Transcription Coupled Repair (TCR)(19-23). The main difference between the two types of NER pathways is that transcription-coupled repair occurs within regions of actively transcribed genes, whereas global genome repair occurs anywhere within the genome at any time, but in a slow and progressive manner. In NER, DNA-damage binding (DDB), and XPC-Rad23B complexes are in constant motion scanning the genome to recognize structural distortions(24). Once a damaged site has been identified, XPC-HR23B recruits

TFIIH and with the aid of ATP unwinds the DNA helix until XPD encounters the modified base. RPA, XPA and XPG then assemble at the site, allowing XPG, due to structure specific endonuclease activity, to make a 3' incision. This allows ERCC1-XPF to bind and create a 5' incision. This dual incision leads to a 25-30 nucleotide gap. RPA remains bound to single stranded DNA (ssDNA), allowing polymerase eta (ε) to re-synthesize the strand and Ligase I to seal the nick(25-30).

Hydrogen peroxide, another industrial chemical, leaves single strand DNA breaks at low concentrations and double strand breaks at higher concentrations due to the combined actions of the Haber-Weiss or Fenton reactions(31, 32). Here, hydrogen peroxide and an iron catalyst react to form a hydroxyl radical and hydroxide anion. The resulting hydroxide radical, a highly reactive oxygen species, has the ability to induce DSBs.

Another form of DNA damage, methylation, can occur exogenously by actions of DNA damage agents, such as MNNG (*N*-Methyl-*N*′-Nitro-*N*-Nitrosoguanidine)(33). MNNG is stable in the anhydrous state, however, when in aqueous conditions alkylating moieties are released leaving them able to bind DNA covalently. Not only can these moieties methylate oxygen and nitrogen atoms of DNA, but they also form altered bases, such as N^7- and O^6-methylguanine, the latter being the most mutagenic lesion(34). Replication through this damage creates DNA mismatches, which are generally resolved by DNA mismatch Repair (MMR). Here, MutS binds to altered base pairs recruiting

MutL and activating MutH. Activation of MutH cleaves the un-methylated strand at the GATC site allowing the mismatch to be removed from the 3' side by an exonuclease. The gap can then be filled by DNA polymerase III and resealed by DNA ligase I(35, 36).

DNA damage can also occur by endogenous cellular processes, such as those resulting from oxidation reactions as a result of intracellular metabolism, errors in DNA replication, and hydrolysis. These types of DNA damage are typically repaired by base excision repair (BER)(37-39). Here, DNA glycosylases remove modified or damages bases by cleavage of the *N*-glycosidic bond between the base and the nucleotide. The type of glycosylase determines the specificity of the repair pathway used. Generally, when the base is removed, the apurinic/apyrimidinic (AP) site is removed by AP endonuclease (APE) by nicking the DNA strand at the 5' or 3' end to the AP site(40, 41). The remaining deoxyribose phosphate residue is excised by a phosphodiesterase and the gap is filled by DNA ligase(42).

DNA Double Strand Break (DSB) Repair. DSB repair is a tightly regulated process critical for cell survival and maintenance of genetic integrity and stability with a single non-repaired DSB being lethal to the cell(43). Most chemotherapeutic agents kill by DSB induction. DNA damaging agents that can induce DSBs include Ionizing Radiation (IR), high doses of Hydrogen peroxide, as well as several known chemotherapeutic agents, such as the alkylating agents

Cisplatin, and Topoisomerase I (irinotecan, topotecan, camptothecin,) and Topoisomerase II poisons (etoposide and doxorubicin). There are two main pathways for DSB repair: Homologous Recombination (HR)(44) and Non-Homologous End joining (NHEJ)(45). Defects in DSB homologous repair have already been associated with breast cancer formation and increased breast cancer risk(46). Breast cancer susceptibility genes, BRCA1 and BRCA2 are largely thought to be involved with HR, while LIG4, XRCC4, and Ku70 are linked to NHEJ(47, 48). Deficiencies in any one of these genes can predispose individuals to breast cancer. In addition to predisposition to breast cancer, altered DNA repair processes can influence chemo- and radiotherapy efficacy by creating resistance to therapy.

Homologous Recombination (HR). HR is only active during late S and G_2 due to the presence of sister chromatids. At these phases of the cell cycle it is considered an error-free method of DSB repair. Some of the proteins involved in this process include Rad51/52/54, BRCA1/2, MRE11, NBS1, and Rad50. Rad51/52/54 promotes ATP-dependent homologous DNA pairing and strand exchange(49, 50). The MRN complex, composed of MRE11, NBS1 and Rad51, has ATP-dependent exonuclease activity and is believed to unwind DNA(51). Rad54 his known to have ATPase activity helping Rad51/52 unwind DNA. This process facilitates access of other DNA repair factors to the sites of DNA damage(52). Following sister-chromatid pairing and strand invasion, HR may

proceed in a non-cross-over event that results from disengagement of the Holliday junction followed by DNA pairing and gap filling. Conversely, a more classical HR pathway may resolve Holliday junctions by endonucleolytic cleavage that can result in either a cross-over event or a non-cross over event(53).

Non-Homologous End Joining (NHEJ). In any given population more mammalian cells are in G_1/G_0 of their cell cycles and do not have sister chromatids. Due to this fact, the majority of DSBs are rejoined by NHEJ in mammalian cells. Characterized proteins known to be involved in NHEJ include Ku70, Ku80, DNA-PKcs, DNA ligase IV, XRCC4, and Artemis. The Ku70/Ku80 heterodimer binds to free ends of broken DNA(47, 54). DNA-PKcs can then be recruited to form the DNA-PK holoenzyme complex resulting in activation of its kinase activity. If the concentration of DNA breaks is high enough, the kinase activity of DNA-PKcs can be initiated in the absence of the Ku heterodimer(55, 56). The DNA-PK holoenzyme can then phosphorylate a variety of DNA-binding proteins, such as the Ku heterodimer (57), XRCC4 (58), Artemis (59), and DNA-PKcs (60). DNA-PK holoenzyme and the XRCC4/DNA ligase IV complex are able to promote end-to-end association of broken DNA that is mediated by contacts between the Ku complex and DNA ligase IV (61), and between DNA-PKcs and XRCC4 (62). The DNA-PK holoenzyme is then able to sequester broken DNA ends and protect them from degradation until end-joining is able to take place (63). DNA-PK holoenzyme complexes are believed to phosphorylate

each other, dissociating themselves from DNA. This allows final processing of the aligned ends to proceed via Artemis and the XRCC4/DNA ligase IV complex (64).

Identification of novel factors involved in NHEJ. Within Non-homologous End joining (NHEJ), and in particular Ku-dependent repair, there remains much to be understood. The function and recruitment of Artemis, as well as enzymatic functions involved in repairing difficult DSBs remains largely unknown. To define and discover, in more detail, the mechanisms and proteins involved in NHEJ, a yeast two-hybrid screen using Ku70 as bait was performed (65, 66). The isolated Ku-binding proteins (KUBs) were partially characterized (66), but KUB5 was found after publication as one of a number of rare (5/495) clones isolated. The majority of Ku70 interacting clones pulled out of the screen was nuclear clusterin (nCLU/KUB1), which binds to and inhibits Ku70 causing cell death (67). Ku80 (KUB2) was also isolated. KUB3 and KUB4 remain unknown proteins, although a role of KUB3 in radioresistance in gliomas was reported (68). KUB5, which was later named HERA by our lab, is a highly conserved protein with homologs found in insects, yeast and plants and was the subject of this work. At the start of these investigations, KUB5/HERA was homologous to the yeast *rtt103* gene, which has a domain name of RPR1B by Genebank. Finally, KUB6 was identified as BAX.

Hypothesis and Specific Aims. Due to its interactions with Ku70, I hypothesize that KUB5/HERA is a novel DSB repair factor involved specifically in NHEJ (Figure 1.1). Alterations in endogenous levels of KUB5/HERA due to genetic amplification or loss in specific human breast cancers plays a major role in chemotherapeutic and/or radiotherapeutic sensitivity via altered capacity to facilitate repair of DSBs in breast cancer cells. This hypothesis was examined by completing three specific aims:

Specific Aim 1: To characterize RTT103 deficient yeast for sensitivity to DNA damage agents and DNA repair capability. The yeast gene, *rtt103,* is thought to be closely related to KUB5/HERA due to sequence similarity. Yeast experiments using *rtt103*-deficient yeast and a subsequent hKUB5/HERA expression in yeast could yield important insight into redundancy of the repair processes across species allowing for us to utilize a model system for the study of this novel DNA repair protein.

Specific Aim 2: To characterize KUB5/HERA interaction with Ku70, including determining functional domains required for KUB5/HERA function and interaction with Ku70. KUB5/HERA most likely interacts with Ku70 through each protein's highly conserved coil-coil domains. This would

indicate that KUB5/HERA and hKu70 are a competitive heterodimer to the known hKu70-hKu80 heterodimer. Such data, along with pathway mutagenesis in yeast using site-directed mutagenesis of known HR and NHEJ pathways, should indicate a novel repair pathway of DSBs directed by KUB5/HERA-hKu70-Artemis.

Aim 3: To elucidate the role of hKUB5/HERA in drug and ionizing radiation (IR) resistance in human breast cancer. KUB5/HERA regulates the resealing of blunt-ended DSBs that are vital lesions to the efficacies of most DNA damaging agents, including IR. We believe that this process could be responsible for acquired resistance to chemo- and radiotherapy in breast cancer cells.

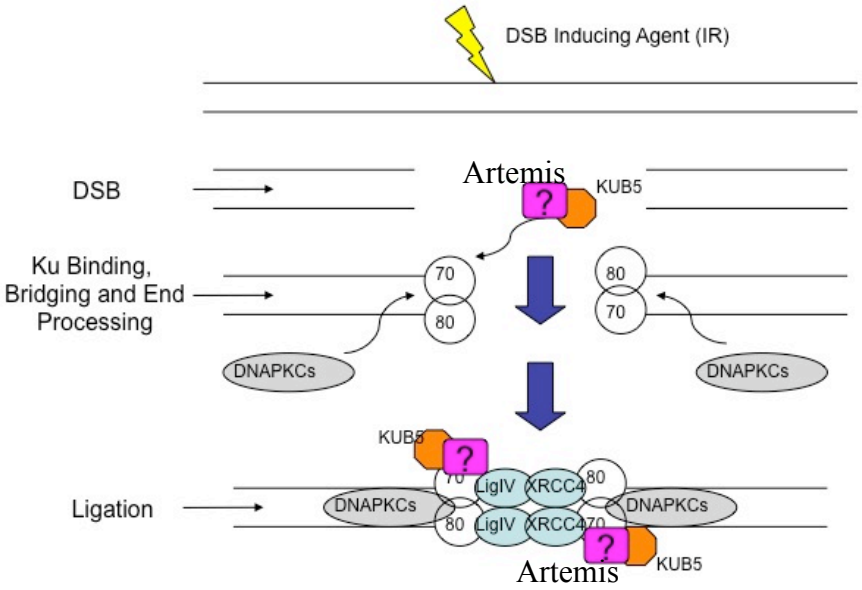

Figure 1.1 – Model for proposed KUB5/HERA involvement in NHEJ. Schematic shows poorly understood areas of non-homologous end joining pathway, such as how some of the NHEJ proteins are recruited to the DNA repair complex. It is believed that upon Ku70/Ku80 binding to the break, KUB5/HERA stabilizes the complex or recruits other repair proteins. Evidence in the lab lean to the possibility that KUB5/HERA may be needed for stabilization and recruitment of Artemis to this complex to facilitate proper NHEJ repair.

CHAPTER II

RTT103, the yeast homolog of KUB5/HERA/HERA, involvement in DNA Double Strand Break repair

INTRODUCTION:

In an attempt to discover novel proteins involved in NHEJ, a yeast two-hybrid analysis of Ku70 binding proteins was performed using human ku70 as bait and a human liver library (65). Ku70 binding protein 5 (KUB5) was one of several proteins isolated as a result of this screen. Ku80 and nuclear clusterin (nCLU) were also isolated and have been largely characterized (66). KUB5/HERA was independently isolated in *Saccharomyces cerevisiae* as the RTT103 gene and the deletion yeast (YDR289C) was generated by the *Saccharomyces* Deletion Project (69). Very few publications exist, and therefore, little is known about the true functions of RTT103 in yeast, and even less is known about its human homolog, KUB5/HERA, function in mammalian systems. Early reports showed that disruption of the *rtt103* gene resulted in a 13-fold increase in Ty1 retrotransposition (70-73). This phenomenon appears to be similar to that observed in yeast deleted in genes with known involvement in DNA end recognition and DNA repair, such as *mre11, rad50*, and *rad57* in yeast (23,27). Yeast Ku70, also known as *hdf1*, was also reported to inhibit non-specific Ty1 retrotransposition, thus supporting another link between RTT103 and hdf1-mediated repair in yeast. These data suggested a correlation existed between KUB5/HERA and Ku70-mediated DNA Repair in humans.

To complicate the elucidation of KUB5/HERA function in mammalian cells, RTT103 also reported to have functions in RNA processing. Recently, RTT103 was found to directly interact with phosphorylated RNA polymerase II C-terminal domain (70). RTT103 in combination with 5'->3' exonuclease RAT1/Rai1 co-localize at the ends of poly Adenine protein coding mRNA transcripts (71). This complex, including RTT103, is thought be required for transcription termination by RNA polymerase II (71). The Torpedo model of transcription termination describes this process, where Rat1 degrades RNA from the 5' end of genes. Upon catching up to RNA polymerase II, Rat1 (also known as Xrn2) acts like a Torpedo to remove RNA polymerase II from DNA. Here, the Rat1, Rai1 and RTT103 complexes are thought to degrade RNA and aid in transcription termination. Mutant RatI can still complex with RTT103 and Rai1, however, transcription does not terminate resulting in the elongation complex and an intact, approximately ~18 nucleotide, RNA-DNA loop(71-73). Furthermore, Rtt103 and Pcf1, a factor important for mRNA poly-adenylation and transcription termination, are shown to act in mRNA termination by interacting with the C-terminal domain of polymerase II largest subunit, specifically when Ser5 is phosphorylated.

The goal of this work was to utilize the well-documented field of yeast genetics to study RTT103 function. Here, I characterized *rtt103* deficient yeast for their sensitivity to DNA damage agents and DNA repair capability.

Experiments using *rtt103* deficient yeast and subsequent rescue by hKUB5/HERA expression could yield important insight into redundancy of the repair processes across species, allowing us to utilize this model system for the study of this novel DNA repair protein.

MATERIALS AND METHODS:

Growth and Synchronization of Yeast in G_1. The *Saccharomyces* Deletion Project generated the deletion yeast strains used in these studies. Haploid yeast strains of wild type (wt), *rtt103*-/- and *hdf1*-/- were created in background BY4741, (MATa *his3_1, leu2_0, met15_0, ura3_0)* yeast. For analysis, one colony from a plate or frozen culture was inoculated and grown on Yeast Peptone Dextrose (YPD) media (For 1 liter; 10 g Dextrose, 10 g Bacto-Peptone, 5 g Yeast Extract, 10 g Agar, adjust pH to 6.5 and autoclave. Add dextrose when cooled to ~ 55^{o}C). For alpha factor G_1 haploid synchronization, 1 colony/loop of a log phase overnight growing culture was inoculated onto 1 ml liquid YPD and grown overnight at 32 C, in a shaker 225 RPM. Add 1 ml to 50 ml YPD media the next day and shake at 225 RPM for 2 Hr until OD_{600} 0.8 is reached. MATa yeast secrete "a" factor and MATα secrete "α" factor in order to undergo mating which occurs in G_1 of the yeast cell cycle. Upon exposure to pheromone (alpha factor), cells arrest in G_1 to prepare for mating(74). For this experiment α alpha was added to MATa yeast to arrest the haploid yeast in G_1 forcing them into NHEJ. α Factor (moth mating pheromone purchased from Abersheim) was added to cultures to a final concentration of 1 μM and put back on the shaker for 3 hours to achieve ~ 98% G_1 arrested haploid cells.

Survival Assays after treatment with DNA damage agents. G_1 arrested haploid yeast were treated with various DNA damage agents. For IR and UV treatment, liquid cultures that have been G_1 arrested were plated onto YPD media plates. After drying for 10 minutes, plates were irradiated and placed in a 32 C growth chamber for approximately 6-9 days until colonies form and are large enough to count. For chemical treatment of yeast, 1 ml liquid cultures were inoculated with indicated doses of Cisplatin, hydrogen peroxide (H2O2), 4-Nitroquinoline 1-oxide (4NQO) and MNNG. These doses were chosen based on a dose response curve in order to determine the optimal concentration range of each agent to use on these haploid yeast. Yeast were then placed in shaker at 225 RPM for 3 Hrs and removed. Yeast were plated onto YPD plates and grown in 32 C chamber for 4-6 days till colonies were large enough to count.

Plasmid Re-ligation Assays. DNA substrate pYES with selection marker, URA3, was used for all plasmid re-ligation assays. Here, an intact correctly repaired pYes plasmid, upon transformation into the yeast, will express the URA3 gene and allow growth on URA- deficient plates. pYES plasmid was digested by various restriction enzymes to create 3', 5' and blunt DNA ends. BAMHI creates a 5' PSS cutting at 5'- G*GATCC-3', SACI creates a 3' PSS cutting at 5'-GAGCT*C-3' and PVUII creates a blunt break cutting at 5'-CAG*CTG-3'. Digests were incubated for 1 Hr and run on 1% agarose gel and visualized using

Ethidium bromide and Ultraviolet light. Digest bands were excised from the gel, digested and purified (Quiagen Gel purification kit) and subsequently used for yeast transformation.

Yeast Transformation. For plasmid re-ligation assays, linearized plasmids were transformed into WT, *rtt103* deficient, and *hdf1* deficient yeast as indicated. The same transformation protocol (modified from Clonetech Laboratories, Yeastmaker^{TM} Yeast System 2 User Manual) was used for generation of hKUB5/HERA expressing *rtt103* deficient yeast and the c-terminal mutants transformed into *rtt103*-/- yeast. Here several solutions are made fresh prior to transformation, 1X TE/LiAc (1ml 10X TE buffer, 1 ml 1M LiAc(10X)), PEG/LiAc Solution (8ml of 50% PEG 3350, 1 ml 10X TE and 1 ml 1 M LiAc (10X)) and 0.9% (m/v) NaCl. Three day cultures were grown on YPD plates and one colony was chosen to inoculate 3 ml of liquid YPD medium. Incubate at 30 ^{o}C for 8 hrs. Transfer 5 μl of culture to 50 mls of YPD in a 250 ml flask. Incubate at 30 ^{o}C overnight (16-20 hrs) shaking at 225 RPM. OD_{600} was monitored to 0.15-0.3 and cells were centrifuged at 700 x g for 5 min at room temperature. Re-suspend pellet in 100 ml YPD, incubate 3-5 hrs at 30 C till (OD_{600} = 0.4-0.5). Cells were centrifuged again at 700 x g for 5 min and split cultures were resuspended from pellet in 600 μl of 1X TE/LiAc. Transformation tubes containing the following; 0.1-1 μg plasmid DNA and 5 μl Herring testes

Carrier DNA were assembled. Competent cells (50 μl) were added and mixed gently by vortex. Add 0.5 ml PEG/LiAc solution and mix gently by vortex. As 20 μl DMSO, mix and place tube in 42 C water bath for 15 minutes vortexing every 5 minutes. Centrifuge to pellet cells high speed 15 sec and re-suspend in YPD media. Plate 100 μl onto selection plate and grow at 32 C for 3-5 days to obtain colonies.

Protein Isolation from yeast and analysis by western blot. Yeast protein extracts were prepared using acid washed glass beads as described in the MATCHMAKER Yeast manual and used for Western blot. Protein concentrations were determined by using Bio-Rad protein concentration reagent and instructions (Bio-Rad Laboratories, Inc. Hercules, CA). Yeast extracts were mixed with SDS-PAGE loading buffer and separated by 10% PAGE gel. Proteins were transferred to PVDF membranes and blocked with 5% non-fat dried milk and 1% BSA. After blocking, membranes were probed with monoclonal KUB5/HERA antibody (generated by our lab) and incubated overnight at 4 C. After washing the membrane 3X in PBS-T, HRP-conjugated anti-mouse secondary antibody was then added and incubated at RT for 1 Hr. After washing, proteins were visualized by ECL and X-ray film. hKUB5/HERA protein was visualized at approximately 34.5 kDa.

RESULTS:

Our data confirmed that KUB5/HERA interacted with Ku70, a protein known to be involved in NHEJ. Sequence homology of *kub5/hera* eluded to a likely yeast homolog, known as *rtt103*. Our hypothesis is that KUB5/HERA and RTT103 both have actions in NHEJ like that of *hKu70* (*hdf1* in yeast), the protein known to have direct interaction with KUB5/HERA. Here, haploid MATa WT, *Rtt103*-/- and *hdf1* -/- (hKu70 homolog) *S. cerevisiae* strains were used to study the role of KUB5/HERA in NHEJ. Due to yeast DNA repair preference they will repair the majority of their damage by homologous recombination in S-phase. In the case of budding yeast, such as *S. cerevisiae* used in this experiment, yeast can live with either a haploid or diploid genome. Haploid cells occur in two different mating types, that of "a" or "α", and is determined by the mating type locus (MAT). Haploid cells can live indefinitely in haploid state, regardless of mating type, until the opposite mating type is introduced. Once this happens the cells fuse and enter the diploid phase of the cell cycle (Figure 2.1a). Using haploid yeast deficient in *rtt103,* we explored the role(s) of this protein. To examine KUB5/RTT103 function in this yeast model it was necessary to generate haploid yeast and force them into G_1 arrest to examine NHEJ. To do this, mating factor (alpha), which arrests haploid cells in G_1, forcing them into NHEJ, was used (Figure 2.1b). After exposure to alpha factor, taking 3-6 hours for 98% G_1 arrest, cells exhibited an "oblong, protruding" schmoo phenotype, consistent haploid G_1

arrested yeast (75, 76) (Figure 2.1c). G_1 arrested yeast by α factor mating, referred to as synchronized yeast, are dependent on NHEJ. Alternatively, yeast left un-treated, referred to as asynchronous yeast, mainly utilize HR for repair of genomic damage. Figure 2.2, shows the radiation sensitivities of wt, *rtt103*-/- and *hdf1*-/- asynchronous yeast versus those treated with alpha factor, in which cells are dependent on NHEJ exclusively. Asynchronous or synchronous yeast were then treated with IR or chemotherapeutic agents. Asynchronous wt, *rtt103*-/- and *hdf1*-/- yeast have similar IR sensitivities (Figure 2.2a). Note that *hdf1-/-,* and *rtt103-/-* yeast likely do not play major roles, if any, in HR. In contrast, synchronized, G_1-arrested haploid yeast, have significant differences in IR sensitivities (Figure 2.2b). Here, G_1-arrested wt yeast display similar IR sensitivity to asynchronous WT yeast. Interestingly, both *hdf1*-/- and *rtt103*-/- G_1 arrested yeast appear to have similar IR sensitivities, both significantly more sensitive than wt G_1-arrested yeast. Most significantly, after treatment with 200 Gy, 76% of wt yeast survived, whereas only 8% *hdf1*-/- or *rtt103*-/- survived the same dose of IR. High doses of IR are required in yeast compared to sensitive mammalian cells due to their smaller genetic material "target" size. These data strongly suggested that RTT103 functions in NHEJ, due to its specific hypersensitivity in G_1 haploid yeast, as well as its similar sensitivity as *hdf1-/-* yeast.

Due to the spectrum of DNA damage caused by IR, which includes DSBs,

SSBs as well as altered base damage and DNA-protein cross-links, the next step was to treat these yeast with DNA damaging agents that result in specific DNA damage that incites specific DNA repair pathways, including NER, BER and MMR (Figure 2.3). Cisplatin, a common chemotherapy drug, creates mono-alkylation lesions that ultimately give rise to inter- and intra- strand cross-links, which after replication, can result in DSBs. After treatment with Cisplatin, haploid G_1-arrested yeast showed significant differences in survival. In particular, WT yeast with 150mM cisplatin resulted in 45% survival, whereas similarly treated *hdf1*-/- or *rtt103*-/- cells resulted in ~13% survival. Due to the creation of a DSB upon treatment and replication through damage, it is expected that *rtt103*-/- and *hdf1*-/- yeast would show sensitivity to this agent supporting the hypothesis that *rtt103* is a novel NHEJ factor and is likely in a similar pathway as hdf1. Further support to this theory came from the data in Figure 2.3c, showing sensitivities of the yeast after H_20_2 treatment. Here, it appears that *hdf1*-/- and *rtt103*-/- yeast once again mirror each other and show increased sensitivity to H_20_2, especially at the higher dose of 10 mM. H_20_2 predominately creates SSBs at lower doses, and at higher toxic doses as a result from the Free radical formation DSBs can be created. Yeast cell lines showed no difference in sensitivity from exposure to UV irradiation, which creates 6,4-photoproducts and pyrimidine dimers that selectively stimulates NER. These data support the idea that RTT103 is not involved in NER, the pathway that repairs these base modifications.

Treatment of G1 arrested yeast with 4NQO resulted in no significant difference in sensitivities between WT, hdf1-/- and RTT103-/- lines. This quinoline derivative and UV mimetic, damages DNA by creating purine dimers, and like damage created by UV, is preferentially repaired by NER. Finally, MNNG treatment yielded interesting and unexpected results. MNNG is a methylating agent, which upon its interaction with DNA, forms O^6-methyl Guanine. The cell upon replication recognizes this base modification as cytidine, creating a DNA mismatch, which is repaired by DNA MMR. In G_1 arrested *rtt103-/-* yeast, there was an increased sensitivity to MNNG, even more than *hdf1-/-* yeast. Yeast responses to DNA damage created by MNNG appear to separate the involvement of hdf1 and RTT103. A possible explanation for this could involve increased DSB lesions in rtt103-/- yeast and PARP1 hyper-activation. Yeast, like mammalian cells, have Poly(ADP) ribosylating Protein (PARP1)(77). The normal function of PARP1 is to bind DNA breaks, and poly(ADP) ribosylate proteins that are ultimately recruited to the site of damage, including itself. At this point, PARP1 is released from the DNA and recycled(78, 79). Our hypothesis is that in *rtt103* deficient yeast treated with MNNG, PARP1 becomes hyperactivated due to increasing DNA damage left unrepaired. This hyperactivation releases PARP1 from DNA leaving the damages ends unstabilized and preventing efficient repair of the damage, creating increased sensitivity to this DNA damage agent.

In addition to studying DNA repair defects by exposure to different DNA damage agents and analyzing the sensitivities of the deficient yeast, we examined the role of rtt103 and human KUB5/HERA more directly in DNA repair by plasmid re-ligation assays. Yeast are especially useful for this study due to the ease of plasmid transformation and selection of recombinant transformants. Here, linearized plasmid DNA digested with various restriction enzymes, each known to leave behind a different type of DNA end, were transformed into wt, hdf1-/- and RTT103-/- yeast. The pYES plasmid was digested using (I) BAMHI (for a 5' overhang break), (II) SACI (for a 3' overhang) or (III) the combination of both BAMHI and SACI (for a non-compatible break) and finally with (IV) PVUII (generating a blunt break). Generally, if the plasmid is successfully repaired, URA expression will be restored allowing the URA-/- yeast to grow on media lacking uracil. This analysis revealed that wt yeast could repair plasmids containing each of the different types of breaks (Figure 2.4), consistent with an intact functioning NHEJ DNA repair pathway. Since haploid G_1 arrested yeast were used, yeast were reliant on NHEJ for survival. In contrast, and as expected, *hdf1*-/- yeast could not repair any of the plasmid DNA ends showing the overall lowest repair efficiency of the three yeast strains which is consistent with known *hdf1* literature (80-82). RTT103-deficient yeast showed significant decreased ability to repair the non-compatible DNA ends generated by the combination of BAMHI and SACI as well as an inability to repair the blunt DNA breaks formed

by PVUII. This suggests a potential role for RTT103 in the repair of DNA breaks requiring specifically NHEJ for repair, consistent with the hypothesis.

After *rtt103-/-* yeast were characterized by specific sensitivities to different DNA damage agents and repair capacities, we then examined whether human KUB5/HERA expression in rtt103-/- could rescue the yeast RTT103 deficiency. Here, KUB5/HERA was cloned into a yeast expression vector, pACT-2, that contains a LEU selectable marker allowing successfully transformed yeast containing the hKUB5/HERA cDNA to be able to grow on media lacking Leucine. In both IR sensitivity and plasmid re-ligation studies, hKUB5/HERA cDNA stably transfected into *rtt103-/-* yeast, resulted in a complete rescue of IR sensitivity compared to responses observed in WT yeast. More importantly, over-expression of hKUB5/HERA rescued the repair defect observed in the plasmid re-ligation assay (Figure 2.5). It is possible that hKUB5/HERA does not completely rescue in the plasmid re-ligation assay due to inherent differences in function of hKUB5/HERA in yeast and RTT103 function in yeast (Table 2.1), where a mere ~23% sequence homology exists between RTT103 and hKUB5/HERA. Alternatively, expression of hKUB5/HERA in rtt103-/- yeast was not at an optimal level (too high, or not equivalent) compared to the yeast endogenous gene. Combined, these data strongly support the hypothesis that RTT103, and therefore hKUB5/HERA are required for repair of blunt DSBs and for fully functional NHEJ.

DISCUSSION:

Yeast genetics have been used to study genes with known homologs in other systems due to the simplicity of the system and depth of information and experimental protocols available. Analysis of potential homologs of KUB5/HERA resulted in identification of RTT103 in yeast showing the highest sequence similarity, ~23%, therefore, making RTT103 a potential functional homolog of KUB5/HERA. Due to known interaction of Ku70 with human KUB5/HERA, the hypothesis was formed that KUB5/HERA is, like Ku70, involved in the DSB repair pathway NHEJ. Yeast DNA repair has been extensively studied, resulting in the identification of several yeast NHEJ proteins that have functional homologs in human NHEJ. Like in mammalian NHEJ hdf1 (human Ku70) and hdf2 (human Ku80) bind DNA breaks to stabilize the ends for recruitment of other DNA repair proteins. An important distinction between yeast and mammalian NHEJ is the involvement of DNAPKcs. In the yeast NHEJ pathway, there are no known functional homologs of mammalian DNAPKcs, which functions in mammalian cells as a recruitment and activation center for polymerase, Artemis and Ligase IV for the repair of a DSB. In addition to yeast not having DNAPKcs, they also have no known functional homolog for Artemis, which in mammalian cells functions to process the broken DNA ends prior to ligation by DNA Ligase IV. Due to the yeast lacking a known homolog for

DNAPKcs and Artemis, reviewers have questioned the significance of studying RTT103 function in yeast and correlating it to KUB5/HERA function in mammalian NHEJ. To address this concern, the most significant data in this chapter shows hKUB5/HERA is able to rescue the IR sensitivity defect seen in G1 arrested yeast (Figure 2.5). These data support the hypothesis that RTT103 is a yeast homolog of human KUB5/HERA, and these proteins functions specifically in NHEJ.

Plasmid re-ligation results further support the hypothesis of RTT103, and therefore hKUB5/HERA involvement in NHEJ by the specific inability of RTT103 -/- yeast to repair blunt and non-compatible DNA ends. Human KUB5 cDNA expression in RTT103-/- yeast was able to rescue this repair defect, however not as efficiently as in the rescue of IR sensitivity. These results suggest RTT103 in yeast may function in several processes, some requiring higher specificity of protein structure, where expression of human KUB5 is unable to mimic. The lack of complete sequence homology between RTT103 and KUB5/HERA could be the reason for this apparent divergence of function. Another possibility for this result could be the re-expression level of human KUB5/HERA was either too high, or not enough in order to allow for the efficient rescue in the plasmid re-ligation assay.

Perhaps the most interesting results obtained from RTT103 studies are those from MNNG treatment and survival assays. MNNG was the only DNA damage

agent negatively affecting RTT103-/- yeast survival more severely than that of hdf1-/- yeast. A possible explanation for this result could be that RTT103 is involved in processes independent of hdf1. One such process could be that of PARP1 hyperactivation. In addition to creating DNA damage in the form of DNA mismatches, MNNG, at high doses, is also known to hyperactivate PARP1, resulting in its disassociation from DNA. Though it is not known exactly how RTT103 functions in this process, one theory is that when RTT103 is absent, PARP1 takes over to stabilize broken DNA ends in order for DNA repair protein to bind and repair the damage. As higher doses of MNNG are applied to these cells, PARP1 becomes hyperactivated, dissociates from DNA and is therefore no longer able to stabilize DNA ends, resulting in defective DNA repair, thus potentially explaining the specific sensitivity of RTT103-/- yeast to MNNG.

A

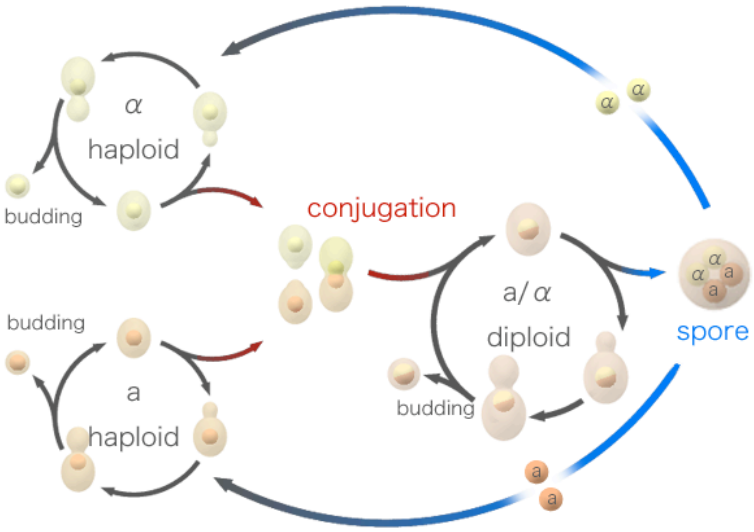

B

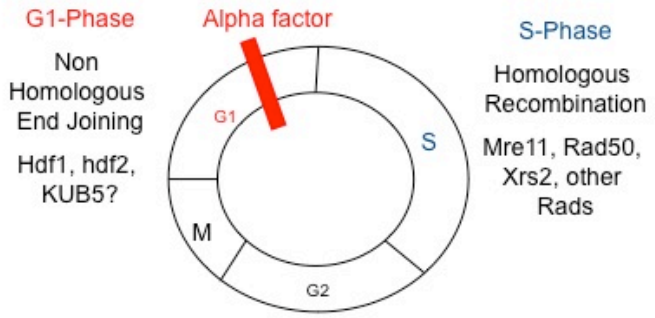

C

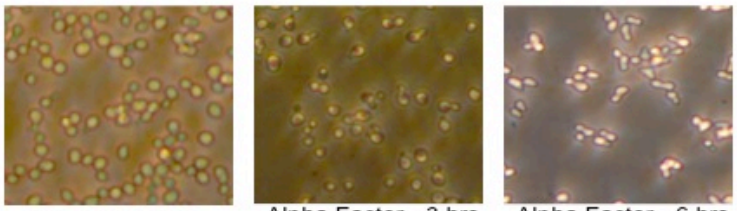

Figure 2.1: **Alpha Factor Arrests Yeast Cells in G_1.** A) Schematic of yeast life cycle borrowed from Websters Dictionary online. Here, yeast begin as haploid yeast being of one of two mating types, a or alpha. Once exposed to mating hormone, and the two types are mixed together, diploid yeast can arise. B) Red

hash mark indicates area of cell cycle where Alpha factor acts, G_1. *S. cerevisiae*, "a" mating type, are forced to undergo non-homologous end joining by being arrested in G_1 phase of cell cycle. Without the presence of alpha factor the cells appear spherical and not necessarily attached to surrounding cells. After three hours of alpha factor treatment the cells begin to show early signs of a "Schmoo" phenotype. The Schmoo phenotype is represented by a change in morphology of the cells shifting from spherical, to oblong and pointed. By 6 hours of alpha factor treatment, nearly all cells exhibited the schmoo phenotype, and in many cases exist in pairs.

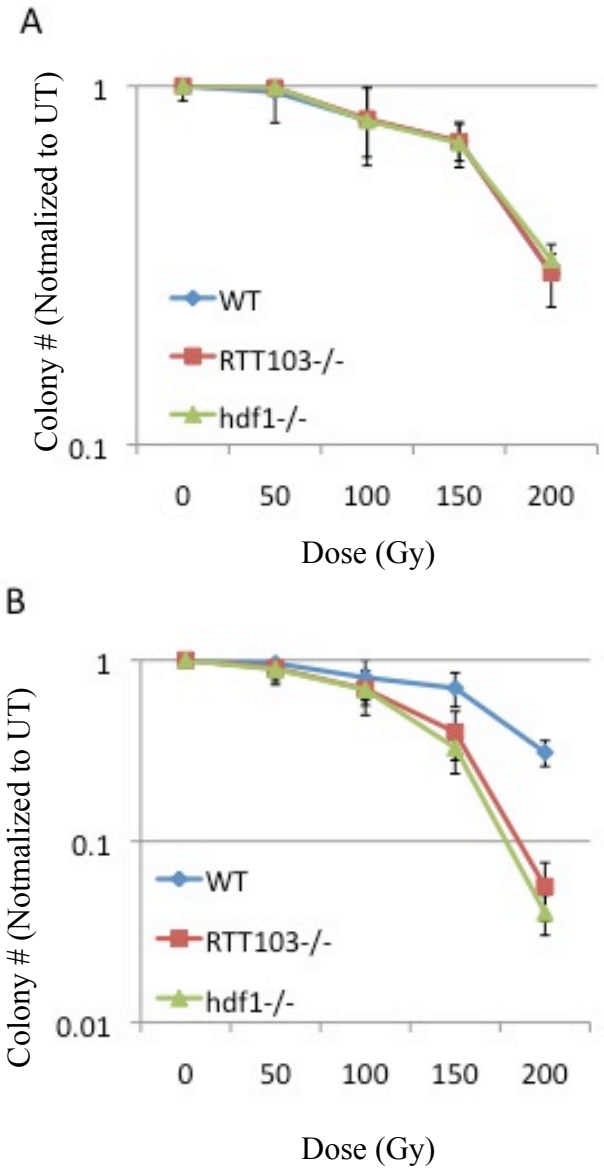

Figure 2.2: **Responses of Asynchronous vs. Synchronous *rtt103-/-* yeast.** Haploid yeast were either unsynchronized (a) or (b) synchronized by alpha factor. Yeast were plated on YPD plates and treated with a range of ionizing radiation doses (0, 50, 100, 150 and 200 Gy). Plated colonies were counted 7-9 days post radiation treatment and graphed. (a) There was no difference in sensitivity to IR between wt, hdf1-/- or RTT103-/- asynchronous yeast. (b) RTT103 and hdf1 were significantly more sensitive to radiation upon synchronization by alpha factor that the wt yeast. (p value < 0.0001).

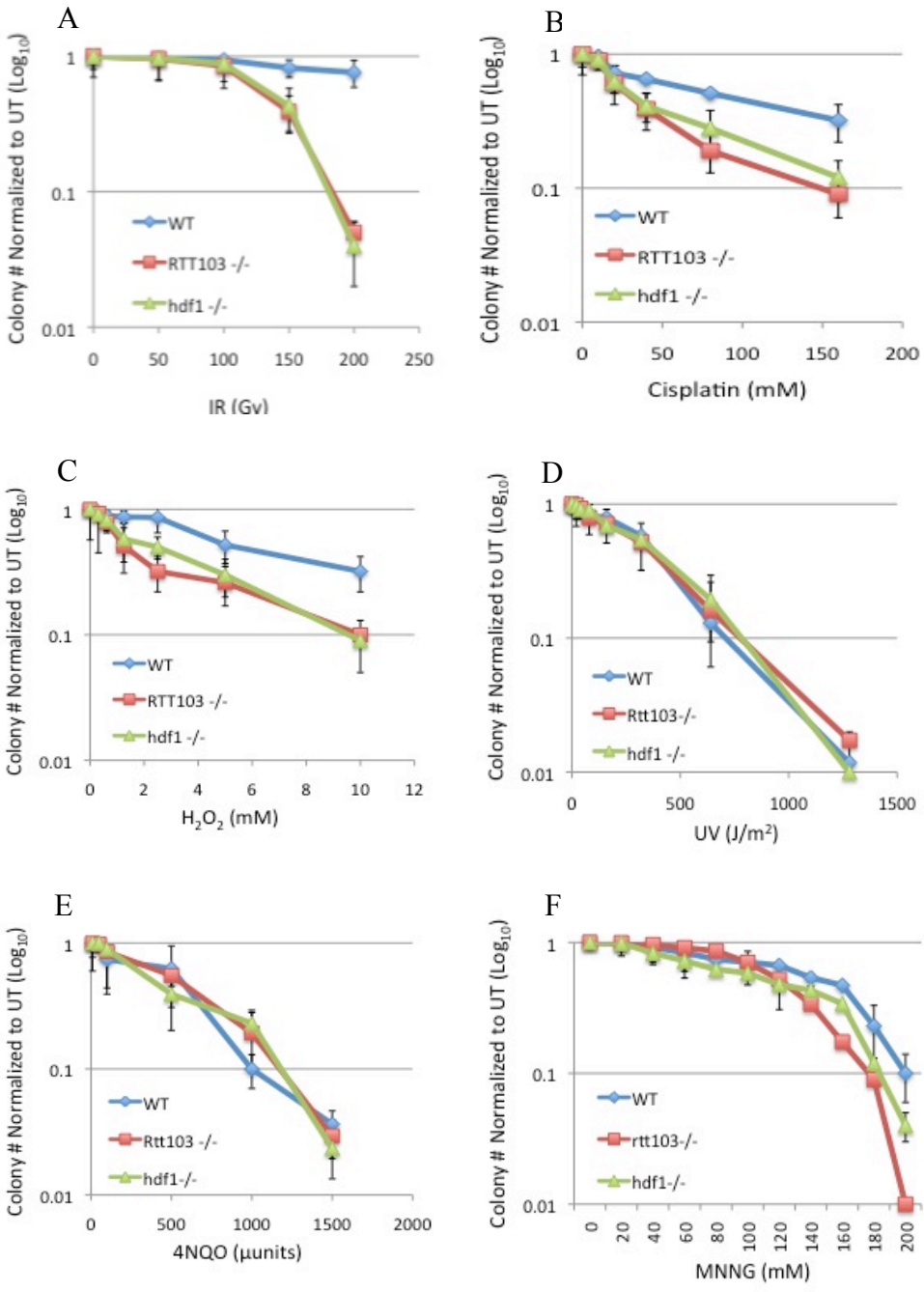
A
Colony # Normalized to UT (Log10)
1
0.1
0.01
0
50
100
150
200
250
IR (Gv)
WT
RTT103 -/-
hdf1 -/-
B
Colony # Normalized to UT (Log10)
1
0.1
0.01
0
50
100
150
200
Cisplatin (mM)
WT
RTT103 -/-
hdf1 -/-
C
Colony # Normalized to UT (Log10)
1
0.1
0.01
0
2
4
6
8
10
12
H2O2 (mM)
WT
RTT103 -/-
hdf1 -/-
D
Colony # Normalized to UT (Log10)
1
0.1
0.01
0
500
1000
1500
UV (J/m2)
WT
Rtt103-/-
hdf1 -/-
E
Colony # Normalized to UT (Log10)
1
0.1
0.01
0
500
1000
1500
2000
4NQO (µunits)
WT
Rtt103 -/-
hdf1-/-
F
Colony # Normalized to UT (Log10)
1
0.1
0.01
0
20
40
60
80
100
120
140
160
180
200
MNNG (mM)
WT
rtt103-/-
hdf1-/-

Figure 2.3: **Survival Analysis of wt, RTT103-/-, hdf1-/- and RTT103-/-(+hKUB5/HERA) yeast after chemotherapeutic or radiation treatments**. G_1 haploid yeast were derived from alpha factor treatment for 6 hours. Cells were then treated with IR, UV or as indicated. A) Yeast treated with IR at various doses (0, 50, 100, 150, and 200 Gy). B) Yeast treated with Cisplatin at various doses (0, 10, 20, 50, 100 and 150 mM) C) Yeast treated with Hydrogen peroxide at various doses (0, .5, 1, 1.5, 2, 5 and 10 mM). D) Treatment with UV at various doses (0, 50, 100, 200, 300, 500, 700 and 1400 J/m^2) E) Treatment with 4NQO at various doses (0, 50, 100, 500, 1000 and 1500 μunits) F) Treatment with MNNG at various doses (0, 20, 40, 60, 80, 100, 120, 140, 160, 180 and 200 mM). Treatments were performed in triplicate for each experiment, using at least 3 replicate experiments for each treatment.

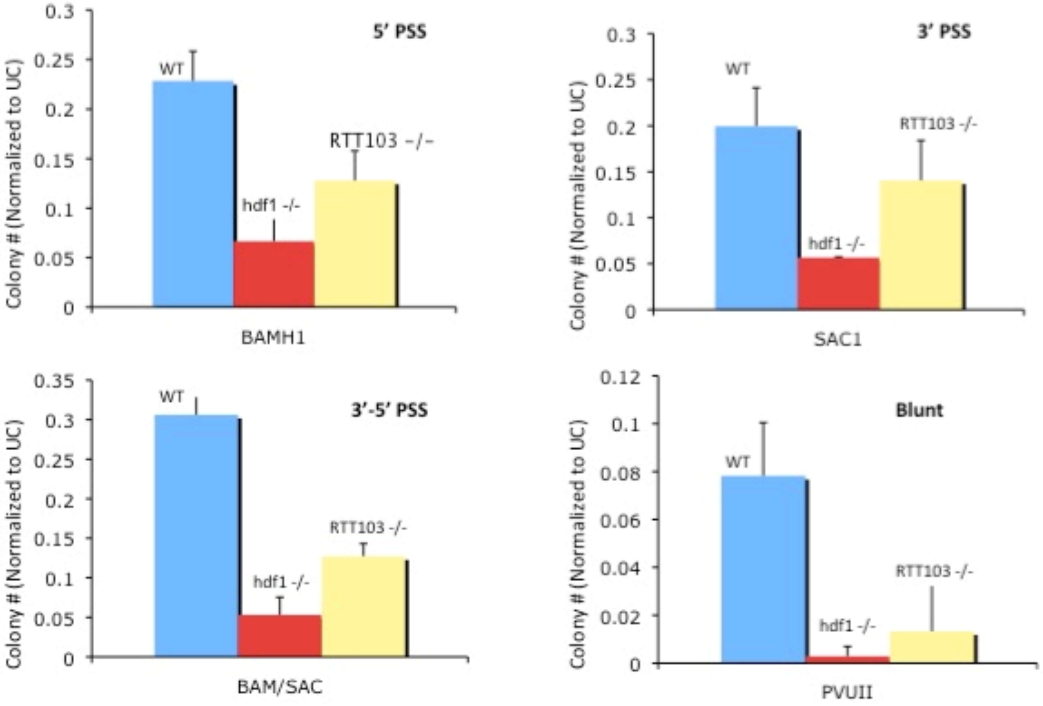

Figure 2.4: ***rtt103-/-* and *hdf1-/-* yeast have an inability to repair several types of DNA breaks.** pYES plasmids were linearized by digestion using either BAMHI, SACI, BAMHI+SACI or PVUII. Each restriction enzyme leaves behind a specific type of DNA break as indicated. Linearized plasmids were transformed into *wt, hdf1-/- or RTT103 -/-* yeast and colonies were selected by the ability to grow on *URA*-/- plates, showing that the plasmid was correctly re-ligated allowing for expression of the selection marker. Wt yeast appeared to be able to repair all the types of damage. *Hdf1 -/-* were unable to repair any of the types of breaks as efficiently as wt yeast. Finally, *RTT103-/-* yeast were specifically unable to repair the non-compatible (BAMHI+SACI digest) ends, as well as the blunt ends (generated by PVUII).

A

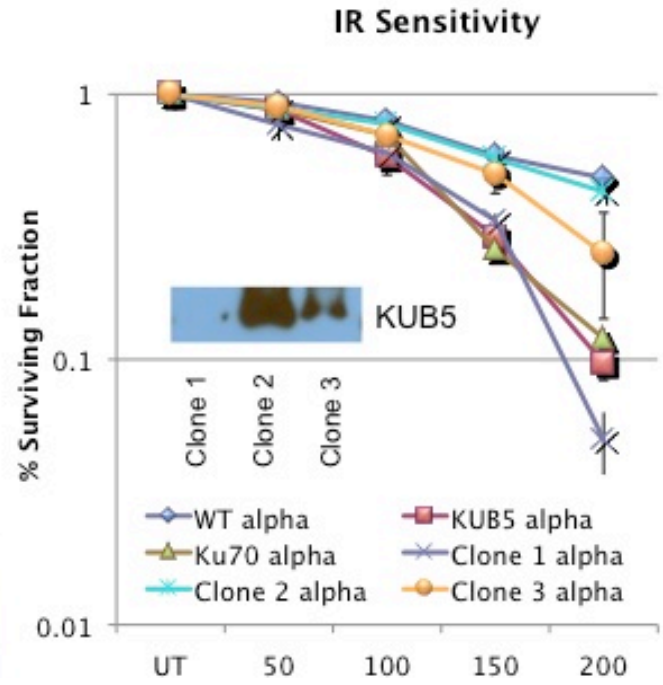

B

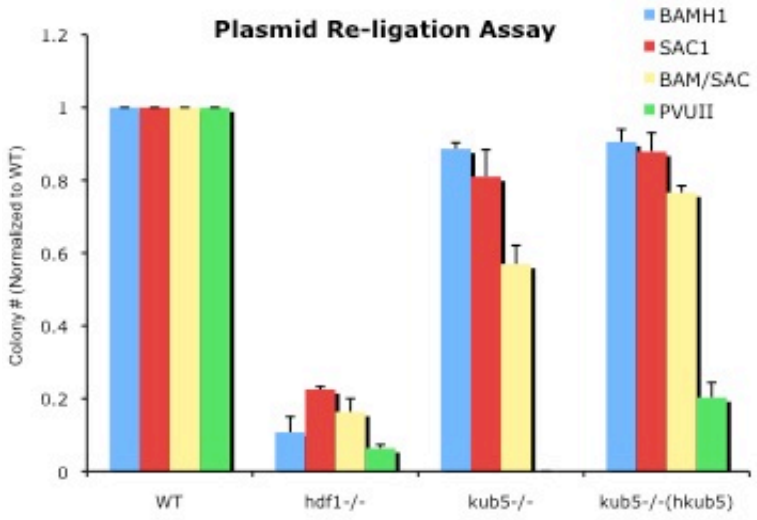

Figure 2.5: **hKUB5/HERA rescues both IR sensitivity of RTT103 yeast, as well as DNA repair defect.** KUB5/HERA was expressed in *RTT103* deficient yeast. Several clones were isolated and probed for KUB5/HERA expression as indicated by western blot in (a) and subjected to (a) IR and (b) plasmid re-ligation assay experiments. In a, the western blot inlet show varied hKUB5/HERA

expression between the clones, with clone 2 expressing the highest hKUB5/HERA level. IR sensitivities of the clones demonstrated that clone 2, with the highest KUB5/HERA expression, also showed the greatest rescue of IR sensitivity. In b, clone 2 was used for plasmid religation analyses. Results indicated that clone 2 did partially rescue the inability of these yeast to repair the blunt and non-compatible DNA breaks.

Yeast gene name	Mammalian gene name	Protein
LIG4	LIG4	DNA ligase IV
LIF1	XRCC4	XRCC4; in collaboration with KU, targets DNA ligase IV to DNA ends
HDF2	XRCC5	Ku80
HDF1	XRCC6	Ku70
This protein is not present in yeast	XRCC7	DNA-PKcs
This protein is not present in yeast	ARTEMIS	Artemis; nuclease regulated by DNA-PKcs; important for preparing DNA ends for ligation

Table 2.1: **Comparison of Yeast DNA repair proteins and pathways to that of Human**. For NHEJ in mammalian cells Ku70 (XRCC4) and Ku80 (XRCC5) bind to the break recruiting DNAPKcs (XRCC7), which allow for recruitment and processing of the break by Artemis and finally the nick ligated by DNA Ligase IV (LIG4). The process is similar for yeast NHEJ, however, yeast do not possess a known homolog for DNA-PKcs or Artemis. Differences, therefore, exist in the repair pathways of the two organisms. Perhaps NHEJ proteins in yeast are not yet fully elucidated, or several proteins in yeast repair have multiple functions yet to be discovered in repair processes.

CHAPTER III

Biochemical and Functional Analysis of KUB5/HERA

INTRODUCTION:

hKUB5 (Genbank accession # NM_021215) is located on chromosome 20q11.21-q12 and the entire gene is ~60 kbps. KUB5 contains 7 exons/8 introns as determined by BLAST using data in the human genome database. All KUB5 homologs contain a highly conserved N-terminal domain (~120 aa). Within its N-terminal region lies an RPR domain that is found in proteins involved in regulation of pre-nuclear RNA, as well as in general transcription, potentially by mediating protein-protein interaction. A Ser/Thr-Gln site found within the RPR domain is may be a phosphorylation target of ATM or related kinase activity. Human KUB5 also contains a leucine-zipper-like coiled-coil domain that appears to be similar to the previously published Ku70 binding domain of nuclear Clusterin (nCLU) (67). Within this coiled-coil domain of hKUB5/HERA lies a potential nuclear localization sequence (NLS) that is also similar to that found in nCLU.

To test the hypothesis that KUB5/HERA is involved in DNA DSB repair, experiments were performed to study hKUB5 expression level both endogenously and after DNA damage. The dependence of DNA repair processes on localization of repair proteins, suggests KUB5 would be localized to the nucleus and perhaps to the sites of DNA damage and repair. hKUB5 localization experiments were performed both with and without DNA damage in an attempt to

differentiate KUB5 function from mere DNA damage detection and signalling indicated by early localization to sites of DNA damage, as in the case of 53BP1 and phosphorylation of H2AX(83, 84). The second major goal of this chapter was to test the hypothesis that KUB5 interacts directly with Ku70 and this interaction is necessary for NHEJ. Experiments were designed to characterize KUB5/HERA interaction with Ku70, including determining functional domains required for KUB5/HERA function and interaction with Ku70 using a yeast two hybrid system to test KUB5/HERA mutants and their ability to interact with Ku70. Conversely, domains of Ku70 important for its interaction with hKUB5/HERA will also be elucidated using GST fusion proteins and immunoprecipitation (IP) experiments.

MATERIALS AND METHODS:

Construction of Expression plasmids. For bacterial purification of hKUB5 protein the hKUB5 cDNA needed to be cloned into bacterial expression vector pQE-80L. This plasmid contains an Ampicillin restriction marker and 6X His tag for protein purification. hKUB5 was subcloned into the MCS region between BamHI restriction and SalI sites.

Sequencing Primers for pQE-80L

5'-CC CGAAAAGTGC CACCTG-3' - Promoter Region

5'-GTTCGAGGTCATTACTGG-3' - Reverse Sequencing

Cloning hKUB5 cDNA into PQE-80L

5'- GCCAGATCTATGTCCTCCTTCTCTGAGTCG-3' – KUB5 Forward N-terminal

5'-CGGCTCGAGCTAGTCAGTTGAAAACAGGTC-3' KUB5 Reverse C-terminal

Subcloning KUB5 into PQE-80L

PCR amplification using primers above were set up as follows. 1 ul template KUB5 cDNA in TOPO expression vector, 2 µl 10X pfu buffer, 2 µl of 5mM dNTPs, 2 µl of 5µM KUB5 Forward N-terminal primer, 2 µl of 5µM KUB5

Reverse C-terminal primer, 0.4 μl Pfu turbo (2.5 μg/μl) and 10.6 μl sterile de-ionized water (SDW). PCR cycle [95°C, 2 min > (95°C, 30 sec > 55°C, 30 sec > 72°C, 1 min 30 sec) 13 cycles > 72°C, 3 min] was used.

PCR product then digested with Bgl II and XhoI at 37°C for 1 hr. At the same time a sample of pQE-80L vector digested with BAMHI an SALI, also at 37°C for 1 hr. PCR products, digestion products and purified plasmid were run on agarose gel. Bands matching expected molecular weights of PCR products were excised from gel and purified from gel using the QIAGEN gel extraction kit, following the QIAGEN handbook guidelines and protocol. Purified PCR products were then used in a ligation reaction mixture of 1μl vector (digested PQE-80L), 7.5 μl insert (purified KUB5 PCR product), 1 μl 10X T4 ligase buffer and 0.5 μl T4 DNA ligase. Samples were incubated at room temperature (RT) for 30 minutes. Resulting ligated plasmids from this reaction were used for propagation in DH5-alpha cells. Transformation of vector into DH5 alpha cells was done by heat shock at 42°C for 30 seconds followed by 1 min on ice. Transformed *E. coli,* were spread on LB plates containing Ampicillin for selection of positive transformants. Positive clones were grown and sequenced to verify intact KUB5 cDNA insert.

YFP tagged KUB5 Generation. Generation of YFP tagged KUB5 and CFP tagged Ku70 utilized expression vectors pcD3F2-YFP and pcD3.1 F2-CFP. The

KUB5 PCR product from creation of the 6 His KUB5 expression system was also used for insertion into the mammalian expression vector for YFP with the selection marker conferring neomycin resistance. For CFP-Ku70, Ku70 was digested from PCNA with BamHI and XhoI and ligated into pcD3.1 F2-CFP and selected under hygromycin. Colonies grown from propagation in DH5-alpha were sequenced to verify correct homology and orientation.

GFP KUB5 Expression in CHO cells. Chinese hamster ovary (CHO) cell lines used were Y-X4-1, Y-X4-2 and Y-X4. CHO cells were grown in HYQ media. For GFP-KUB5 cells a FUGENE protocol was employed used as stated in FUGENE manual. Transformed cells were selected for on media containing Neomycin (200 μg/ml) and selected for 3 days prior to preparation for microbeam analysis.

Microbeam Analysis. Microbeam-laser system was combined with fluorescence microscopy in order to visualize DNA damage created by the laser. Analysis was carried out using 63X objective lens and filter #5. Contrast of camera was set to DICII. Laser energy was set to 75 and pulse centered between 1 and 10 pulse per second. Data acquisition was carried out under multidimensional acquisition, C-TAG with exposure time 800 ms.

hKUB5 expression and isolation for purification. BL21 bacterial cells were used to express and purify His tagged hKUB5. Here pGEX-6p-1 was used as a control plasmid, and pQE-80L-His-KUB5 was used for transformation into BL21 cells. 50 μl BL21 cells for 5 μl purified plasmid DNA were incubated on ice for 30 min. Samples underwent heat shock at 42 ^{o}C for 30 seconds and placed back on ice for 2 minutes. Sampled were added to 500 μl SOC media and incubated in a 37 ^{o}C shaker for 1 hour. 50 μl of sample were plated on media containing ampicillin to select for positive transformations. Expression of KUB5 protein was carried out by using 1ml log-phase BL21 cells with IPTG added to a final concentration of 5 mM. Cells were incubated at 37^{o}C for 3 hours. Protein was isolated by spinning down cells and re-suspending in SDS buffer and stored at -20 ^{o}C.

hKUB5 protein purification. KUB5 protein isolated from BL21 cells contains a 6X His tag. Samples can be purified by both Ni-NTA and by HPLC. For Ni-NTA, BL21 cells were treated with 0.5 mM IPTG for 6 hours. Ni-NTA beads (200 μl bed volume) were washed 3X with TBS-T. 10 ml of protein isolate from BL21 cells, using extraction buffer (50 mM Tris 7.5, 500 mM NaCl, 5 mM imidazole, 1% NP-40, protease inhibitors), was added to beads and rotated at 4^{o}C for 30 minutes. Beads were then washed 2X with 500 mM NaCl buffer (50 mM Tris 7.5, 150 mM NaCl, 5 mM Imidazole, 0.1 % NP-40), and 1X with 150mM

NaCl (50 mM Tris 7.5, 500 mM NaCl, 5 mM Imidazole, 0.1 % NP-40, 10% glycerol). 25 μl of 2M solution Imidazole was then added to beads followed by 600 μl elution buffer (50 mM Tris 7.5, 150 mM NaCl, 200 mM Imidazole, 0.1% NP-40, 10% glycerol). After 5 minutes, samples were spun and supernatant was analyzed for protein concentration. Purified protein samples were stored at -80^{o}C after flash-freeze in liquid nitrogen. Prior to use for interaction studies protein samples were dialyzed to remove traces of imidazole in sample using dialysis buffer (20 mM Tris 7.5, 150 mM NaCl, 10 mM $MgCl_2$, 10 % glycerol, 0.1% NP-40.

Size Fractionation by FPLC. BL21 purified KUB5 protein was adjusted to 4mg/ml, and 200 μl was loaded onto a Superdex 200 separation column (Amersham Biosciences). Protein was eluted in elution buffer (20mM HEPES, pH 7.5, 250 mM NaCl, 1 mM EDTA, o.1% B-mercaptoethanol and 0.01% Tween20). Fractions were collected at 0.5 ml/min in tubes containing 10 μg bovine serum albumin (85). Proteins were precipitated with 1 ml Acetone at -20 C overnight. Protein was pelleted at top speed and dried before being re-suspended in SDS buffer for SDS-PAGE electrophoresis and western blot analyses.

Gel Shift Assays. Gel shift assay was employed to confirm direct interaction of KUB5 and Ku70 in the presence of DNA. Here 100 pmol oligos (2, 43-mers) were combined in 50 μl water. Samples were then boiled for 10 minutes and cooled. Protein isolates were run on 12% polyacrylamide gel, visualized under UV light and bands excised from gel and placed in a solution containing 0.5 M Ammonium acetate and 10 mM Magnesium Acetate. Samples were rotated overnight at RT. Ethanol precipitation of protein was performed using 0.1 volume 3M sodium acetate and 3 volumes 100% ethanol. Precipitation was allowed to occur for 20 minutes at -20^{o}C. Samples were spun and washed in 70% ethanol. Pellets were air-dried and re-suspended in water, or TE. Oligos were then labeled with ATP^{32} using the following method: 8 μl boiled DNA was added to 35 μl water. 5 μl 10X bacteriophage T4 polynucleotide kinase buffer (PKB) was added and sample taken to protective radiation hood. Here 1 μl of 10 mCi/ml γ p^{32}/ATP (50 pmoles) was added along with 1 μl T4 polynucleotide kinase (10 units). Samples were incubated at 37^{o}C for 1 hr and run through Superdex G-50 pre-made column. DNa can then be stored at 4^{o}C until needed. For DNA binding reactions reaction buffer (100 mM KCL, 25 mM Tris pH8, 1 mM DTT) was made. Purified Ku70/80 (a generous gift from David Chen laboratory) was added to 10 μl reaction buffer with 1 μl labeled oligos. Solution was left on ice for 30 mintutes. When adding multiple proteins the order of application of proteins can be varied. The best interaction of KUB5 and Ku70/80 protein was obtained by

first incubating in KU70/80 then after 1 hr adding purified KUB5. Samples were washed in 1X TBE prior to running on acrylamide gel. Radio-labeled oligos and protein complexes were identified by Typhoon Imager (Acquisition mode: storage phosphor, orientation R, 200 microns, scan time 6 min). All gels in this experiment were run using TBE buffer (5X TBE buffer – 54 g Tris, 27.5 g, Boric Acid, 20 mM 0.5 M EDTA).

Nuclei Isolation Protocol for protein lysates. Adherent mammalian cells were washed wish PBS and scraped. Pelleted cells were washed again in PBS and re-suspended in 400 μl Buffer A (10mM HEPES pH 7.9, 10 mM KCl, 0.1 mM EDTA pH 8, 0.1 mM EGTA) and carefully pipetted up and down to avoid bubbles. Cells were allowed to swell on ice for 15 minutes. 25 μl NP-40 (10%) was added and samples vortexed and pelleted. Resulting supernatant was removed (cytoplasmic fraction) and pellet was re-suspended in 50 μl ice cold Buffer C (20 mM HEPES pH 7.9, 0.4 M NaCl, 1 mM EDTA pH 8 and 1 mM EGTA) and rotated for 15 minutes at 4^{o}C. After top speed spin, supernatant was collected as nuclear fraction.

Co-Immunoprecipitation (Co-IP). Protein isolated from any of the mechanisms (RIPA, whole cell, or nuclear fractionation) are all treated equally for Co-IP experiments. Here Protein A/G beads are washed with TBS-T and incubated with

antibody, KUB5 monoclonal at 4^{o}C rotating for 1 hours. Beads are spun and washed with TBS-T 3X and suspended in TBS-T with protein lysate added. Lysate and beads are rotated again for 2 hrs at 4^{o}C. After washing another 3X beads attached to protein complexes are suspended in SDS buffer and boiled prior o running on SDS-PAGE gels.

GST Fusion Proteins and interaction Assay. Purified GST Ku70 protein, and mutants of Ku70 were created from David Chen laboratory. His KUB5 purified protein was used for direct protein-protein interaction studies using glutathione conjugated beads. Here purified protein was generated using lysis buffer (20 mM Tis HCl pH 8, 200 mM NaCl, 1 mM EDTA pH 8, 0.5% NP-40 and just prior to use adding protease inhibitors at the following concentrations: 2 μg/μl apoprotinin, 1 μg/μl leupeptin, 0.7 μg/ml pepstatin and 25 μg/ml phenylmethylsulfonyl fluoride (PMSF)). Purified GST Ku70 fusion protein was incubated with 50 μl of a 50% slurry of glutathione agarose beads washed in TBS-T, for 2 hours at 4^{o}C. Pelleted beads were washed with 1 ml ice-cold lysis buffer. Purified KUB5 protein was added to Ku70-Bead complex suspended in lysis buffer and rotated for another 2 hrs at 4^{o}C. Protein:bead complexes were then washed and suspended in 10 μl 2XSDS buffer and run on polyacrylamide gel.

Yeast Two Hybrid screen for domains responsible for Ku70 and KUB5/HERA binding. AH109 yeast strain (*his*3,*lacZ,trp1,leu2*) will be used in two-hybrid structure/function analyses as described [MatchMaker Two-Hybrid System 2 Protocol, Clontech Laboratories (PT1030-1)]. Using this protocol, deletion mutants can be inserted into either pGADT7 or pGBKT7 vectors (generous gift from Paulo Scaglioni Laboratory, from Clontech Laboratories, Inc., Palo Alto, CA) as prey or bait [20]. KUB5/HERA and Ku70 mutant proteins will be generated by PCR using splicing by overlapping extension (SOE)(86, 87). Human KUB5/HERA cDNA fragments, generated by PCR, encoding aa residues in table will be subcloned in-frame into the pGADT7 vector. Ku70 will form a hybrid protein with the GAL4 DNA binding domain (GAL4-DBD) at its N-terminus. Once sequenced, GAL4-Ku70 can be co-transfected with various GAL4-KUB5/HERA fragments into AH109 yeast using the protocol provided in the MATCHMAKER (Clontech Laboratories, Inc., Palo Alto, CA) manual. AH109 yeast carry both GAL4-responsive LacZ (for detection) and GAL4-responsive HIS3 (a selection marker) genes. Stable transformants grown on selection can then be subjected to on-filter -galactosidase assays, with X-gal as a substrate yielding a positive reaction when colonies turned blue within first 120 min of incubation with X-gal. Negative reactions when blue colonies are not observed indicate no association (Yeast MATCHMAKER protocol, clonetech). This same experiment will be performed in reverse using full length

KUB5/HERA and various mutants of KU70.

Transient down regulation of hKUB5/HERA by siRNA. Pooled siRNA was purchased from Fisher Scientific (SMARTpool MU-013787-00-0005, 5 nmolx4, C20orf77). siGenome duplexes were as follows: duplex 1 sense sequence GAAGAAAUCUCUGAAACGAUU, duplex 2 sense sequence GCAAGAUGUUUCUCUAUUGUU, duplex 3 GACCUGAAUUCACUAGAGAUU and finally duplex 4 sense sequence GAACAUCUGGCAAGAACGAUU. Oligos were suspended in buffer (200 μl resuspension buffer and 800 μl RNAse free water) to a final concentration of 100 μM for stock. siRNA transient transfection was carried out using ExtremeGene protocol for transfection as indicated in manual. Cells were incubated in transfection reagent and oligos overnight and media replaced.

Flow Cytometry Analysis. Cells were prepared for flow cytometry by washing plates with PBS. Cells were craped into PBS and centrifuged (500xG). Pellets were washed in PBS and re-suspended in 1 ml 95% ethanol and stored overnight at -20^{o}C. Cells were labeled for cell cycle analyses using propidium iodide (PI) by re-suspending pelleted cells and washed ethanol fixed cells in PI solution (100 μg/ml RNAse, 50 μg/ml PI, 2% FBS). Samples were incubated for at least 1 hr at

37^{o}C prior to flow cytometry analyses. Flow cytometry was performed using a flow cytometer as described by (67, 88).

RESULTS:

KUB5/HERA steady state protein levels appear to be highly stable in several different cell lines and from genetic backgrounds analyzed (example in Figure 3.1a). The hKUB5/HERA protein resolves at 34.5 KDa and engodenous levels of the protein do not appear to change in response to DNA damage treatment, such as after IR exposure (Figure 3.1b). In addition to protein levels remaining unchanged after DNA damage, the localization of hKUB5/HERA within the nucleus (Figure 3.2a) appears to remain the same, as well as after pulsed laser DNA damage (Figure 3.2b). A possible explanation for this result could be the ubiquitous expression of KUB5/HERA within the nucleus similar to that documented for Ku70, which also does not accumulate at the sites of DNA damage in the form of accumulated foci, however Ku80 is able to localize to sites of DNA damage (89, 90).

A. Protein-Protein Interactions using Whole Cell Lysates.

To study the physical interaction of hKUB5 and Ku70, several methods were employed. First, whole cell protein lysates were collected and immunoprecipitated with KUB5/HERA antibody generated in our lab. Here, the KUB5/HERA antibody was able to pull-down both KUB5 and Ku70 protein from a whole cell lysate confirming association of the two proteins either directly or

within a complex (Figure 3.3). Interestingly, the reverse immunoprecipitation using Ku70 antibody, did not result in KUB5 being pulled down in the reaction. A possible theory for this result is that the intracellular level of Ku70 is so much greater than that of KUB5 that a very small percentage of Ku70 interacts with KUB5. This could be due to the broad functions of Ku70, since it is known to have many interacting partners, such as nuclear clusterin, BAX, and Ku80(65). It is possible that these other protein complexes containing Ku70 are in much greater concentration within the cell than that of the KUB5/HERA:Ku70 complex.

B. Protein-Protein Interactions using Purified Proteins

Co-immunoprecipitations (Co-IPs) from whole cell lysates may only indicate that proteins exist within the same complex, not necessarily that they directly interact. For example, other proteins may be required for complexation between Ku70-KUB5/HERA. In order to test if these proteins directly interacted, pure protein from bacteria was generated. Here, an expression plasmid, PQE-80L, was used to construct hKUB5 cDNA fused to a 6X-His tag. Protein expression was confirmed in BL21 bacterial cells after IPTG induction by SDS-PAGE and western blot analyses (Figure 3.4). Further protein purification was also performed by FPLC using a SuperDEX 200 column (Figure 3.5). In collaboration with Drs. Weterings and Chen, gel shift analysis, after FPLC

purification, confirmed the interaction of the two proteins in the presence of DNA (Figure 3.6). Further analyses showed that increased magnesium dissociated the KUB5/HERA:Ku70 protein complex in the presence of DNA. Using gel shift assays, we also showed that Artemis did not appear to complex with KUB5 and Ku70 in the presence of DNA (data not shown). Further co-IP analyses using purified KUB5, Artemis, Ku70/Ku80 heterodimer and Ku70/Ku80(c-terminal deleted) revealed insight into the complex (Figure 3.7). Here, the KUB5 antibody pulled down Ku70 and KUB5, however Ku80 was not resolved or present in the complex (Figure 3.7, lane 1). Furthermore, the KUB5 antibody in the absence of KU(Ku70:Ku80), did not pull down Artemis, confirming the gel-shift data suggesting that KUB5 and Artemis do not directly interact (Figure 3.7, lane 2). Thus, the KUB5 antibody, in the presence of KUB5, KU and Artemis purified proteins only KUB5 and Ku70 were co-immunoprecipitated. (Figure 3.7, lane 3). Using a mutant form of KU, Ku70/Ku80 (c-terminal domain deleted) was used in pure protein co-IPs. Here, the KUB5 antibody in the presence of purified KUB5, and Ku70/Ku80(c-terminal domain deleted) resulted in KUB5 and Ku70 being pulled out of the reaction (Figure 3.7, lane 4). These data support the hypothesis and previous data suggesting a direct interaction between KUB5 and KU70, and this interaction appears to be independent of KU80 (Ku86).

C. GST-Fusion Protein Analysis

Consistent with data from both endogenous and pure protein co-IPs and the original yeast two hybrid screen for Ku70 binding proteins, the data from GST-fusion protein analyses supported the notion that KUB5 and KU70 directly interact. It is important to further study this interaction by identification of specific residues responsible for KUB5:Ku70 interaction. Ku70 as been well published as a binding partner with many important proteins in DNA damage sensing and repair pathways. Domain analyses of Ku70 revealed a c-terminal coiled coil domain that was largely responsible for its interaction with these proteins, including nuclear clusterin and BAX. In order to determine if this is also the case with KU70 interacting with KUB5, GST fusion proteins (from Dr. David Chen laboratory) were used in binding reactions with KUB5 (Figure 3.8a). Co-IP experiments were performed using glutathione beads mixed with purified GST Ku70 fusion proteins, followed by addition of pure KUB5. Reactions were then separated on SDS-PAGE gels and visualized by western blot for KUB5 and Ku70. KUB5 antibody probing of the western blot revealed pure KUB5 protein in the control lane. The fusion proteins corresponding to Ku70(493-575), KU70 full-length, Ku80 full-length and Ku80(509-732) were unable to interact with bacterial purified KUB5 protein. Importantly, the GST-Ku70(524-609), which contains a Ku70 c-terminal domain showed interaction with KUB5 being pulled down in the reaction. These data support the hypothesis that KUB5/HERA, like

many other Ku70 interacting proteins, interacted with Ku70 via its C-terminal coiled-coil domain.

D. Yeast Two Hybrid Analyses of KUB5/HERA interaction with Ku70

S. cerevisiae, in addition to being a simple and versatile model system for studying DNA repair, is also useful as a tool to study protein-protein interactions. Preliminary data suggested direct interaction of hKUB5/HERA and hKu70, such as the original Yeast-2-Hybrid screen using Ku70 as bait where KUB5/HERA was discovered. This same system was employed to study, in more detail, the interaction of Ku70 with wild-type and mutant forms of hKUB5/HERA. Here, yeast-2-hybrid analyses were used to study the direct interaction of KUB5/HERA with Ku70 (Figure 3.9). Point mutations and domain deletions of hKUB5/HERA (Figure 3.10) were generated by PCR and cloned into pGADT7, the "prey" vector. hKU70 was cloned into pGBKT7, also known as the "bait" vector. When both plasmids were successfully transformed into the yeast, they were able to grow on –leu, -Trp media (Table 3.1). Controls were especially important in this experiment in order to demonstrate proper functioning of the assay and specific selection. Here, the negative control, pGBKT7 (Lamin) and pGADT7 (Large T- Antigen), both transformed in yeast allowed for growth on –leu, -trp media. However, these yeast did not grow on the stringent selection on media lacking Histidine, nor did the colonies turn blue upon X Gal treatment when

grown on –Leu-Trp media. This is due to the fact that Lamins are known to not interact with many proteins, including Large T Antigen. The positive control, pGBKT7 (p53) and pGADT7 (Large T Antigen), was used for the well-known ability of p53 to bind Large T-Antigen. Therefore, when both plasmids were transformed into the yeast, they grew on the stringent selection media (-His, -Leu, -trp, -ade), and the colonies also turned blue when grown on media containing X Gal. After the conditions for the controls were met, the human KUB5/HERA, KUB5/HERA point mutants and domain mutants were analyzed for their ability to bind Ku70. Results indicated that the full-length human KUB5/HERA interacted with Ku70 directly in the Y2H system (Table 3.1). Furthermore, most KUB5/HERA mutations generated in this investigation did not affect Ku70 binding to KUB5/HERA. The only mutations that showed inhibition of interaction were mutants generated with the C-terminal domain deleted, as well as the following point mutations; L276A, LL269, 276 AA, L269, 273, 276A as well as LL269, 276PP. The common amino acid present in all the mutants with abolished KUB5:Ku70 interaction was L276 within the C-terminal domain of KUB5/HERA. (Table 3.1). These data are consistent with the known involvement of the C-terminal coiled-coil domain in protein-protein interaction, and therefore important for KUB5/HERA interaction with Ku70.

Due to the significance of the KUB5/HERA c-terminal domain in its ability to interact with Ku70, we hypothesized that perhaps KUB5/HERA's interaction

with Ku70 is important for proper NHEJ. To test this, C-terminal deletion mutants were analyzed for their sensitivities to IR. We previously established that hKUB5/HERA has the ability to almost completely rescue the IR sensitivity noted in the *rtt103-/-* yeast. These *rtt103-/-* were transformed with the PGADT7 vector containing hKUB5/HERA (c-terminal del), the same that showed an inability to interact with Ku70 by Y2H. Consistent with our hypothesis, these yeast remained sensitive to IR, therefore hKUB5/HERA with the c-terminal domain deleted was unable to rescue the IR sensitivity noted in the *rtt103*-/- yeast (Figure 3.11). These data suggest that not only is RTT103 likely involved in NHEJ, but in particular, its interaction with Ku70 is important in normal functioning of the NHEJ pathway and repair.

E. Identification of KUB5 Higher Complexes Using Gel Filtration.

These data confirmed my original hypothesis that there is direct interaction between KUB5 and Ku70, however, it is still not known how many different complexes KUB5 are present in cells before or after cell stress. To test this, whole cell protein lysates were fractionated by FPLC analyses (Figure 3.12). Fractionation and subsequent western blotting revealed KUB5 likely exists in three different fractions of distinct molecular weights. The largest KUB5-

containing fraction corresponded to 1000 KDa fraction. It is not known yet what complexes containing KUB5 could be within this fraction however, a likely possibility would be that of transcription complexes, which would be consistent with the hypothesis of KUB5 acting in transcription termination. These fractions, in the future, should be analyzed for RNA polymerase and other transcription complexes. The second largest MW fraction containing KUB5 was that corresponding to a 115 KDa complex. Western blotting of this fraction confirmed that it contained hKUB5 and Ku70. Finally, the last fraction containing KUB5 was eluted at a volume that corresponded to 40 KDa. Though these data are preliminary, they suggest KUB5 exists in more than one MW complex and these data support the hypothesis that KUB5 and Ku70 exist in a complex together.

DISCUSSION:

Domain analyses of KUB5/HERA and Ku70 revealed the importance of the Ku70 C-terminal coiled-coil domain and the Leucine 276 amino acid of KUB5/HERA for interaction of the two proteins. Though yeast two-hybrid results and purified protein IPs confirmed a direct interaction of KUB5/HERA and Ku70, the purified GST full length Ku70 alone was unable to bind KUB5/HERA. A likely explanation for this result is illustrated in the SDS-PAGE gel shown above the western blot (Figure 3.8b). Here, the lane with full-length Ku70, as well as that of full length Ku80 showed faint banding for the purified protein. Possible structural stability dependence of Ku70 interaction with Ku80 could be necessary for stable interactions, and when the two are purified separately they are unstable and therefore do not interact with their known binding partners. This instability could be preventing Ku70 full-length protein from interacting with KUB5.

Purification of highly concentrated KUB5/HERA in large amounts provided the necessary components for performing X-ray crystallization to determine the 3-D structure of the protein. This proved difficult, as the protein could not be crystallized by any of the conventional methods. This inability for KUB5 to be crystallized led to the hypothesis that KUB5 is a largely hydrophobic protein, and may require interaction with another protein, maybe Ku70, for

stability. In the future, it will be necessary to study KUB5 by purifying and crystallizing specific domains alone, rather than the entire protein.

Gel filtration analyses were performed in order to test the hypothesis that KUB5/HERA has the ability to exist in more than one complex. Preliminary results indicate that KUB5 exists in at least three different protein complexes two of which could also contain Ku70. Further analysis will be performed in order to test for additional proteins existing in the KUB5 containing fractions, including IP experiments to look for proteins directly interacting with KUB5. Ku80, Artemis, RNA polymerase II and DNAPKcs would all be possible candidates that could be in a complex with KUB5. Previous IP experiments showed that KUB5 antibody can IP Ku70 with KUB5, however Ku70 antibody does not IP KUB5/HERA with Ku70. These data led us to hypothesize that Ku70 exists in the nucleus at much higher levels than KUB5 due to its involvement in several processes and complexes, most of which may not rely on KUB5. The gel filtration analyses support this hypothesis due to nearly every fraction containing Ku70 protein, therefore providing evidence to support several Ku70 complexes. Conversely, KUB5/HERA only existed in three distinct fractions, significantly fewer than Ku70.

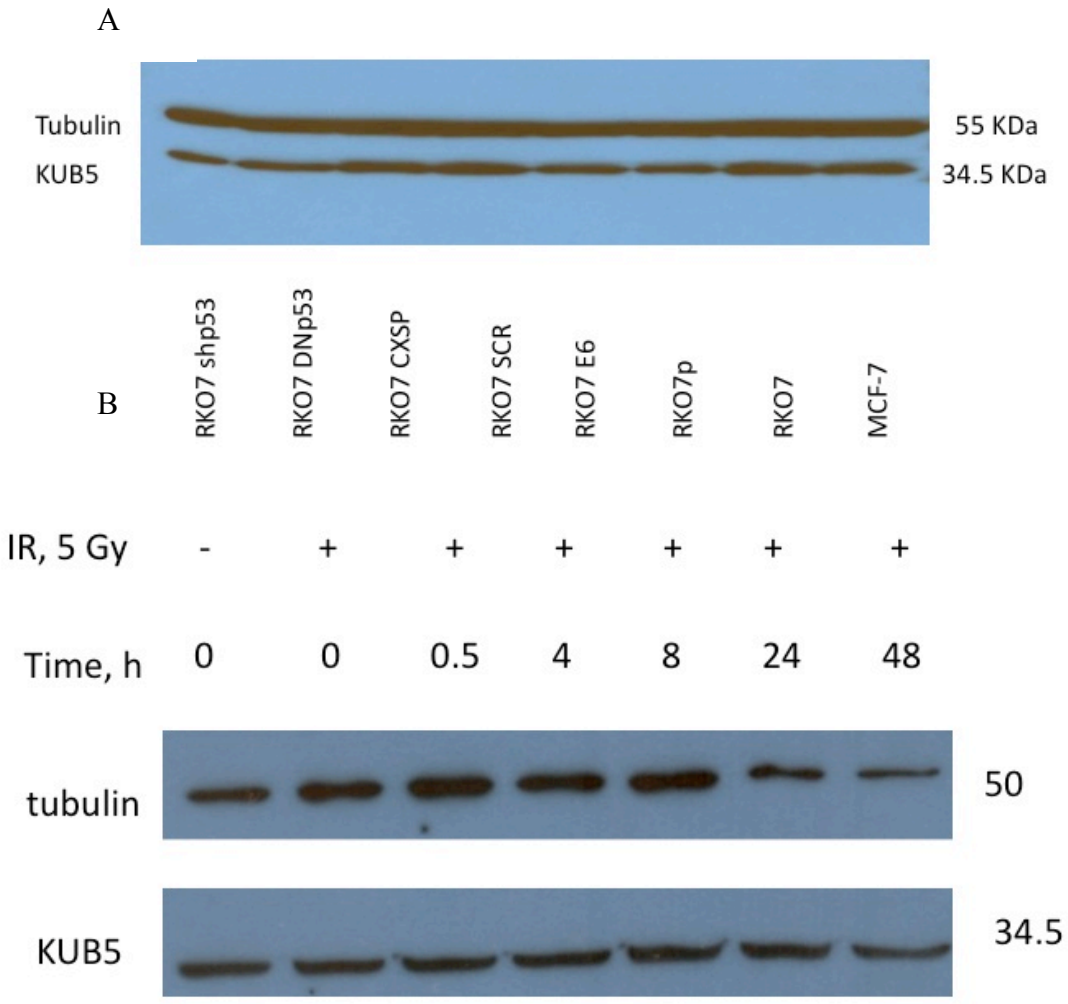

Figure 3.1 – **Endogenous KUB5 protein levels appear tightly regulated across cell lines and levels do not change after DNA damage.** A) Western blot illustrating a small subset of early screenings of cell lines and their KUB5 levels. In most cases KUB5 levels appear to be steady, and at relatively equal expression across cell lines, including those that have been altered in cell cycle regulators such as p53. B) After IR treatment KUB5 protein levels remain steady. Results indicate that KUB5 is not an IR inducible protein.

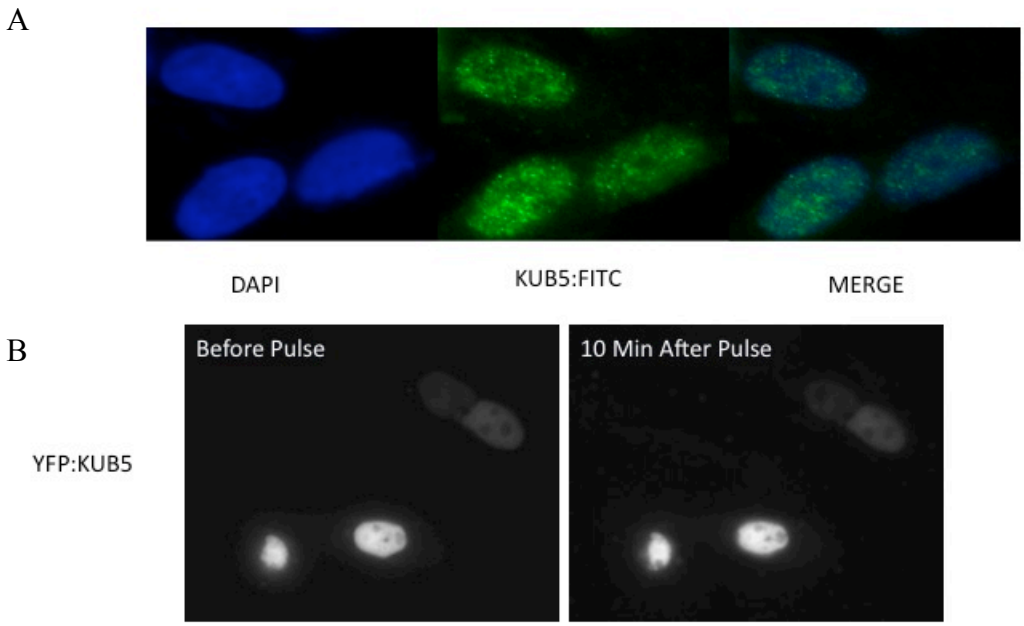

Figure 3.2 – **KUB5 protein expression is localized to the nucleus**. A) KUB5 antibody was used for immuno-histochemistry analysis yielding KUB5 expression solely in the nucleus of cells, co-localizing with DAPI. B) Pulse Laser DNA damage does not affect KUB5 localization in CHO cells transformed with GFP-KUB5 expression vector. Figure is representative, similar results were taken out to longer time points, the longest being 3 hours post laser pulse, all with the same result of no change in KUB5 localization.

A

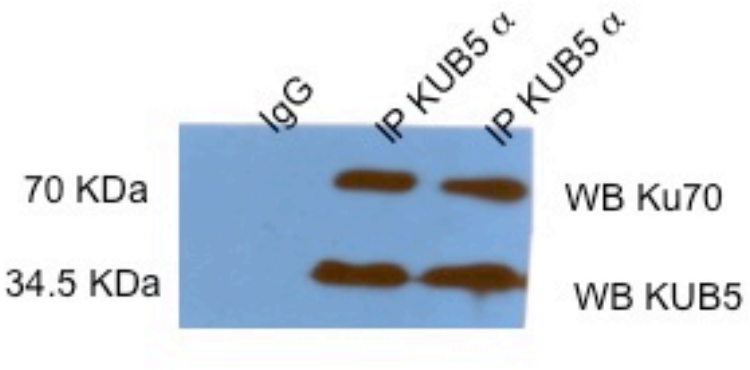

B

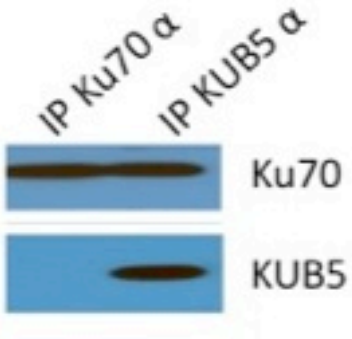

Figure 3.3 – **Whole cell protein lysate Co-IPs reveal KUB5 interaction with Ku70.** A) Whole cell protein lysates were co-IPed using KUB5 antibody resulting in pull-down of KUB5 protein and Ku70. B) Whole cell lysate IP using Ku70 antibody, pulled down Ku70 however KUB5 was not detected on resulting western blot.

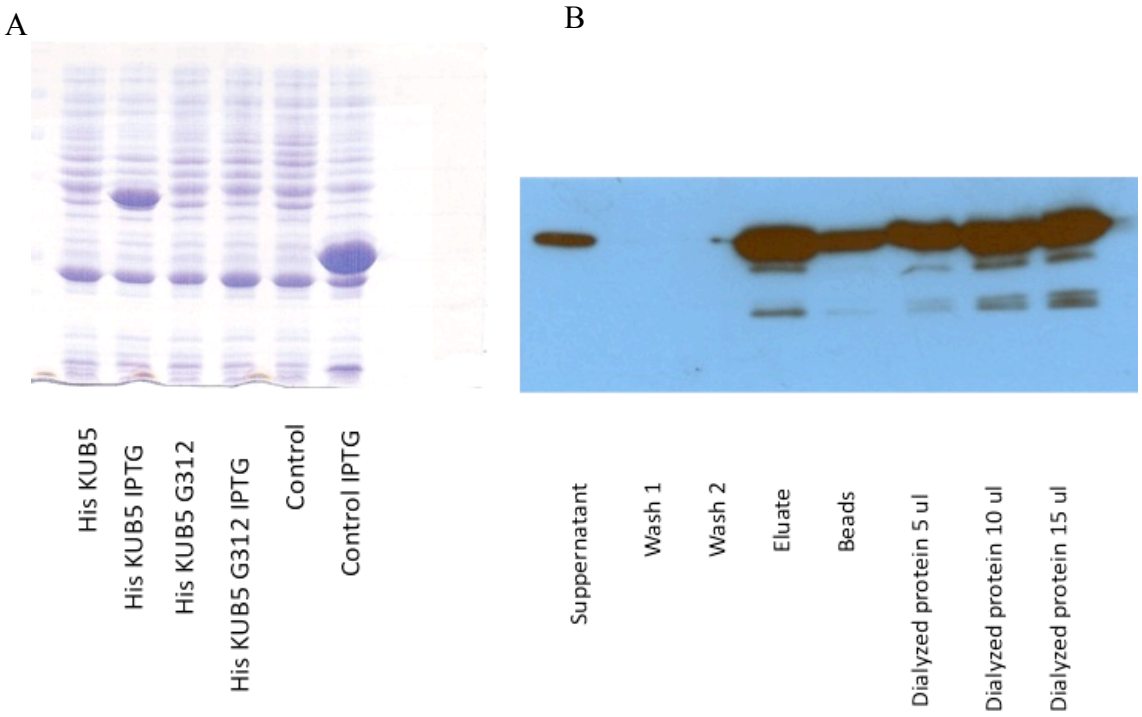

Figure 3.4 – **hKUB5 protein can be purified by Ni-NTA after expression in BL21 cells with high yield and purity**. A) SDS-PAGE showing effect of IPTG induction of KUB5 expression in BL21 cells for various clones and mutants of KUB5. The highest induction clone was used for all later purifications. B) Western blot showing KUB5 antibody probing pure protein lysates direct from Ni-NTA purification prior to FPLC.

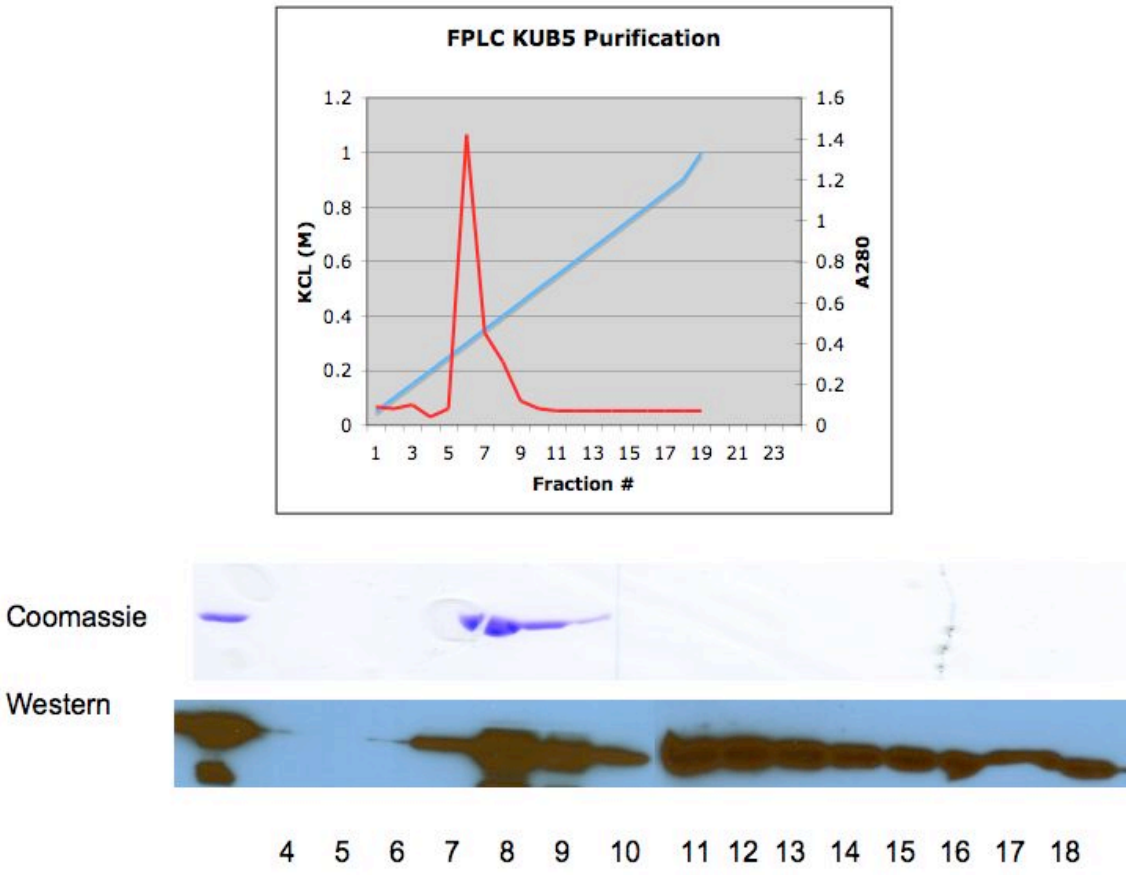

Figure 3.5 – **KUB5 purification by FPLC successfully purified and concentrated KUB5 protein.** FPLC analysis was carried out and monitored by UV as indicated in materials and methods. Fractions were collected after initial 15 mls excluded. Protein containing fractions were further analyzed for KUB5 purity by SDS-PAGE and western blot analyses for KUB5 expression. Fraction 8 contained the highest level of purified KUB5 protein and was used in following experiments.

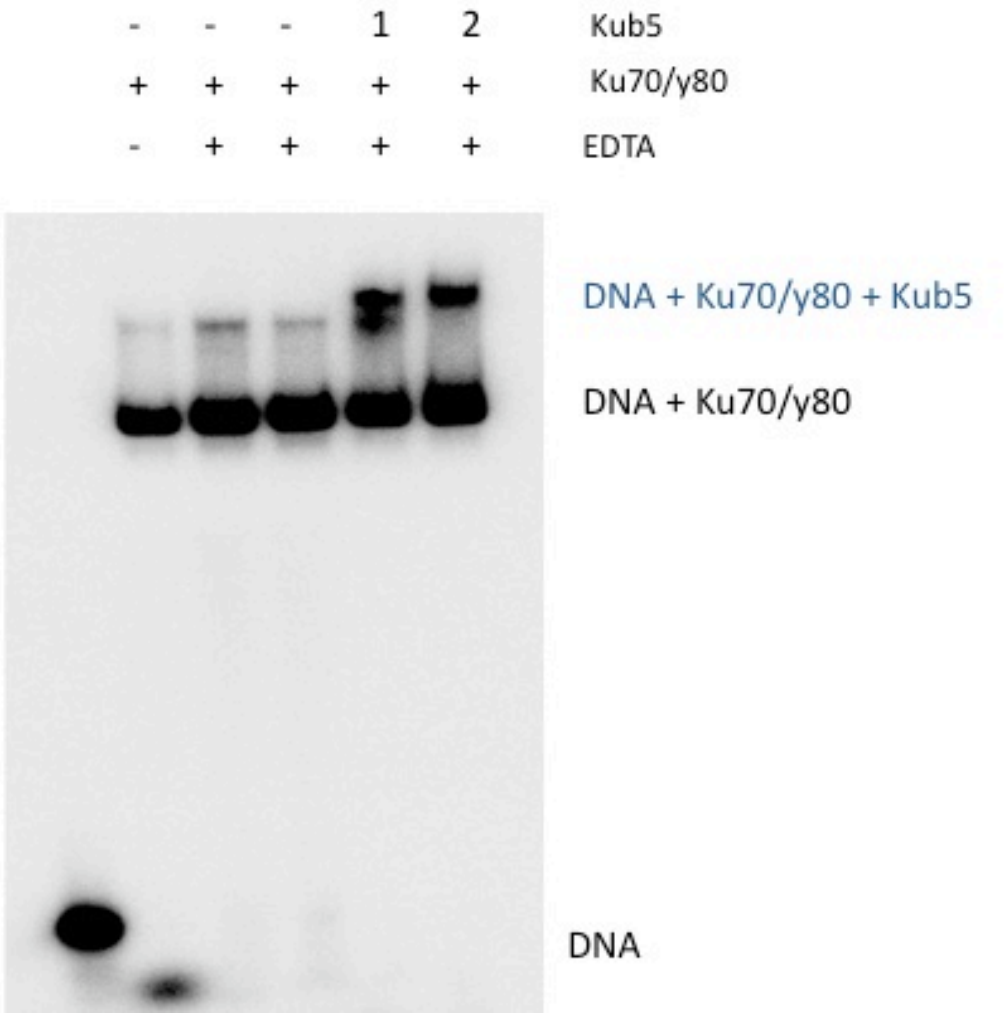

Figure 3.6 – **Gel Shift analysis confirms interaction of KUB5 and KU70 in the presence of DNA.** Radiolabeled DNA ends were conjugated to Ku70/Ku80. This was then allowed to incubate with purified KUB5 resulting in a MW shift, illustrating a DNA bound complex of Ku70/Ku80 and KUB5.

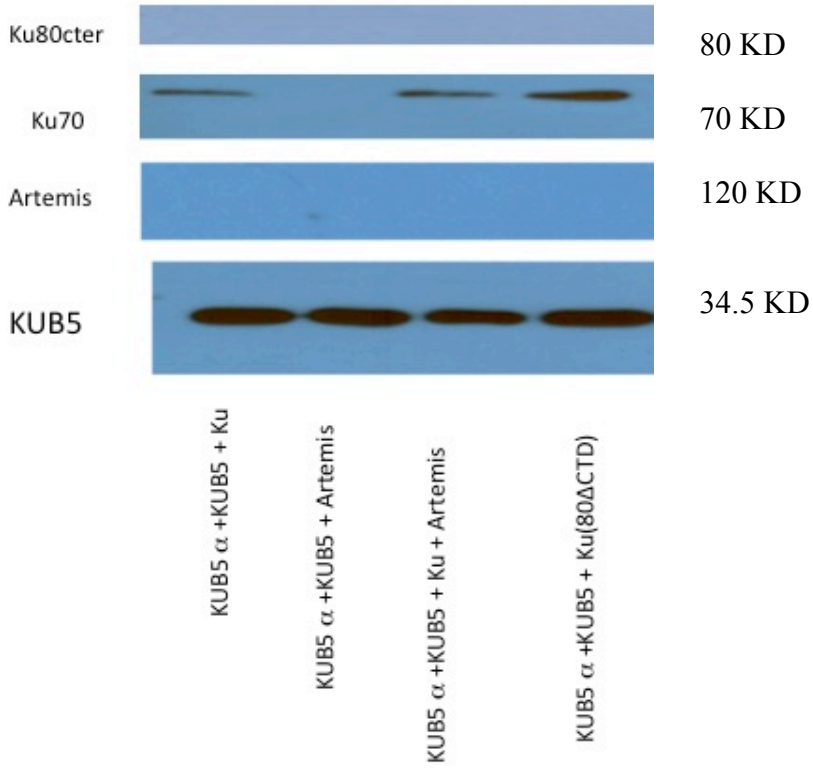

Figure 3.7 - **Pure protein Co-IPs reveal KUB5 interaction with Ku70.** Purified protein obtained from FPLC fractionation was used for immunoprecipitation using KUB5 monoclonal antibody. Purified Ku70, Ku80 and Artemis were supplied as a generous gift from Dr. David Chen laboratory. Proteins were run on SDS-PAGE gel and western blotted for KUB5 (34.5 KDa), Artemis (120 KDa), Ku70 (70 KDa) and Ku80 (80 KDa). Results indicate KUB5 direct interaction with KU70 and not Ku80 or Artemis by pure protein Co-IPs.

A

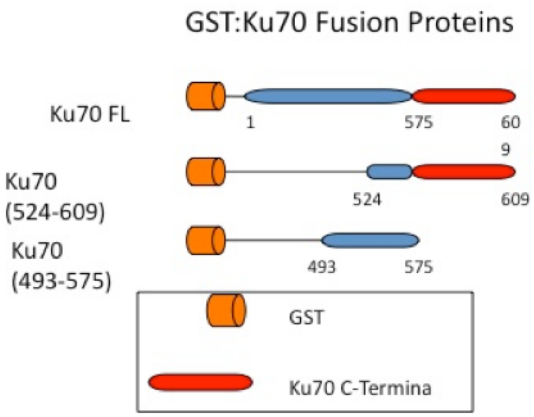

B

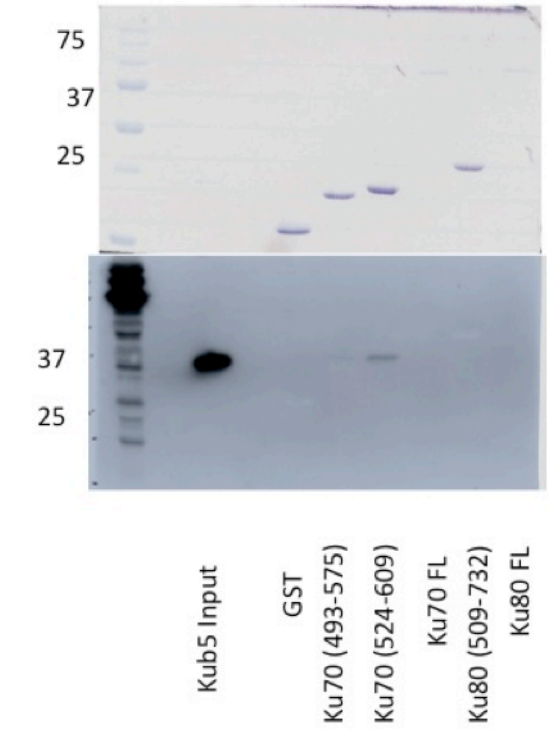

Figure 3.8 – **GST fusion proteins of Ku70 and Ku80 protein binding reactions with purified KUB5 revealed a dependence on Ku70 c-terminal domain for interaction of Ku70 and KUB5.** GST fusion proteins shown in A, were incubated with glutathione beads followed by incubation with Ni-NTA purified

KUB5 protein. Full-length Ku70 and full-length Ku80 proved too instable for interaction assays as proteins couldn't resolve on SDS-PAGE gel. In B, western blot analysis probing for KUB5 shows interaction of KUB5 with the c-terminal domain of Ku70, and not with any of the other GST fusion proteins.

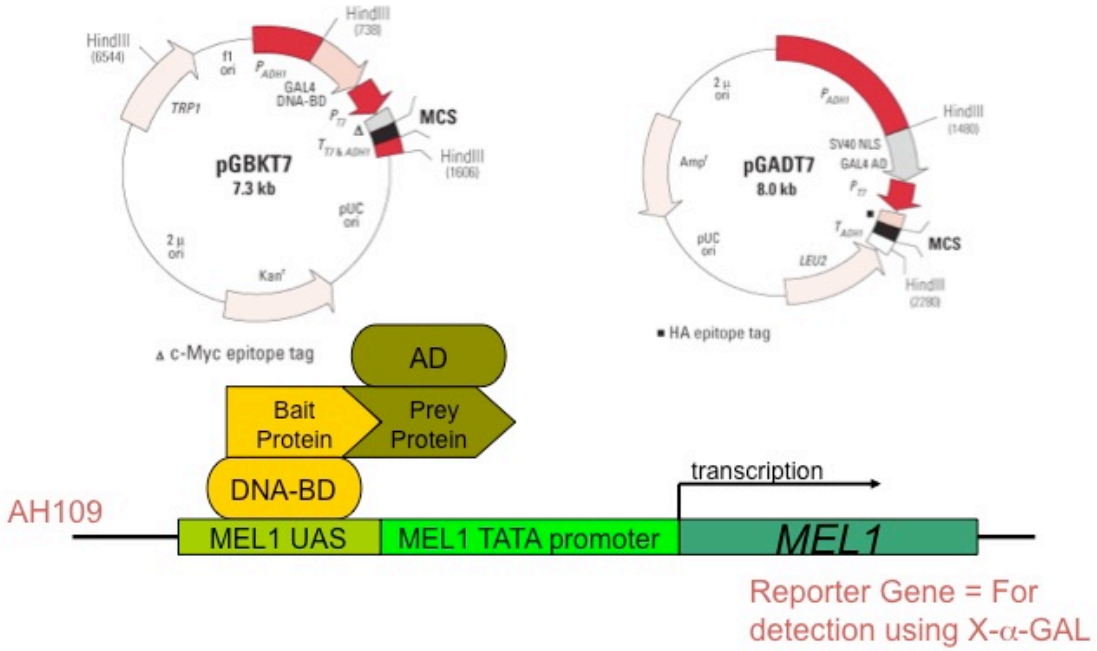

Figure 3.9: **Yeast Two Hybrid Experimental Design**. Due to the auto-activation phenomenon seen with Ku70, it was necessary to clone human Ku70 into pGBKT7 so it would not give false positive readings by X Gal treatment. KUB5/HERA was, therefore, cloned into pGADT7. The carrier yeast, AH109, contain both GAL4-responsive LacZ (for detection) and GAL4-responsive HIS3 (a selection marker) genes. Upon transformation of both plasmids into AH109, growth on (-Leu, -Trp) media indicates successful dual transformation. Stable transformants are then grown on plates containing a more stringent selection of (-His, -Leu, -Trp, -Ade) and subjected to on-filter β-galactosidase assays, using X-gal as a substrate yielding a positive reaction when colonies turned blue within first 120 min of incubation. Negative reactions when blue colonies were not observed indicate no association.

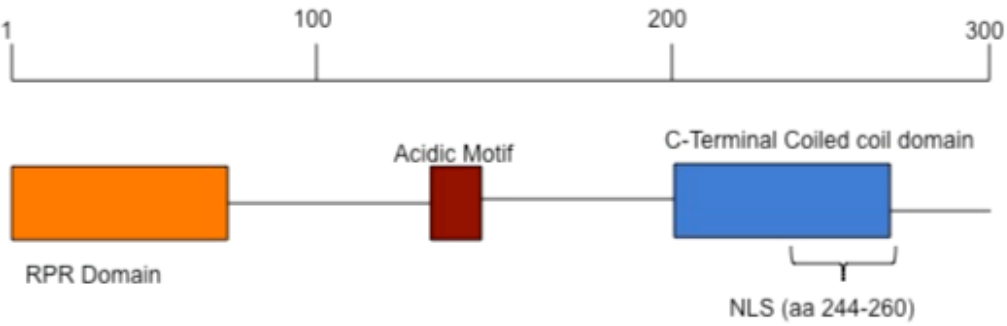

Figure 3.10: **KUB5/HERA Protein motifs of interest.** The KUB5/HERA human protein contains a c-terminal coiled-coil domain whose function is expected to be important in protein-protein interactions. Within this c-terminal domain also lies a putative nuclear localization sequence (NLS). Near the N-terminal region of the protein lies an RPR domain whose function could be important in RNA processing and transcription processes. Within this domain there is a Ser/Thr-Gln consensus sequence that could be regulated by PI3-like kinases such as ATM, ATR and DNAPK.

Mutation	-Leu-Trp	-His-Ade-Leu-Trp	X α Gal
pGBKT7(Ku70) + pGADT7(Empty)	+	-	-
pGBKT7(Lamin) +pGADT7(Large T-Antigen)	+	-	-
pGBKT7(p53) + pGADT7(Large T-Antigen)	+	+	+
pGBKT7(Ku70) + pGADT7(KB5)	+	+	+
C-Terminal Domain Alone	+	+	+
L276A	+	-	-
LL269,276AA	+	-	-
L269A	+	+	+
L269,273,276A	+	-	-
LL269,276PP	+	-	-
S19D	+	+	+
S19A	+	+	+
Q20A	+	+	+
Q21A	+	+	+

Table 3.1: **KUB5/HERA c-terminal domain deletion and point mutation L276A was sufficient to abrogate binding with Ku70.** The final lane in a) shows pGBKT7(Ku70) and pGADT7(KUB5/HERA) and the fact that the X Gal successfully turned the colony blue indicating direct interaction of the proteins. The table on the left b) indicates the different KUB5/HERA mutants and whether they appear to interact (+) or not (-) determined by their ability to grow on stringent selection media as well as X Gal activity. Point mutants were generated within the region of the coiled-coil such as L276A, L276A, as well as combinations of these mutations, LL269,276AA and LL269, 276AA. According to these data amino acid L276 is required for hKUB5 interaction with Ku70.

Y2H controls indicated in left showing not only selection on minimal selection media (-leu, -trp), but also showing the differential detection by X Gal. Negative controls include Ku70 alone in pGBKT7 and pGADT7-empty, as well as Lamin and Large T Antigen. Both sets of negative controls should not have direct interaction, therefore, should not turn blue when grown on X Gal containing media. The positive controls include pGBKT7 containing p53 and pGADT7 containing Large T Antigen. Here the proteins are known to interact, and this is confirmed by the appearance of the blue color when grown on X Gal-containing media.

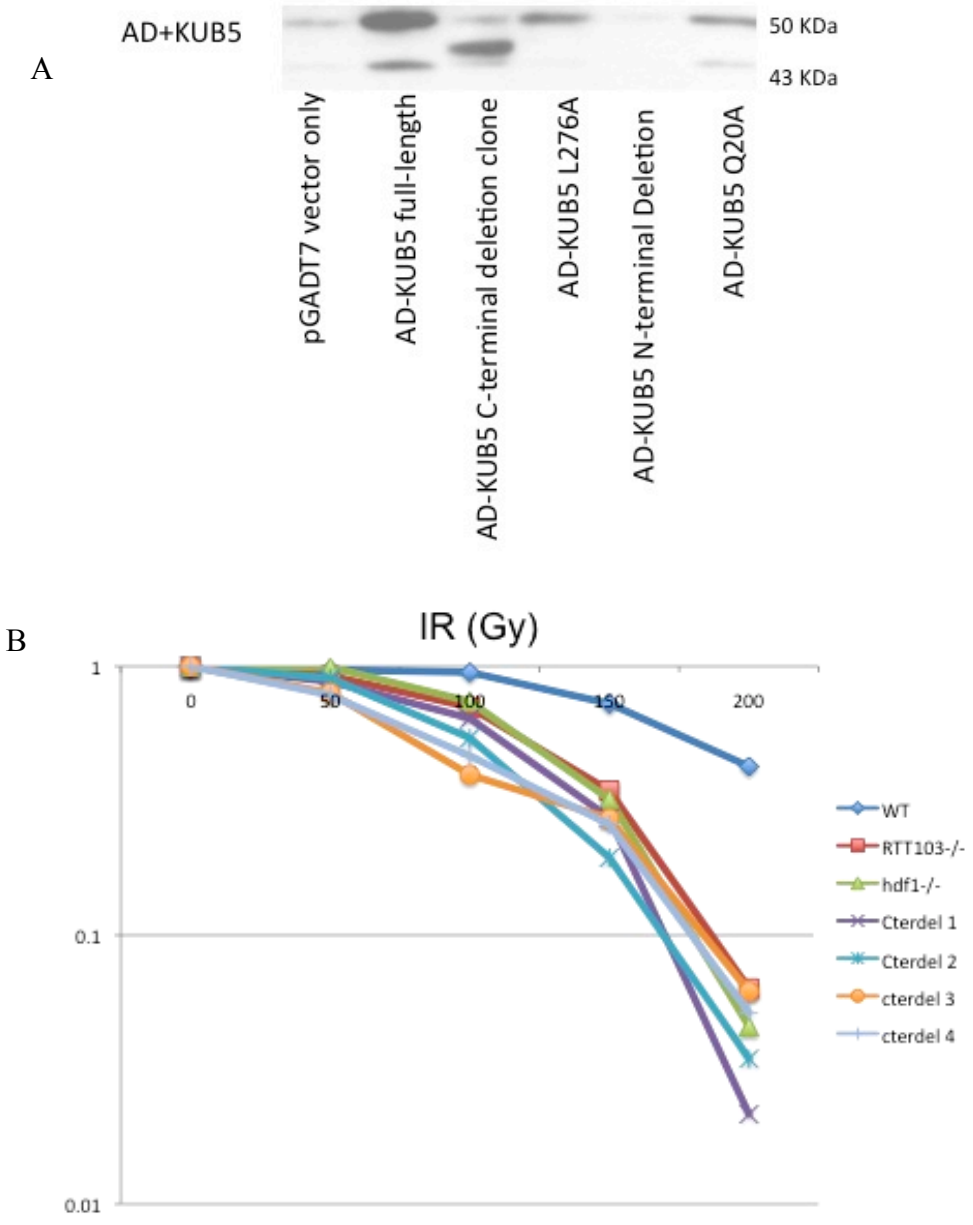

Figure 3.11: **C-terminal domain deletion in hKUB5/HERA also affects IR sensitivity.** A) Western blot showing protein expression in some of the Yeast 2

Hybrid reactions. Note Activation domain size of ~ 14 KDa is responsible for the offset of predicted molecular weight for hKUB5. Not all yeast used in experiment when probed with KUB5 antibody seemed to express the protein as in the case of n-terminal deletion. This could also possibly be due to antibody no longer recognizing protein, due to absence of epitope. In B) Human KUB5/HERA c-terminal deletion mutants were transformed into *RTT103-/-* yeast. Several clones were generated and tested for sensitivity to IR alongside wt*, hdf1-/- and RTT103-/-* yeast. IR Doses used were 0, 50, 100, 150 and 200 Gy. WT yeast showed relative resistance to IR, whereas the c-terminal deletion mutants, *hdf1-/-* and *RTT103-/-* mutants all showed similar increased sensitivity to IR.

IR 45 min - dark

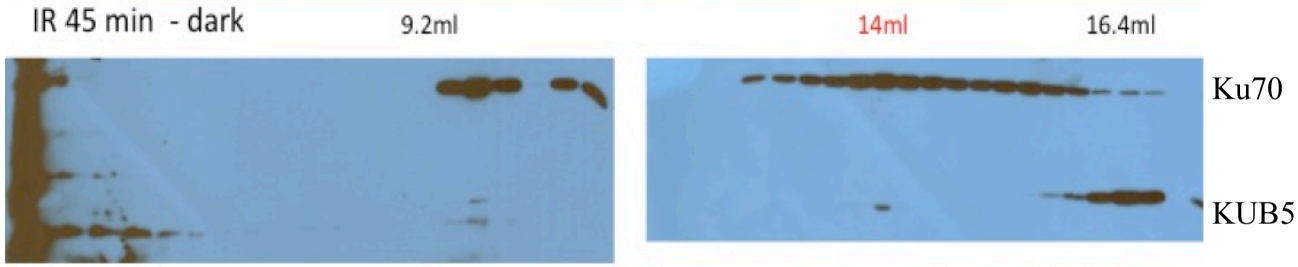

Protein Size	Volume Elute
669 KD	11ml
440 KD	12ml
150 KD	13.5ml
81 KD	14.5ml
43 KD	16.5ml

~1000 KD 660 KD — Potential transcription complex – dissociate for repair???

220 KD — KUB5/KU70/ Artemis??

115 KD — KUB5/KU70

40 KD — KUB5

Figure 3.12 – **Whole cell lysate factionation reveals KUB5 existance in several molecular weight fractions.** Whole cell lysates were prepared and separated into fractions by FPLC analysis. Fractions were collected and run on SDS-PAGE gel and western blotted for KUB5 and Ku70. Volumes collected correspond to MW fractions, 9.2 ml being 100 KD, 14 ml being 115 KD and finally 40 KD corresponding to 40 KD.

CHAPTER IV

Cells Survive KUB5 loss when p53 is mutant.

INTRODUCTION:

The p53 transcription factor plays an important role in the cellular response to stresses such as DNA damage and oncogene activation. Once a cell encounters DNA damage or stress, p53 is stabilized by phosphorylation allowing it to bind DNA resulting in transcriptional regulation of genes involved in DNA repair, cell cycle arrest, and apoptosis (91-93). In mice, loss of a single copy number for p53 results in increased cancer predisposition, likely due to loss of tumor suppression, which would normally be active to prevent accumulation of somatic mutations (94, 95). The role of p53 in apoptosis and genome protection has led to cancer therapies involving re-introduction of p53 in the cancers with mutant or loss of p53 function (96). WT p53 re-introduction into myeloid leukemia cells decreased cell viability and showed signs of apoptosis such as chromatin condensation and DNA fragmentation. In addition to lack of p53 showing importance in cancer formation, it also results in the ability of the cells to survive significant genetic mutations, loss of genetic regulation and genomic instability. This is supported by data showing genetic losses with early embryonic lethality being rescued by p53 mutation or loss. In the case of BRCA1 loss, the early embryonic lethality and cell dependence on this gene, made it difficult to study its function until a p53 null mutation was induced concurrently in the embryos, allowing partial survival in order to obtain BRCA1-/- MEF cell

populations (97). In this chapter, KUB5 loss in cancer cell lines will be investigated for affects on cell survival in order to test the hypothesis that KUB5 is a necessary gene for cell functioning, and maintenance of genomic stability. In addition to these studies, concurrent transient knockdown of KUB5 in MEFs deleted in various DNA repair proteins may be able to suggest a pathway KUB5 might be involved.

RESULTS:

Transient knockdown of KUB5 was achieved by siRNA oligos designed to the 5' un-translated region of the KUB5 gene. Transfection resulted in efficient knockdown of KUB5 protein, in several cell lines as shown by western blot (Figure 4.1). RKO7 parental and several other sublines including RKO7 shp53 were monitored after transfection for doubling time alterations by growth assays. Interestingly, RKO7 parental cells appeared to show a sharp early decline in population doubling compared to that of RKO7 shp53, which growth appeared unchanged by the knockdown (Figure 4.2). Further analysis of this phenomenon by western blot showed that parental RKO7 cells, after siRNA knockdown of KUB5, appeared to show phosphorylated p53 at Serine 15 (Figure 4.3). This stabilization of p53 in these parental cells could be the reason these cells are unable to survive upon KUB5 knockdown. These data show that after KUB5 knockdown in wild-type p53 background, cells are likely dying through a p53 dependent pathway. Conversely, in the RKO7 cells with shp53, the cells survive, likely due to a lack of p53 signaling which would have otherwise caused cell death(98-102). This fact, could allow for the possibility of KUB5 modification in cancer that would only be possible in cells or tumors where p53 activity is down-regulated allowing damaged cells, by means of accumulated DNA damage due to loss of KUB5, to survive and bypass cell cycle arrest and apoptosis.

The immortalization process of generating mouse embryonic fibroblasts (MEFs) involves spontaneous mutation within the p53 pathway(103-105). It is due to this, mutant p53 pathway, that siRNA to KUB5 was transfected into wild-type MEFs and the cells survive (Figure 4.4a). The laboratory of Dr. Sandeep Burma has generated several MEF cell lines with genetic alterations in DNA damage sensor and repair proteins. MEFs treated with siKUB5 and deleted in DNAPK as well as those deleted in Ku80 were able to survive knockdown (Figure 4.4b and c). Interestingly, in the ATM-/- MEFs, siKUB5 resulted in complete stalling of cell doubling (Figure 4.4d). The cells appeared to swell and maintained adherence to dish throughout the time points selected, however no population growth was seen. ATM deficient cells already display abnormal G1 and G2 checkpoint response, and are deficient in HR (106), so when the addition of a KUB5 knockdown, these cells, have even more trouble in repair. Also, due to the bypass of the checkpoint by both los of ATM and p53, these cells are unable to induce apoptosis, and are likely stalled or senesced. Finally, in MEFs deficient in Ku70, concurrent transient knockdown of KUB5 by siRNA resulted in a clear cell death (Figure 4.4e). Here, unlike in the case of ATM-/- with siKUB5, the cell growth line turns negative, below that of the starting cell number, indicating cell death. After siKUB5 treatment, the cells can be seen floating in the media and are no longer adherent. This strong response to the dual knockdown of Ku70 and KUB5 could be due to the fact that perhaps upon Ku70

loss the pathway more depends on Ku70, and conversely upon KUB5 loss, the pathway depends more on Ku70. Therefore, when both proteins are lost, this creates a detrimental problem for the cells, with a complete inability to survive even in the absence of a functional “apoptosis inducing” p53 pathway.

DISCUSSION:

Heterozygous KUB5 +/- mice were purchased and timed mated in order to create a colony of homozygous KUB5-/- mice to study the effects of loss of KUB5 *in vivo*. The hypothesis was that, like other mice with severe DNA repair defects, these KUB5 -/- mice would be at an increased risk of developing early onset lymphomas due to genomic instability resulting from the accumulation of un-repaired DNA damage. The generation of KUB5-/- mice in this manner proved impossible without additional genetic manipulation due to the early embryonic lethality of homozygous KUB5 deletion mice. The lethality occurred too early for KUB5-/- MEFs to be isolated, indicating importance and dependence of KUB5 expression in early embryonic development. The data presented in this chapter supports these results further by showing that a loss of KUB5 is lethal to the cells, unless p53 is mutant, or null. In these experiments, normal RKO7 cells transiently knockdown for KUB5 by siRNA showed significantly decreased survival initially, at the time points corresponding to the greatest knockdown of KUB5. Later time points, when KUB5 was beginning to be re-expressed, cells overcame lethality and survival improved. Interestingly, knockdown of KUB5 in shp53 RKO7 cancer cell lines did not have the same effect on cell survival, in fact there appeared to be no effect and the cells survived. This is also reported in the case of loss of BRCA1, perhaps KUB5 loss requires concurrent loss of p53 function in order for the cells to survive. This is due to the ability of the cell to

bypass normal cell cycle checkpoints and apoptosis triggers when p53 is null. Unfortunately, in terms of cancer, this could be a reason why tumors are able to survive genetic instability and loss of important cellular factors, even those involved in DNA repair. In these cases, losing p53 activity and making the cells impermeable to the adverse affects of accumulated DNA damage is a survival mechanism. Under normal functioning p53, DNA damage would normally be repaired by functional HR, NHEJ, or even result in apoptosis, all of which would be unfavorable to a tumor.

The experiments involving transient knockdown of KUB5 in MEF cells was made possible by the inherent mutant p53 status created during generation of the immortalized MEF cell lines allowing the WT MEF cells to survive KUB5 transient knockdown by siRNA. As a generous gift from the laboratory of Dr. Sandeep Burma, several MEF DNA repair protein knockout MEF cell lines were donated including DNAPK-/-, Ku80-/-, ATM -/- and Ku70 -/-. The hypothesis was that KUB5 is involved within the pathway of NHEJ, therefore studying the dual KUB5 and NHEJ protein knockdown, could give valuable insight into where in the pathway KUB5 is acting. Interestingly, in Ku70-/- MEFs, KUB5 transient knockdown resulted severely decreased cell viability, ultimately resulting in complete detachment of cells from plate indicating either apoptosis or necrosis. Interestingly, this cell death occurred in a p53 mutant MEF cell line, indicating cell death occurred independently of p53. This result could indicate that KUB5

and Ku70 lie in parallel pathways involved in NHEJ, and when both are lost, this results in a complete inability for the cells to repair DSBs, resulting in cell death. This idea is supported with evidence that loss of NHEJ by inhibition or mutations of several known factors including DNA-PKcs, Ku, DNA ligase IV and XRCC4 results in delayed processing of DNA breaks, however repair still takes place, though much slower than traditional NHEJ. This evidence allows for the possibility of an alternative DNA DSB repair pathway (107). In the case of ATM-/- MEFs, upon KUB5 transient knockdown the cells exhibited a senescent morphology. Known results of ATM loss are genomic instability and cancer predisposition (108). This result could be due to an additive effect of loss of both detection of DSBs and repair of DSBs, and since p53 is mutant in these cells, they undergo a senescent phenotype to avoid apoptosis (109).

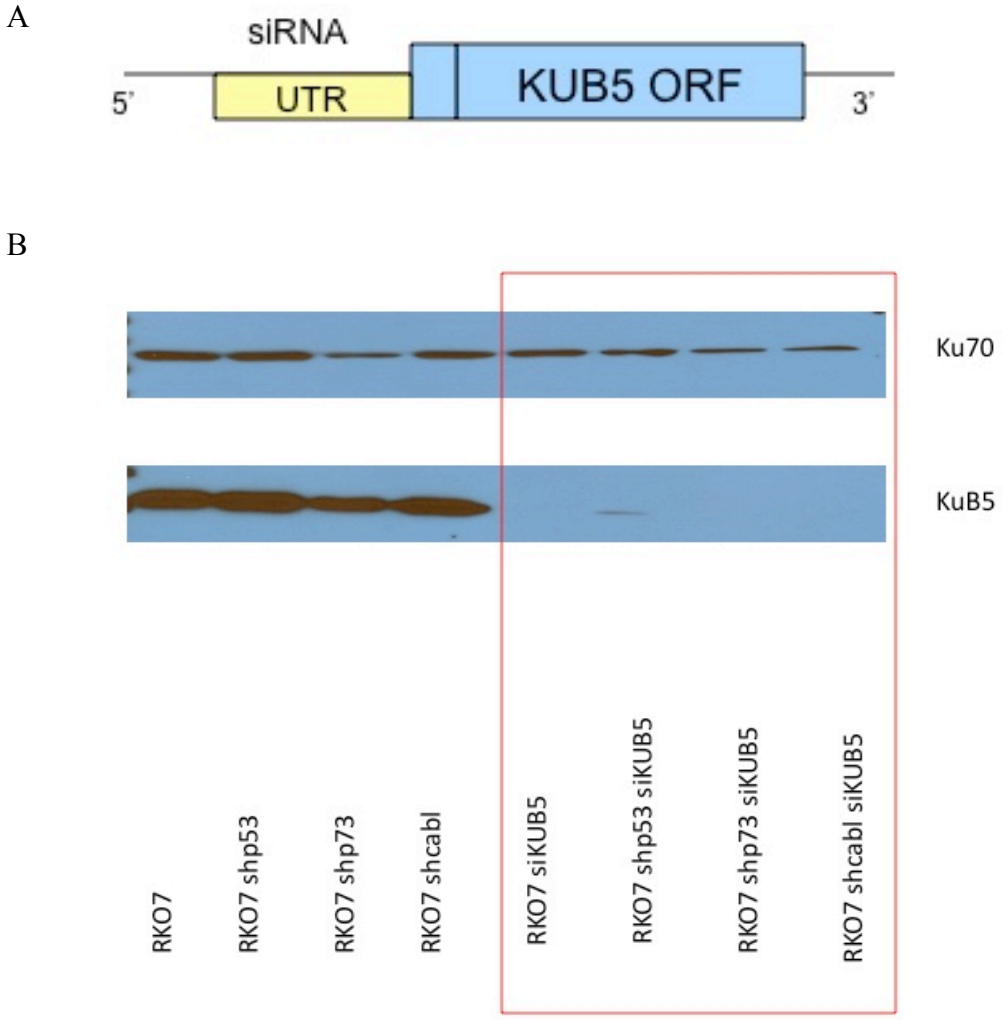

Figure 4.1 – **iRNA to KUB5 sucessfully knocked down KUB5 protein levels.** Transient transfection of siRNA to 5' un-translated region of KUB5 gene resulted in efficient knockdown of KUB5 protein. A) Schematic representation of siRNA design for 5' untranslated region of KUB5 gene. B) Western blot showing successful KUB5 knockdown in RKO7 cell lines both parental and shp53.

A

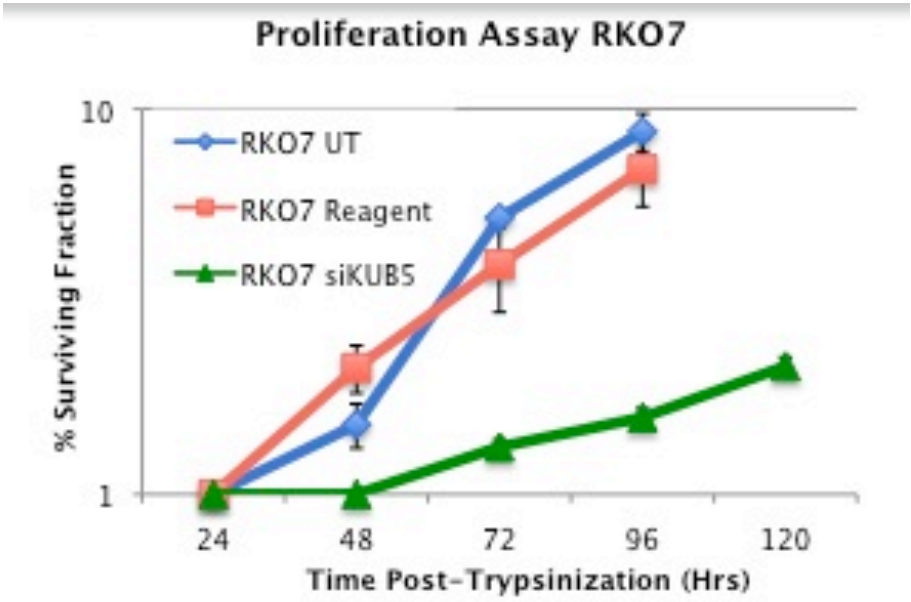

B

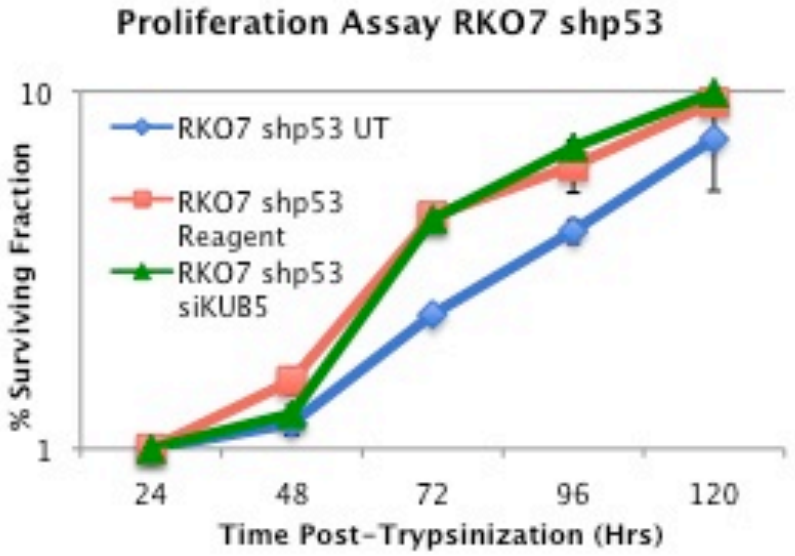

Figure 4.2 – **Transient knockdown of KUB5 resulted in death in cells with functional p53.** Survival curve post-transfection for A, ROK7 parental and B, RKO7 shp53. Cells could only survive loss of KUB5 if p53 is concurrently lost. Transfection reagent alone had no affect on cell survival.

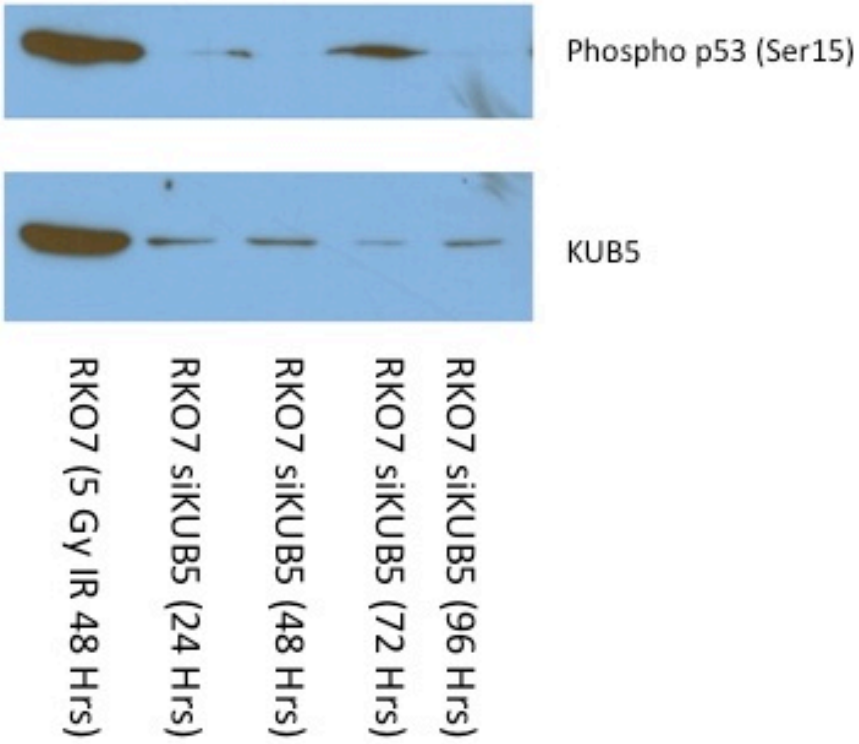

Figure 4.3 – **Transient KUB5 knockdown resulted in phosphorylation of p53 (Ser15) at 72 hours.** Whole cell protein lysates from RKO7 cells treated with siRNA and media replaced two days after transfection. Protein samples were taken at the following time points after media replacement: 24, 48, 72, and 96 Hrs, therefore a sample taken at 24 hours, corresponds to 72 hours post-transfection with siRNA oligos. Protein was run on SDS-PAGE and western blotted for KUB5 and Phospho-p53(Ser15). KUB5 blot showed efficient KUB5 knockdown by 24 hours post- transfection.

A

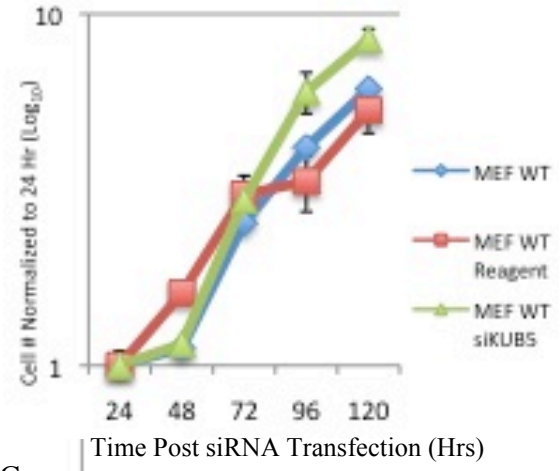
10
1
Cell # Normalized to 24 Hr (Log10)
24 48 72 96 120
Time Post siRNA Transfection (Hrs)
MEF WT
MEF WT Reagent
MEF WT siKUB5

B

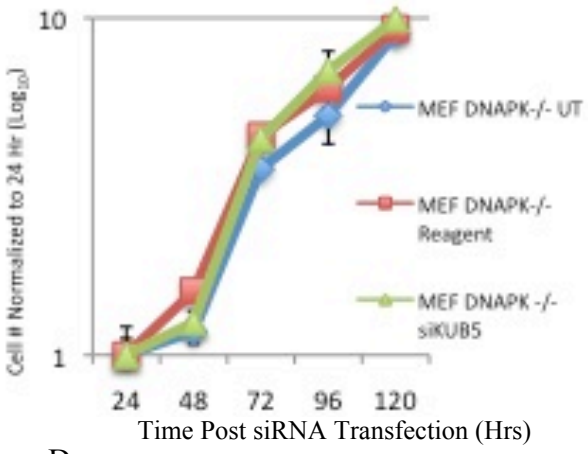
10
1
Cell # Normalized to 24 Hr (Log10)
24 48 72 96 120
Time Post siRNA Transfection (Hrs)
MEF DNAPK-/- UT
MEF DNAPK-/- Reagent
MEF DNAPK -/- siKUB5

C

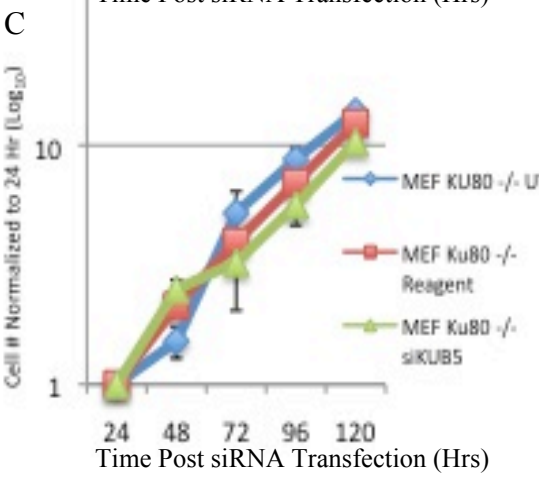
10
1
Cell # Normalized to 24 Hr (Log10)
24 48 72 96 120
Time Post siRNA Transfection (Hrs)
MEF KU80 -/- U
MEF Ku80 -/- Reagent
MEF Ku80 -/- siKUB5

D

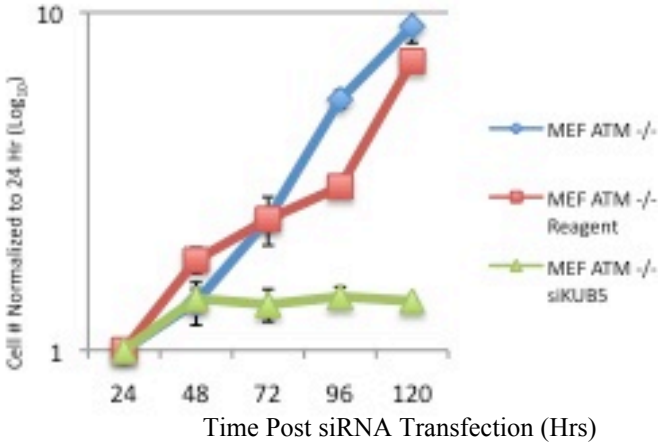
10
1
Cell # Normalized to 24 Hr (Log10)
24 48 72 96 120
Time Post siRNA Transfection (Hrs)
MEF ATM -/-
MEF ATM -/- Reagent
MEF ATM -/- siKUB5

E

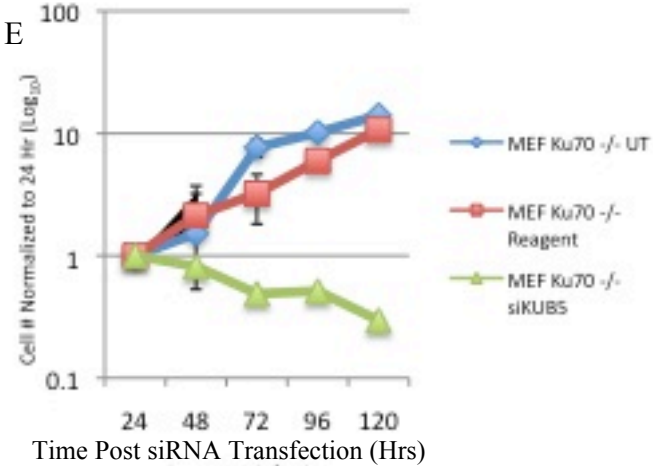
100
10
1
0.1
Cell # Normalized to 24 Hr (Log10)
24 48 72 96 120
Time Post siRNA Transfection (Hrs)
MEF Ku70 -/- UT
MEF Ku70 -/- Reagent
MEF Ku70 -/- siKUB5

Figure 4.4 – **KUB5 knockdown in MEFs cells lacking Ku70 or ATM result in changes in cell survival.** Transient knockdown of KUB5 was carried out using siRNA and cells were counted 24, 48, 72, 96 and 120 hours post-transfection. In A), siRNA to KUB5 was transfected into wild-type MEFs. In B), DNAPK -/- MEFs were treated with siKUB5. In C), siKUB5 transfected into Ku80 -/- MEFS. In D), ATM-/- MEFs were transfected with siKUB5. And finally in E), MEFs deficient in Ku70 were transfected with siKUB5 oligos. Cell survival was determined by counting cell number after 0, 24, 48, 72, 96 and 120 hrs post siRNA treatment. Experiments were carried out in triplicate and repeated at least three times. Standard error is reported.

CHAPTER V

KUB5/HERA Involvement in Breast Cancer Chemo- and Radio-Resistance

INTRODUCTION:

Importance of DNA Repair in Disease. Chemo- and radio-therapies can be common and fairly efficacious treatments for most early stage human breast cancers, though unfortunately, many patients present with advanced disease. Treatment of metastatic breast cancer remains a very challenging goal. It is, therefore, important to understand the molecular events that occur in both the tumor and surrounding normal tissues to exploit cancer cell differences that may enhance the efficacy of therapy. Comparative genomic hybridization studies (CGH) studies in human breast cancers suggested an increase in copy number at locus 20q11-13.2. Since hKUB5/HERA is located within this region (110, 111), these data suggested the possibility that KUB5/HERA was amplified in breast cancers and derived breast cancer cell lines. Since shRNA or siRNA knockdown of KUB5/HERA expression increased sensitivity to IR and other chemotherapeutic agents (Chapter 3 and 4), minor changes in copy number (provided this correlated well with protein levels) may correspond and correlate with sensitivity (low levels) or radio-resistance (elevated levels). Its over-expression could result in an increased capacity for DSB repair via non-homologous end joining (NHEJ) due to its interaction with Ku70, and therefore, result in resistance to chemotherapy and/or radiation-induced DNA damage. Since NHEJ is error-prone, another consequence of altered levels of KUB5/HERA could be causative for genomic instability. The overall goal of my

work was to examine KUB5/HERA expression in breast cancer cells and correlate the expression of this single gene with radio-sensitivity. Based on these observations, I hypothesized that understanding KUB5/HERA expression and functions will be key to the development of new treatments to enhance chemo- and radio-sensitivities of breast cancer cells.

Drug Resistance and DSB Repair. Chemotherapy and/or radiation therapies play vital roles in the treatment of breast, as well as all cancers. Several drugs are commonly used in the treatment of advanced breast cancer disease. These include cisplatin, as well as the drug combinations CMF (cyclophosphamide/methotrexate/5-fluorouracil) and more recently, TAC (docetaxel/doxorubicin /cyclophosphamide). These drug combinations benefit only 15% of patients with favorable responses, including occasional complete remissions. However, a significant number of women experience relapses, with an average survival of 2 years (112). New treatments involving monoclonal antibodies, such as trastuzumab, have been used in the for HER2/neu-positive breast cancer, however, these therapies are limited by the fact that only a fraction of patients benefit. This monoclonal antibody treatment, as well as chemo- and radiotherapies, have a common problem: the emergence of resistance to therapy (112). Thus, there is a clear need for additional understanding of the molecular mechanisms responsible for resistance to therapy, as well as development of strategies to modulate resistance to provide more efficient treatment for patients.

Breast cancer drug resistance could result from one or a combination of several factors, including tumor micro-environmental changes, drug metabolism, drug target modifications, apoptotic mechanisms, and finally DNA repair. The hypothesis to be tested by this proposal is that increased or altered DSB repair capacity is mediated by over-expression of a novel Ku70 binding protein, KUB5/HERA. Since KUB5/HERA levels appear to be much lower than those of Ku70, it is possible that KUB5/HERA levels are rate limiting and determine DSB repair capacity in cells. Thus, expression of KUB5/HERA could be a molecular determinant for chemo- and radio-resistance in breast cancer cells and tumors *in vivo*.

NHEJ in breast cancer. Increased breast cancer risk has been reported to be associated with single nucleotide polymorphisms (SNPs) in the NHEJ genes Ku70 and XRCC4 (46). Deficiencies in any one of these genes can predispose individuals to breast cancer with altered DNA repair processes, creating resistance to chemo- and/or radiotherapies. The tumor suppressor gene, BRCA1, is linked to inherited breast cancer and has been documented to participate in several cellular processes, including chromatin remodeling, DNA repair (HR and NHEJ(in yeast)), cell-cycle control, and apoptosis (113). There is growing evidence to suggest that BRCA1 is involved in, or regulated by, NHEJ and is important in maintaining genomic stability in yeast (114-116). Research using BRCA1 mutant MEFs indicate a deficiency in end-joining activity, providing evidence for the possible contribution of NHEJ to BRCA1-related breast cancer

development(117-124).

MATERIALS AND METHODS:

Colony Formation Assays (CFAs). CFAs were performed as described (125, 126); log-phase breast cancer cell lines were cultured in DMEM supplemented with 5% FBS. Cells were counted and 10^3 cells plated in 3 cm dishes and allowed to adhere overnight. Treatment by IR, UV or various drugs and DNA damage agents were performed 24 h post-plating as indicated below. The doubling time of MDA-231 cells was determined to be ~26 h, therefore, 5-7 days was allowed for colonies to form >50 normal appearing cells (in controls) for staining. After 7-10 days, plates were washed 2X with phosphate buffered saline (PBS) and plates were fixed/stained in crystal violet/methanol as described (125). Colonies were counted under a dissecting microscope to calculate those with $\geq$50 normal appearing cells. Large senescent-like colonies were excluded and only viable colonies scored. All experiments were normalized to the untreated controls and performed a minimum of three times. Statistical analyses of the data were performed using Student's T tests and p values reported.

shRNA Transfection: Media from shKUB5 lenti-virus producing cells and 10 μg/ml polybrene was added to plates and incubated overnight to improve infection efficiency. Lenti-containing media was removed and replaced with fresh DMEM. Cells were grown 48 h before Puromycin containing selection media were added. Selection was carried out for ~4 days until parental cells (un-

infected) were killed off. Colonies were isolated from pooled knockdown pooled populations by serial dilution in 96 well dish as needed. Puromycin selection (1 μg/ml) was maintained on pooled and clonal populations for 3 weeks after confirmation of clones (parental cells die off). Responses in pooled populations were also examined in CFAs as descried above. In all experiments, cells were not incubated with antibiotics, and cells were grown for at least 24 h prior to initiating any experiments with clones or pooled populations. SCR cells had a doubling time of 26 h and shRNA-KUB5/HERA had doubling times only slightly slower of 28 h for clone 11 and 26 h for clone 2.

Foci formation as a measure of DNA damage using immunohistochemistry (IHC): DNA foci formation for various DSB repair factors was performed using log-phase human MDA-231 breast cancer cells grown in DME medium as described above as previously described. Briefly, UV sterilized cover slips in dishes were overlaid with approximately 10^3 cells in 100 μl of media, followed by the addition of an additional 3 mls media over top. Cells were allowed to adhere to cover slip overnight. The next day, cells were treated with 1 Gy ionizing radiation using a Mark I cesium X-ray generator. Covers slips were removed and fixed in 2% sucrose and 3% paraformaldehyde in PBS for 5 minutes at room temperature at time points 0, 0.25, 0.5, 0.75, 1, 1.25, 1.5, 1.75 and 2 h. Cover slips were washed in PBS 3X and suspended in Permeabilization buffer (0.5%

Triton, 20mM HEPES, 50 mM NaCl, 3 mM $MgCl_2$ and 300 mM Sucrose in sterile water) and chilled on ice for 30 mins. Cover slips were washed 3 X in PBS and then placed face down in 100 μl blocking buffer (5% FBS in PBS) on parafilm and allowed to sit for 20 min at RT. Cover slips were washed 1X in PBS and then turned facedown in 100 μl aliquot of primary antibody H2AX (1:1000 in PBS) for 1 Hr. Cover slips were washed in PBS 3 X and then laid face down in 100 μl secondary antibody (stock: 2 μl Hoescht, 10 μl fluorescent secondary antibody 10 ml PBS) for 30 min in the dark. Cover slips were washed 3X in PBS and mounted face down on microscope slides in vectashield and sealed with clear nail polish. Experiments were performed three independent times in duplicate and data were analyzed using Student's T tests. p values were reported as indicated.

Comet Assays. MDA-MB-231 breast cancer cells (10^6cells/10 mm dish plate) were plated and allowed to grow for 24 h. Cells were then treated with DNA damage agents, UV or IR as indicated. Low melting point agarose was warmed up (1% solution in water) and kept at 37 ^oC. Cells after collected at time point were scraped and washed with PBS. Cells were re-suspended in 1 ml PBS and 15 μl counted. The calculation Counted cell number/4x10,000=cell number/ml X ml = total number was used. Cells were diluted to 300 cells/μl and 25 μl added to 250 μl warmed agarose and immediately 75 μl of mixture was added to each comet slide circle making sure that no bubbles or gaps remain. The slides were

then places in the dark at 4 ^{o}C for 30 minutes or until 0.5 mm clear ring appears around edge of agarose on slide. Slides were immersed in pre chilled lysis solution (Trevigen) and kept at 4 ^{o}C for 1 h. Excess buffer was then removed and slides were placed in Alkaline solution (300mM NaOH, 1 mM EDTA and ddH2O) for 1 hour in dark at RT. Slides were then washed in 1XTBE buffer and placed in a horizontal electrophoresis chamber. The electric current was supplied to the slides for 10 minutes in cold room at 1 volt per cm (23 volts or 4 mA). Samples were removed and air-dried overnight in dark at RT. Before imaging 50 µl SYBR Green I solution (1 µl in 10 ml TE buffer) was added to each dried agarose circle. (TE buffer: 10mM Tris-HCl, 1 mM EDTA) SYBR GreenI's maximum excitation and emission are 494 nm/512nm. Foci/nuclei were calculated and experiments were performed three independent times in duplicate. Data were analyzed by Student's T tests and p values were calculated as appropriate.

Isolation of human mammary epithelial cell (HMEC) populations. Fresh patient fibroadenoma samples were obtained from the Tissue Procurement Shared Resource (UT Southwestern Simmons Cancer Center) and logged into the appropriate database. Tissue was minced using razor blade and collagenase digested (1µg/ml collagenase in MEGM media) overnight at 37 ^{o}C under rotation. The next part of the protocol used centrifugation to separate fibroblast cells from

epithelial. Here the cells are spun at 80 x G for 30 seconds, this is considered step 1. The supernatant is removed and further spun at 200 x G for 3 minutes. Again supernatant is removed and spun at 3500 x G for 5 min. The pellet from this spin is mainly fibroblasts and can be grown in DMEM media with 10% FBS. The pellet resulting from the 200 x G spin is washed in PBS and 1 ml trypsin added and incubated for 3 minutes at 37 ^{o}C. 10 ml TNS is added and spun at 1000 RPM and cells plated on MEGM media (this population is mostly epithelial and minor fibroblast mix). The pellet obtained from the initial spin in step 1 is washed in PBS and 3 ml trypsin added. Similar to the pellet treatment before TNS is added and the cells plated on MEGM media. Over the course of 3-5 weeks the cells will be short trypsinized (trypsinization for 30 seconds, monitor by microscopy when fibroblast cells begin to pull away from plate) and re-plated in an attempt to remove all contaminating fibrobasts from cellular mix as fibroblasts are more sensitive to trypsin than epithelial cells.

Subcutaneous Injection of MDA-231 in Mice Using sterile technique, nude mice were injected with MDA-MB-231 (SCR and shKUB5) cells. Cells were trypsinized and counted into a final volume concentration of 10^6 cells/ 100 μl. 70% alcohol was used to sterilize the site of injection and a 23-gauge needle was placed just under the upper skin (Sub-cutaneous) to inject 100 μl of the cell suspension. Tumor growth was monitored over time by palpation, then by caliper

measurements. Tumor volumes in mm^3 were reported over time for 5 animals per group (SCR and shKUB5). Mice were sacrificed when tumor volume reached 10 mm^3 and tumors removed for IHC.

Bioluminescence (BLI). To image mice they need to be placed in the sleeping chamber. The CO_2 tank should be on and the Isofluorane set to 2.5. Pre-mixed luciferin solution was mixed at 2.5mg/100μl concentration in sterile PBS and filter sterilized under hood. Each mouse was injected with 100μl luciferin solution behind neck under skin. Protocol carried out as stated (126, 127).

KUB5 antibody purification for IHC analysis – KUB5 antibody was first generated from lab hybridoma strain. Media from cells was collected and used in a Melon Gel Purification Kit to purify KUB5 monoclonal antibody. 4 mls of Melon IgG beads were washed in Melon Regenerant buffer. After spinning at 1000XG supernatant was removed and hybridoma added to beads. Beads and hybridoma mixture was allowed to rotate at 4 ^oC for 4 hours. Beads were spun down again at 1000xG and washed with regenerate buffer. Gel Purification buffer was then assed to appropriate volume needed for antibody concentration, for KUB5 4 mls. Solution and beads was rotated at 4 ^oC for 1 hour and supernatant removed and frozen down in 50 μl aliquots to -80^oC.

RESULTS:

Homozygous deletion of KUB5/HERA was early embryonic lethal at less than 8 days not permitting the generation of KUB5/HERA-/- MEFs. Since KUB5/HERA knockdown cells showed hypersensitivity to IR, I performed studies using heterozygote KUB5/HERA murine epithelial fibroblasts (KUB5/HERA+/- MEFs). Figure 5.1a shows a representative western blot analyses of KUB5/HERA MEF+/+ and MEF +/- cells with two different amounts loaded (30 μg and 15 μg). KUB5/HERA protein expression in KUB5+/- MEFs appeared half the level of wild-type KUB5/HERA (+/+) cells. Ku70, Ku80 and tubulin levels were unchanged with the loss of a single copy of mouse KUB5/HERA. Interestingly, in KUB5/HERA+/- MEFs, p53 was phosphorylated at Serine 15, suggesting the presence of endogenous DNA damage and potential genomic instability within these cells. The doubling rate of both KUB5/HERA+/+ and KUB5/HERA+/- cells was 18 days. KUB5/HERA+/+ and +/- MEFs were then treated with various doses of IR (0, 1, 2, 3, 4, 5 Gy) and survival was measured by cell number count and colony forming assays (CFAs) (Figure 5.1b, CFA results). KUB5/HERA +/- MEFs showed significantly increased sensitivity to IR compared to wt KUB5/HERA+/+ cells. These data support our previous findings, and the hypothesis that loss of KUB5/HERA confers increased sensitivity to DNA damage from IR.

Results from transient KUB5/HERA knockdown in RKO7 parental and

RKO7 shp53 summarized in chapter 4, suggested that p53-mediated cell arrest and cytotoxicity responses could prevent isolation of stable knockdown cells, consistent with the embryonic lethality of KUB5/HERA-/- mice. To further study KUB5/HERA function in human breast cancer cells, mutant p53-expressing MDA-MB-231 cells were generated with stable shRNA-KUB5/HERA knockdown. Cells were generated using shRNA generated to the 5' un-translated region of the human KUB5/HERA gene using Lenti-virus with Puromycin-resistance ($Puro^R$) as a selectable marker (vector made by Tomoyuki Mashimo, PhD). Control cells were transfected with shRNA-Scr under $Puro^R$. $Puro^R$ cells were analyzed by western bloting for KUB5/HERA expression (Figure 5.2a). Clones 2 and 16 showed no significant knockdown, whereas clones 4 and 11 showed significant KUB5HERA protein knockdown compared to parental and scrambled (SCR) MDA-231 cells. KUB5/HERA knockdown did not affect Ku70 protein expression similar to data obtained from previous studies of loss of KUB5 in RKO7 and MEF cells. CFAs were employed to study the hypersensitivities of these clones to IR (Figure 5.2b). Radiation sensitivity curves of the clones indicate that the clones with the highest KUB5/HERA protein knockdown (i.e., clones 4 and 11) exhibited the greatest increase in IR sensitivities versus clones 2, 16, and parental and SCR MDA-MB-231 cells. This radiation sensitivity was similar to that observed previously when studying yeast deficient in RTT103. The hypersensitivity could be due to either a higher endogenous DNA damage as

a result of improper or lack of repair of normal DNA damage resulting from DNA replication, or other normal endogenous processes that, upon damage, becomes cumulative and difficult for the cell to repair. This theory was tested by measuring DNA damage by the activation and phosphorylation of DNA damage sensors at DNA lesions. Analyses of DNA damage monitored by γ-H2AX foci DNA damage detection and repair was carried out as indicated (128). For this experiment, DNA damage foci created by γ-H2AX phosphorylation at serine 15 were imaged by fluorescence microscopy after IR treatment. These data are summarized in Figure 5.3a and 5.3b. Here, KUB5/HERA knockdown clone 2 (showing normal KUB5 levels) and clone 11 (showing significant KUB5 protein knockdown by western blot) were treated with 1 Gy and fixed for immunohistochemical (IHC) analyses at various times (t=0, 0.25, 0.5, 0.75, 1, 2, 4, 6, 7, 12, 24 h) post-IR treatment. Cell nuclei were counter-stained with blue fluorophore by DAPI. Green foci corresponded to γ-H2AX, and showed DNA damage detection by H2AX phosphorylation as a result of the activation of Ataxia telangiectasia mutant kinase (ATM); key images were recorded at time points: t=0, 0.5, 2, 8 and 12 h post-IR (Figure 5.3a). At 2 h post-IR, the number of γ-H2AX foci in clone 11 (lowest KUB5/HERA protein expression) were elevated in number/nuclei compared to those for clone 2 that had levels of KUB5/HERA that were identical to parental MDA-MB-231 cells. Over time, clone 2 appeared to repair the DNA damage normally and foci disappear by 2 h post-IR. In contrast,

clone 11 foci persisted up to 8 h post-IR. These data, summarized in the graph in Figure 5.3b, support the hypothesis that hKUB5/HERA is required for normal repair of DSBs, since its loss led to higher basal levels and the inability to repair damage created by IR. Importantly, loss of KUB5/HERA did not affect the cell's ability to detect DNA damage and activate ATM, as evidenced by the near-equivalent γ-H2AX phosphorylation foci formed in KUB5/HERA knockdown versus irradiated SCR or parental cells.

In order to study the DNA damage and repair defect in KUB5/HERA knockdown or knockout cells more directly, alkaline comet assays were performed. KUB5/HERA KD or Scr clones were treated with either H_2O_2 (200 μM), etoposide (200 ng/ml) or IR (40 Gy) and collected at 15 min intervals for 2 h. The theory behind this assay is that damaged DNA within the nucleus loses tight association with matrix proteins, resulting in relaxed DNA. When the cells are embedded into soft agarose and lysed in alkaline conditions, the damaged DNA protrudes out of the cells into the soft agarose, whereas the undamaged DNA remains tightly associated with matrix proteins within the nucleus (129-131). An electric current is then passed through the cells allowing visualization of cells with damaged DNA by the presence of DNA "comets". Under alkaline conditions, all DNA lesions are assessed, including AP sites, SSBs and DSBs. MDA-MB-231 KD and Scr clones were treated with a positive control, etoposide, which is known to create DSBs (132, 133) and H_2O_2 known to create SSBs at low

concentrations and DSBs at high concentrations (134, 135). Increased number and length of comet tails in KUB5/HERA KD clone 11 (low KUB5 protein level) cells were noted after 30 mins treatment with etoposide and H_2O_2 (Figure 5.4). Treatment of cells at 4 ^oC required a dose of 40 Gy in order to visualize comets, whose repair could be monitored over time (Figure 5.5). Cells were placed on ice prior to IR treatment, and the initial time point of 15 min post-IR was collected from a plate remaining on ice after treatment. All other time points were collected from plates placed in growth chamber after IR treatment. Initially, DNA damage was visualized by the presence of a long comet tail. Over time, these tails rapidly shorten due to DNA repair with biphasic responses as in foci formation and repair (Figure 5.5b). Thus, the kinetics of DNA repair were determined by measuring comet tail lengths over time (mins or h). These data, summarized in Figure 5.5a and 5.5b, indicate persistence of DNA damage in KUB5/HERA+/- clone 11 cells (low KUB5 protein level) taking nearly 1 h and 15 mins to begin resolving DNA damage versus clone 2 (normal KUB5/HERA protein levels) that began repairing damage as early as 30 mins post-IR. In clone 2, the appearance of comet tails disappeared by 1 h, where clone 11 comet tails persisted for 1 h and 45 mins. These data support the hypothesis that KUB5/HERA was required for repair of DNA damage created by IR, and in the absence of KUB5/HERA DNA repair was significantly delayed.

DNA damage created by IR can leave several types of DNA lesions

including both DSBs and SSBs, however, the broad spectrum of damage created upon IR treatment makes it difficult to determine specifically which DNA repair pathway KUB5 might be working. To test this, MDA-231 parental, SCR and KUB5 knockdown cells were treated with several DNA damage agents including those used in breast cancer therapy (Figure 5.6a-f and Figure 5.7a-c). In Figure 5.6a, the IR sensitivity of KUB5 knockdown cells supports previous data also showing increased IR sensitivity of KUB5 transient and stable knockdown cells. In Figure 5.6b, H_2O_2 treatment is known to create SSBs at low concentrations and DSBs at high concentrations(134, 135). In KUB5 knockdown cells, there appeared to be an increased sensitivity to this agent at particularly the higher concentrations, where DSBs are likely being formed. In Figure 5.6c, cells were treated with increasing doses of Cisplatin, an agent known to create inter- and intra- DNA strand cross-links. KUB5 knockdown cells showed increased sensitivity to this agent, likely due to stalled replication forks resulting in DSB formation. In Figure 5.6d, cells were treated with MNNG, an alkylating agent known to create O^6 methyguanine, as well as other minor DNA adducts. The cell recognizes this altered base as cytidine, and as a result creates a DNA mismatch upon replication (136). DNA MMR can recognize these mismatches and at high doses of MNNG create DSBs in exposed cells. Interestingly, KUB5/HERA knockdown cells showed an increased sensitivity to MNNG, similar to that seen in yeast RTT103-/- cells. These data further support the hypothesis that in both

rtt103 deficient yeast and KUB5 deficient mammalian cells, treatment with MNNG results in DSB formation at high doses, for which KUB5/HERA was required for survival. High doses of MNNG could also hyperactivate PARP1 if not repair, suggesting that KUB5/HERA knockdown cells were hypersensitive to this agent due to unrepair damage (78, 79). The normal function of PARP1 is to bind DSBs, and poly(ADP) ribosylate proteins that are recruited to the sites of DNA lesions, including itself. At this point, PARP1 is released from the DNA and recycled (78, 79). This hyperactivation releases PARP1 from DNA leaving the damages ends unstabilized and preventing efficient repair of the damage, creating increased sensitivity to this DNA damage agent. In figure 5.6e, cells were treated with UV, known to create damage resolved by TCR(137, 138). In contrast to agents that create frank DSBS, there was no difference in survival between parental, SCR and KUB5/HERA shRNA-knockdown cells in response to UV treatment. In Figure 5.6f, cells were treated with etoposide, an agent known to create DSBs by forming a timeric complex with DNA and Topoisomerase II, after cleavage of DNA, therefore, preventing resealing of the break created when unwinding the DNA (132, 133). KUB5/HERA knockdown cells were more sensitive to this DNA damage agent compared to parental and SCR 231 cells. Figure 5.7a-c, continues this study using common chemotherapeutic drugs Doxorubicin, Topotecan and Taxol. In figure 5.7a, cells were treated with Taxol, a clinically effective drug used to treat metastatic breast cancer targeting the

tubulin/microtubule system (139-141). It is suspected that Taxol can also induce certain types of DNA damage, including SSBs that can be converted to DSBs after DNA replication (142, 143). Nevertheless, KUB5/HERA knockdown cells did not show a significant difference in sensitivity to Taxol compared to parental and SCR cells. In figure 5.7b, cells were treated with increasing doses of doxorubicin (aka., adriamycin). Doxorubicin functions by intercalating into DNA and poisons DNA topoisomerase II (Topo II), which unwinds DNA for replication and transcription (144-146). KUB5/HERA knockdown cells show hypersensitivity to Doxorubicin versus parental and SCR MDA-MB-231 cells. In figure 5.7c, cells were treated with Topotecan, a compound that forms a trimeric complex with topoisomerase I (TOPO-I) and DNA, which poisons TOPO-I). Upon DNA replication, a collision occurs between this ternary complex and the replication fork resulting in a stalled replication forks and the formation of DSBs (147, 148). KUB5/HERA knockdown cells were more sensitive to topotecan than parental or SCR cells. These combined data support the hypothesis that KUB5/HERA is directly involved in DSB repair.

KUB5/HERA knockdown cells were generated using an shRNA to KUB5/HERA designed to its 5'-untranslated region (5'-UTR), allowing for re-expression of human KUB5 cDNA to test restoration of function. KUB5/HERA KD clone 11 cells were transfected with a CMV-directed mammalian expression vector containing the hKUB5/HERA cDNA, and transformants were selected in

Neomycin-containing media. Western blot analyses showed the re-expression of human KUB5 in knockdown clone 11 (Figure 5.8a). Pooled population 1, showing a high level of KUB5 re-expression was then treated with IR and assayed for survival at doses 0, 0.5, 1, 1.5, 2, 2.5, 3, 3.5 and 4 Gy (Figure 5.8b). Re-expression of KUB5/HERA in clone 11 knockdown cells rescued the radiation sensitivity seen in the knockdown cells (Figure 5.6a). These data confirm that the lenti viral shRNA to KUB5 has little to no non-specific activity, and is likely only affecting KUB5.

Previous data in chapters 2, 3 and the first part of chapter 4, supported the hypothesis that KUB5/HERA was a novel DNA repair protein, and that alterations in this protein's expression conferred changes in sensitivity to DNA damage agents, such as IR. The final goal of this thesis was to investigate the possibility that KUB5/HERA expression in breast cancers could be correlated with sensitivity to IR, potentially setting the framework for KUB5/HERA as a biomarker for 'predictors of response' to therapy. Due to known amplifications in several cancers at regions at or near the position of the KUB5/HERA locus, a screen was performed through a Comparative Genomic Hybridization (CGH) database provided by the UT Southwestern SPORE and Dr. John Minna's laboratory. Results for breast cancer cell lines were summarized in Figure 5.9a. Breast cancer cell lines were ordered from left to right, from greatest amplification at locus C20orf77 (KUB5/HERA), to greatest loss of copy number

at the KUB5/HERA locus. All samples were normalized to the copy number of the KUB5/HERA locus of normal HMECs. Significant gains or losses are those above 0.2, and less than -0.2. A copy number gain or loss correlating with +/-0.5 is approximately equal to one copy number gain or loss. Though most CGH values correlated to only a single copy number loss or gain, these data were considered significant in light of the subsequent radiation sensitivity and western blot data obtained from a single copy number loss in mouse cells heterozygous for KUB5/HERA+/- MEFs (Figure 5.1). The western blot data in Figure 5.9b summarizes several breast cancer cell lines used in the CGH analyses and their relative KUB5/HERA protein levels. Figure 5.9c illustrates, by graphing relative KUB5/HERA protein levels to CGH, a strong correlation between relative KUB5/HERA protein levels and copy number, with a p-value of 0.0013.

Breast cancer cell lines chosen from the CGH screen were further analyzed for their sensitivities to IR (Figure 5.10a). Cell lines exhibiting the greatest resistance to IR were HCC1419, HTB26 (MDA-231) and HTB122, which expressed the highest levels of KUB5/HERA protein and gene copy number by western blotting and CGH analyses, respectively. The cell lines exhibiting the greatest sensitivity to IR included HCC202, HCC2185 and SKBR3. Consistently, HCC202 and HCC2185 also had the lowest levels of KUB5/HERA protein and the lowest copy number by CGH analyses. SKBR3 cells appear to be an interesting exceptional case, where KUB5/HERA protein levels and copy

numbers by CGH amplification are extremely high, but these cells appear to be extreme sensitivity to IR. This inconsistency could be due to other, more important, alterations in DNA repair capacity within these cells, perhaps a loss of HR factors necessary for repair. Another option is that KUB5/HERA within these cells may alterations, point mutations preventing its action in the efficient repair of DNA damage created by IR. Figure 5.10c illustrates a comparison of LD_{50} values of these breast cancer cell lines after exposure to IR, plotted against their relative KUB5/HERA protein levels as measured by western blotting (Figure 5.9b). Statistical analyses of these data, excluding SKBR3 cells, shows a significant p value less than 0.0001. Thus, it seems possible to correlate KUB5/HERA protein levels within cell lines to IR hypersensitivities. Table 5.1 shows a summary of these breast cancer cell lines, including CGH copy number values, IR responses, p53 statuses, as well as HER2, ER/PR and BRCA1 statuses. Within this table there are 4 of 11 cell lines that are known to be triple-negative (HER2/ER/PR) and the protein levels of KUB5/HERA correlate well with the IR sensitivities of these cells, potentially indicating that KUB5/HERA levels may be a sensitive biomarker to use to predict radiation sensitivity in triple-negative breast cancers.

Analyses of KUB5/HERA expression with sensitivity to radiation to this point have only examined breast cancer cell lines, which typically retain several other problems that could lead to sensitivity to DNA damage agents. One of the

problems with studying cell lines is the immortalization process, since this can affect several processes, most importantly, those controlling the cell cycle (149). To determine whether or not the immortalization process had an affect on KUB5/HERA expression, primary cells were generated from a normal fibro-adenoma mass taken from a patient, and analyzed with both immortalized and matched non-immortalized cell lines obtained from the laboratory of Dr. David Euhus. Generating primary cell populations from a patient sample requires extensive maintenance in order to separate out fibroblast from epithelial cell populations (Figure 5.11a). After successful purification of epithelial HMECs, named 4077 and 2424, these primary cells were analyzed with matched 4341 or 4341 immortalized cells, as well as with 348t HMEC cell lines. Immortalized cell lines were generated from Euhus laboratory by ectopic expression of lentiviral-mediated cdk4 and telomerase. Figure 5.11b, shows western blot analyses obtained from protein isolates from all HMECs, as well as two breast cancer cell lines, MCF-7 and SKBR3. Results show that the immortalization process did not appear affect KUB5/HERA protein expression levels in this brief and limited screen. In addition to the immortalization process having no affect on KUB5/HERA expression, it appears that, in general, breast cancer cells have a much higher expression level of KUB5/HERA versus normal HMECs. This indicates that changes in KUB5/HERA expression level may allow the tumor to survive the series of genomic instabilities caused by carcinogenesis that promote

changes in the cell cycle and p53 status. Radiation treatment of normal HMECs showed that these cells were significantly more sensitive to IR than most breast cancer cell lines.

We confirmed that loss of KUB5/HERA results in hypersensitivity to DNA damage agents, specifically those that kill by creating DSBs. Screening of breast cancer cell lines by western blotting demonstrated varied KUB5/HERA expression that correlated well with radiation sensitivity. For this work to have a hope of being useful in the clinic, it is necessary to generate a simple means of detecting changes in KUB5/HERA protein expression levels, including IHC. The final goal of this breast cancer work was to try to work out conditions to use our KUB5/HERA monoclonal antibody in the detection of changes in KUB5/HERA expression in tissue slices taken from tumor samples. For this, MDA-MB-231 shKUB5 and SCR cells were infected with lentivirus containing a CMV-luciferase (CMV-luc) vector, and cells were injected subcutaneously in athymic nude female mice (18-20 gms). Tumor growth was measured and quantified by bioluminescence (BLI) and direct caliper measurements until tumor volumes reached 10 cm^3. At this point, mice were sacrificed to remove tumors and frozen tissue was processed for tissue slicing and IHC slide prep. IHC analyses revealed that KUB5/HERA levels could be detected in 231 SCR cells, indicated in red nuclear staining (Figure 5.12). Conversely, in MDA-MB-231 shRNA-KUB5 knockdown cells, the KUB5/HERA antibody could not detect significant protein

staining. Of note, however, a significant cross-reaction with the KUB5/HERA monoclonal antibody occurred along the edge of the tissue, which we believe may be due to cross-reactivity with surface epithlium in mouse tissue. Overall, these data provide evidence that KUB5/HERA protein levels could be a predictive biomarker to determine radiation sensitivities of tumors, and its expression can be detected by IHC.

DISCUSSION:

Due to the early embryonic lethality of the KUB5/HERA-/- mice, *in vivo* studies were limited to using KUB5/HERA+/- MEFs. A single copy number loss in KUB5+/- MEFs conferred significantly increased IR sensitivity compared to WT KUB5/HERA+/+ mice, supporting prior data within this thesis that loss of KUB5/HERA resulted in increased radiation sensitivity. Interestingly, cells and tissue from KUB5/HERA+/- mice showed stabilization of p53 levels and phosphorylation of p53 at serine 15. This could be explained by endogenous DSBs causing DDR responses, resulting in genomic instability even in the absence of DNA damage. The significance of these data span beyond this model into the breast cancer CGH analyses in Figure 5.9a. Here, a single copy number loss in the KUB5/HERA locus by CGH analyses can be directly correlated with radiation sensitivities of various breast cancer cell lines. Combined, these data support the hypothesis that KUB5/HERA function within the cell is important and necessary in normal cells, as only a single copy number loss appears to be required for a significant affect on the cell's ability to survive through both exogenous and endogenous DNA damage.

My initial hypothesis was that KUB5/HERA was necessary for efficient DSB repair and its loss would lead to increased sensitivity to IR and other DNA damaging agents. This hypothesis appears to be supported by nearly all of the

data generated in this thesis. Here, stable KUB5/HERA knockdown in MDA-MB-231 cells expressing mutant p53 resulted in significant loss of KUB5 protein expression and hypersensitivity to IR as well as all agents that killed via the creation of DSBs. The p53 mutant status likely allowed these cells to survive this knockdown, consistent with previous data from chapter 4. KUB5/HERA knockdown also resulted in significant increased sensitivity to other DNA damage agents, where DSBs are created in their mechanism of cell killing. Comet and H2AX phosphorylation assays further supported the hypothesis that loss of KUB5/HERA resulted in delayed repair of DNA damage. Loss of KLUB5/HERA did not, however, affect the initial detection of DNA damage (as monitored by γH2AX). These data supported the hypothesis that KUB5/HERA was involved in the repair of DSBs and disruption of its function was not required for the early detection of DSBs and downstream DNA damage signaling. More importantly, re-expression of KUB5/HERA cDNA back into the knockdown cells rescued the IR sensitivity, confirming that the effect of stable knockdown of KUB5/HERA was due to the specific loss of KUB5/HERA protein and not by other non-specific effects of clonal selection. These results were similar to those in yeast, where human KUB5/HERA re-expression restored IR hypersensitivity in rtt103-/- yeast.

In summary, the data generated throughout my thesis support the overall hypothesis that KUB5/HERA is an important, novel factor in DSB repair in eukaryotic cells, and appears to play a significant role in human breast cancer

radio-resistance. The significant correlation of KUB5/HERA relative protein levels and radiation sensitivity could prove to be an important finding that may lead to the development of KUB5/HERA as a biomarker for how a specific tumor may respond to DNA damage-inducing therapy. In order for this to become a reality, further analyses and conditioning will need to be done so pathologists could be able to screen and quantify KUB5 levels in tumor tissue by IHC analyses.

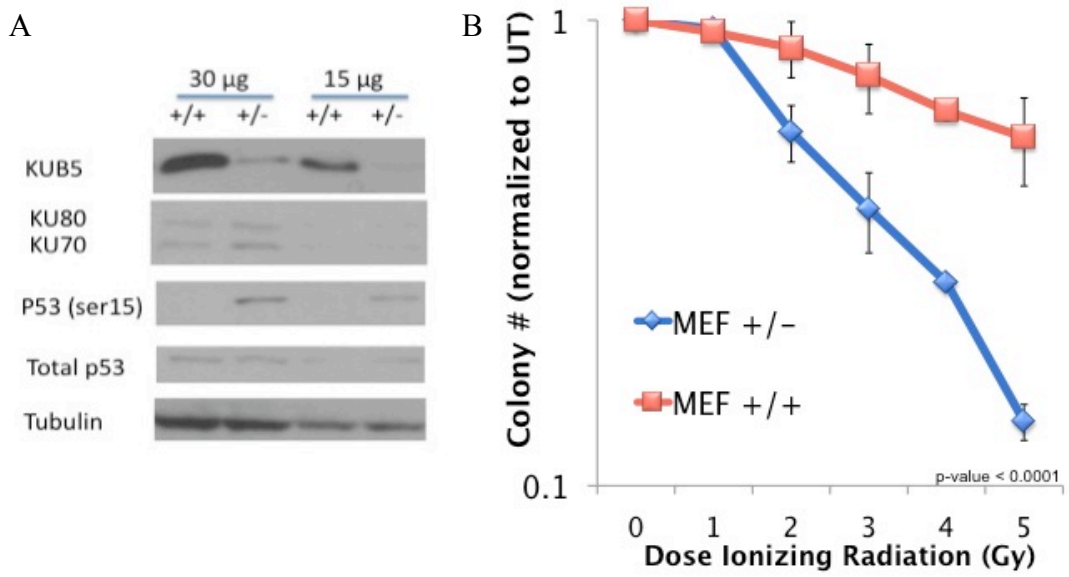

Figure 5.1 – **Single copy number loss in MEF cells results in significantly decreased protein expression and increased radiation sensitivity.** In A) protein was extracted by whole cell RIPA extraction in MEF +/+ and +/- cell lines and western blotted to KUB5 expression as well as other DNA repair proteins (Ku70, Ku80, total p53, phosphorylated p53 (ser15). In B) MEF +/+ and +/- cell lines were treated with doses or IR including 1, 2, 3, 4, 5 Gy and growth assays performed to determine survival of cells after treatment. Statistics indicate R^2 value for MEF +/+ = 0.78 and for MEF +/- = 0.92 with an overall p value < 0.0001.

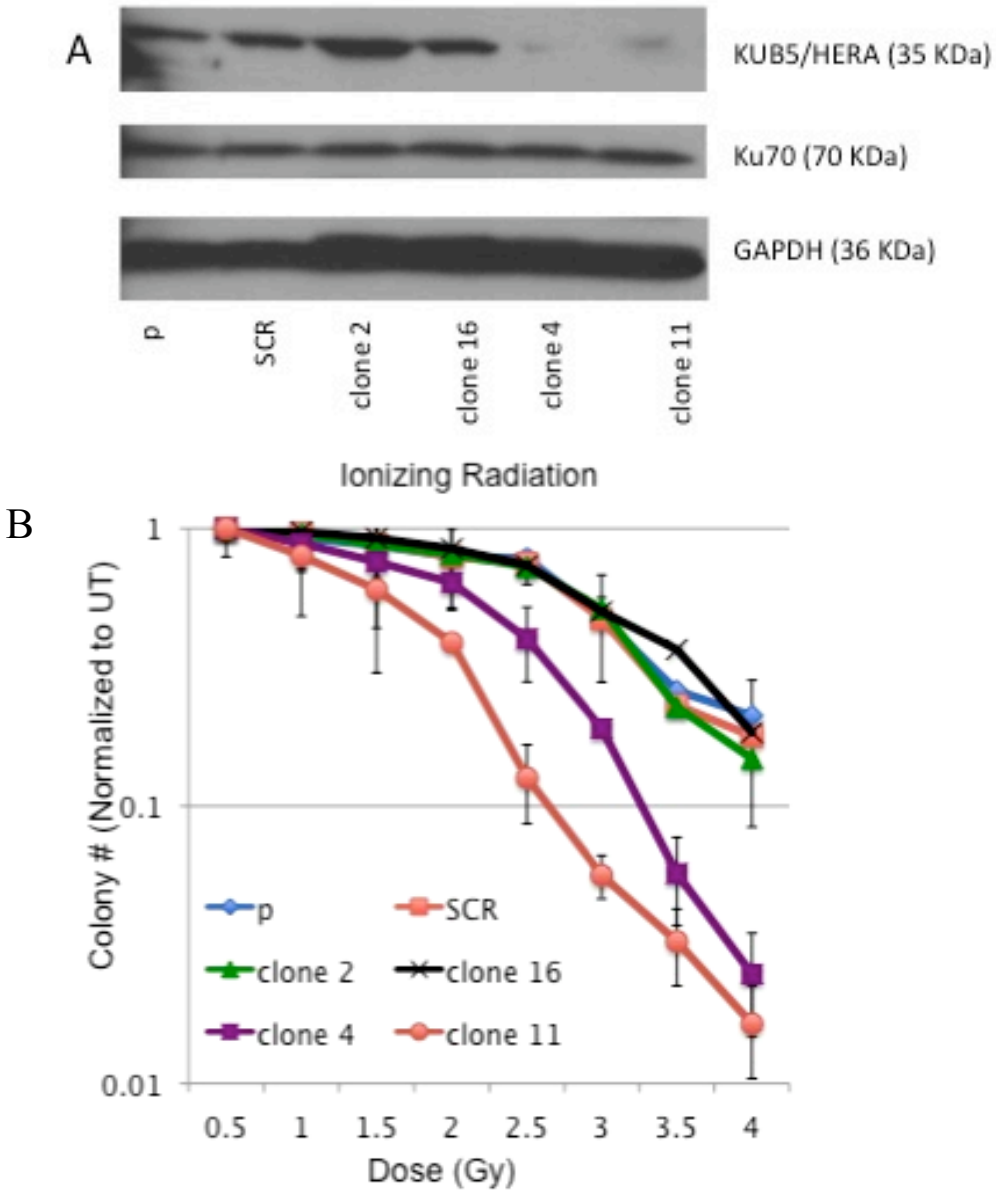

Figure 5.2 – **Stable knockdown of KUB5 protein by shRNA resulted in increased sensitivity to IR.** In A), shKUB5 knockdown clones were isolated and total protein extracted using RIPA extraction buffer. Lysates were separated by SDS-PAGE and western blotted for KUB5, Ku70 and loading control GAPDH. In B), shKUB5 knockdown clones, parental and SCR lines were treated with IR and colony formation assays performed to analyze growth and survival. The

curve for parental and clone 11 (clone showing least KUB5 expression by western blot analysis) were shown to be statistically significantly different with p-value<0.0001.

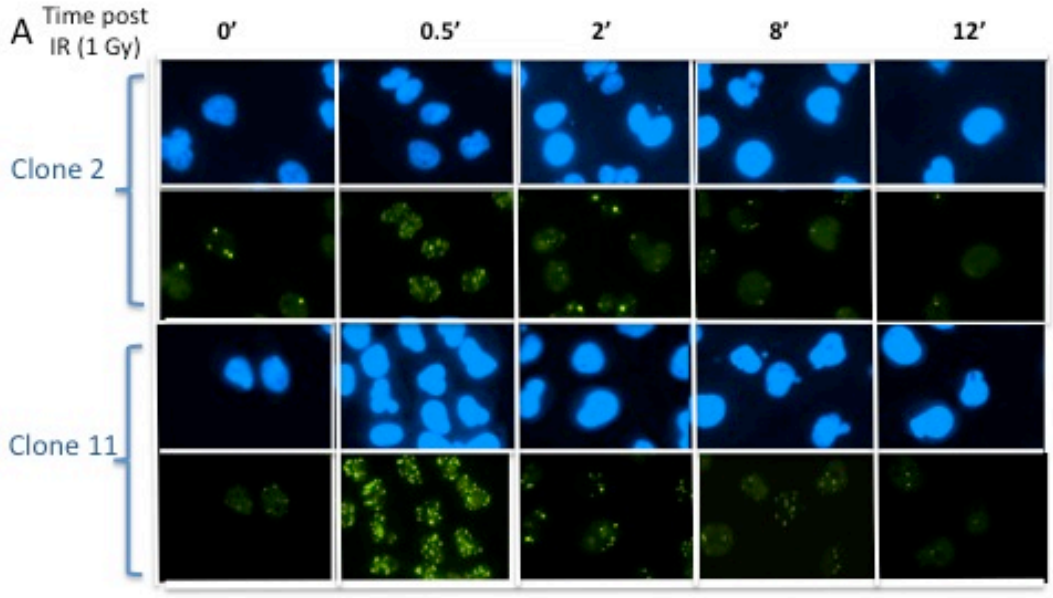

B

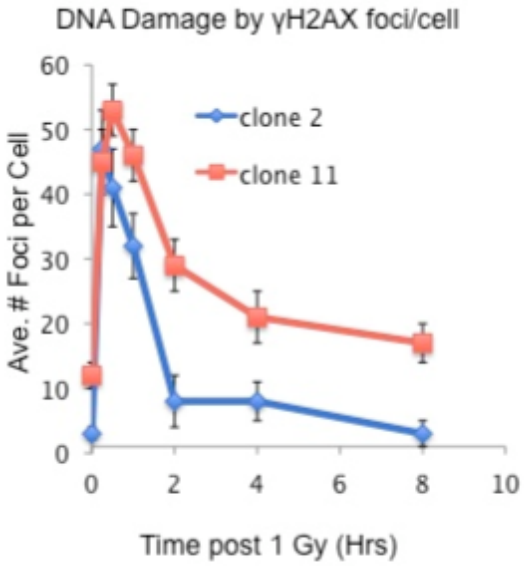

Figure 5.3 – **KUB5 shRNA treatment results in increased basal H2AX phosphorylation and persistence of foci compared to untreated.** In A), γ-H2AX foci were quantified over time after treatment with 1 Gy IR. Foci were counted at time points 0, 0.25, 0.5, 0.75, 1, 1.25, 1.5, 1.75, 2, 4, 8, 12 and 14

hours post IR treatment (not all data shown). Only panels taken from time points 0, 0.5, 2, 8 and 12 hours post IR treatment are shown to summarize the results. Clone 2, showing normal KUB5 expression level is shown in the top two lanes of panels with DAPI on top and the corresponding γ-H2AX shown under. Clone 11, known to express KUB5 protein at very low levels is shown in the bottom two lanes of panels. DAPI represented in 3rd lane and γ-H2AX represented in forth lane. In B), results from counting the foci of 100 cells, in three different experiments are summarized in the graph. Here, clone 2 γ-H2AX foci appear to disappear quickly after IR treatment and are mostly gone by 2 hours post IR treatment. Clone 11 appears to be delayed in γ-H2AX foci disappearance with high levels of foci persisting through 8 hours and resovled by 12 hours post IR treatment.

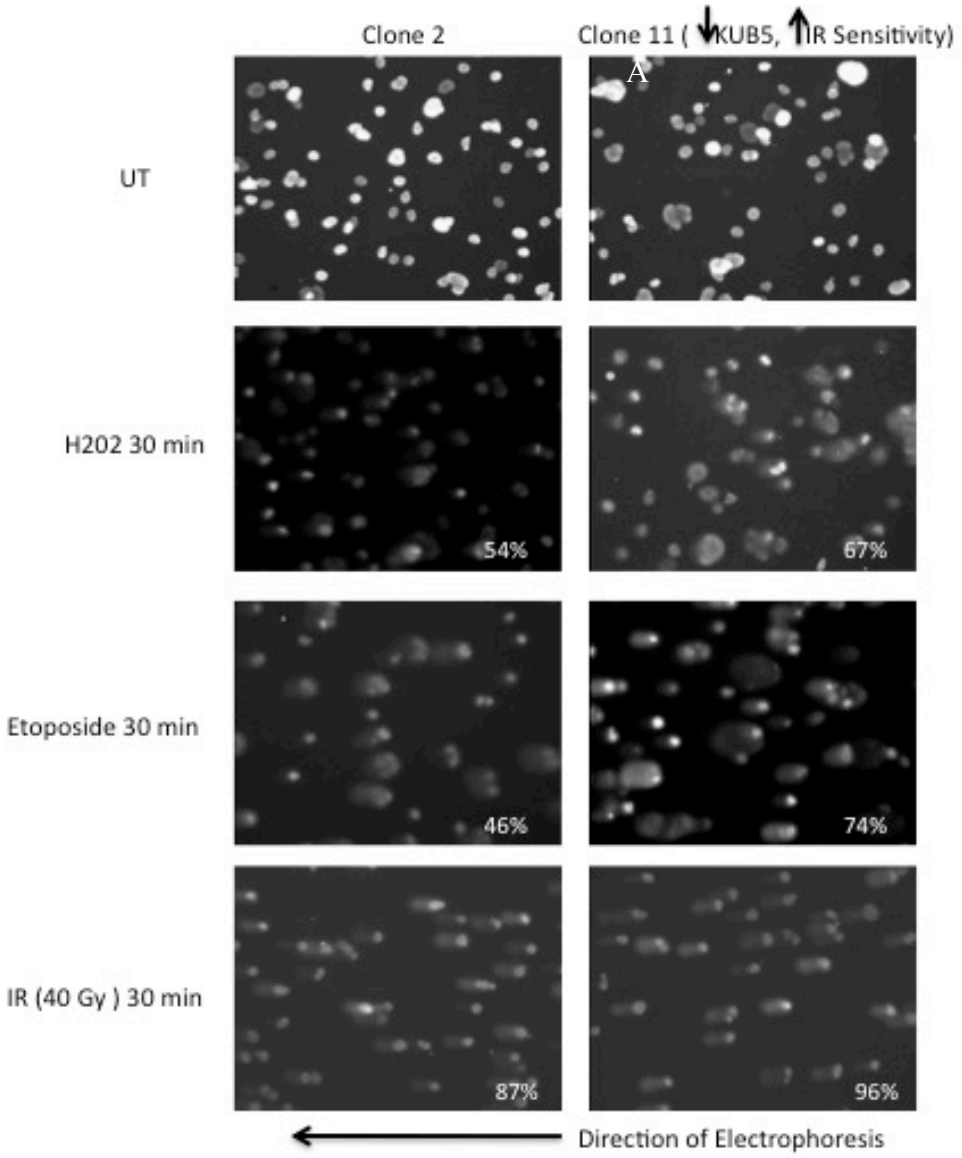

Figure 5.4 – **Comet assay shows KUB5 knockdown cells have more DNA damage foci 30 minutes after treatment with either hydrogen peroxide, etoposide or IR. C**omet assay panels on the left summarize data from treatment with each agent for clone 2, the clone showing normal KUB5 expression levels. Comet assay panels on the right summarize data from treatment with each agent for clone 11, the clone showing decreased KUB5 protein expression, and also showing increased radiation sensitivity. The top panels represent the untreated cells after comet assay is performed showing intact, mostly undamaged DNA. The second set of panels represents treatment with H_2O_2 at 200 μM for 30

minutes. Here, clone two shows roughly 54% cells with comets, and clone 11 shows 67% cells with comets. The third row of panels represents the comet assay after treatment with 200 ng/ml etoposide for 30 minutes. Clone 2 shows only 46% comets and clone 11 shows 74% comets. The final row represents comet assay 30 minutes after treatment with 40 Gy IR. Here clone 2 shows 87% cells with comets, and clone 11 shows 96% cells with comets.

A

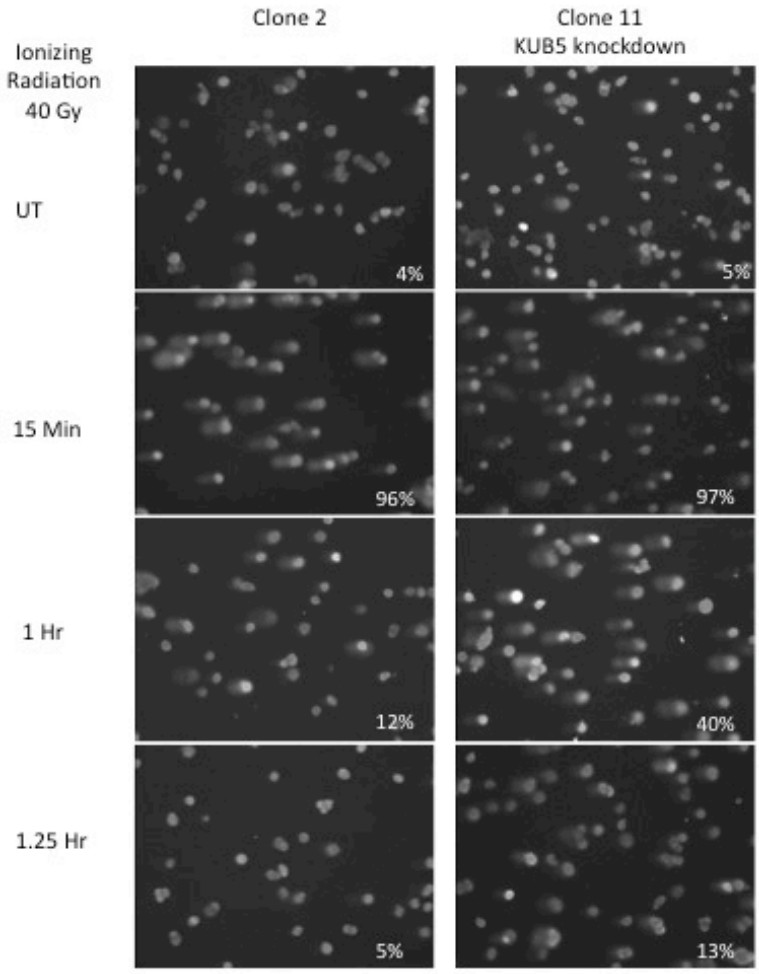
Clone 2
Clone 11
KUB5 knockdown
Ionizing Radiation 40 Gy
UT
15 Min
1 Hr
1.25 Hr
4%
5%
96%
97%
12%
40%
5%
13%
Direction of Electrophoresis

B

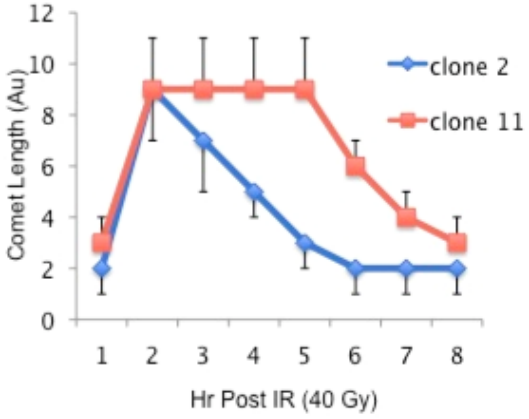
Comet Length (Au)
Hr Post IR (40 Gy)
clone 2
clone 11
0
2
4
6
8
10
12
1
2
3
4
5
6
7
8

Figure 5.5 - **Comet Assay shows repair of DNA damage over time, with loss of KUB5 resulting in persistent DNA damage.** In A), Panels were chosen from several time points taken every 15 minutes after IR treatment up to 2 hours. Panels on the left correspond to the time points for clone 2, and on the right for clone 11. For clone 2, panels represent UT, 15 min, 1 Hr and 1.25 Hr post IR treatment. 15 minutes after IR treatment there are approximately 96% of the cells containing comet tails, by 1 hr this number is diminished to only 12 % cells containing comets and by 1.25 hours post-IR treatment all the comets tails have disappeared. For clone 11, 15 minutes after IR treatment, 97% of the cells contain comets tails, and at 1 hour post treatment 40% of the cells contain comets. And by 1.25 hours still 13% of cells contain comets. In panel B), the graph represents the comet tail length over time, which corresponds to DNA repair. As the comet tails shrink, the DNA is being repaired. For clone 2, where KUB5 expression is normal, the comet tails resolve by 1 hr post treatment. Conversely, in clone 11, where KUB5 levels have been significantly knocked down, the comet tail length persists until 1 hour, where it begins to shorten. Results were collected from 3 independent experiments, with each experiment in duplicate.

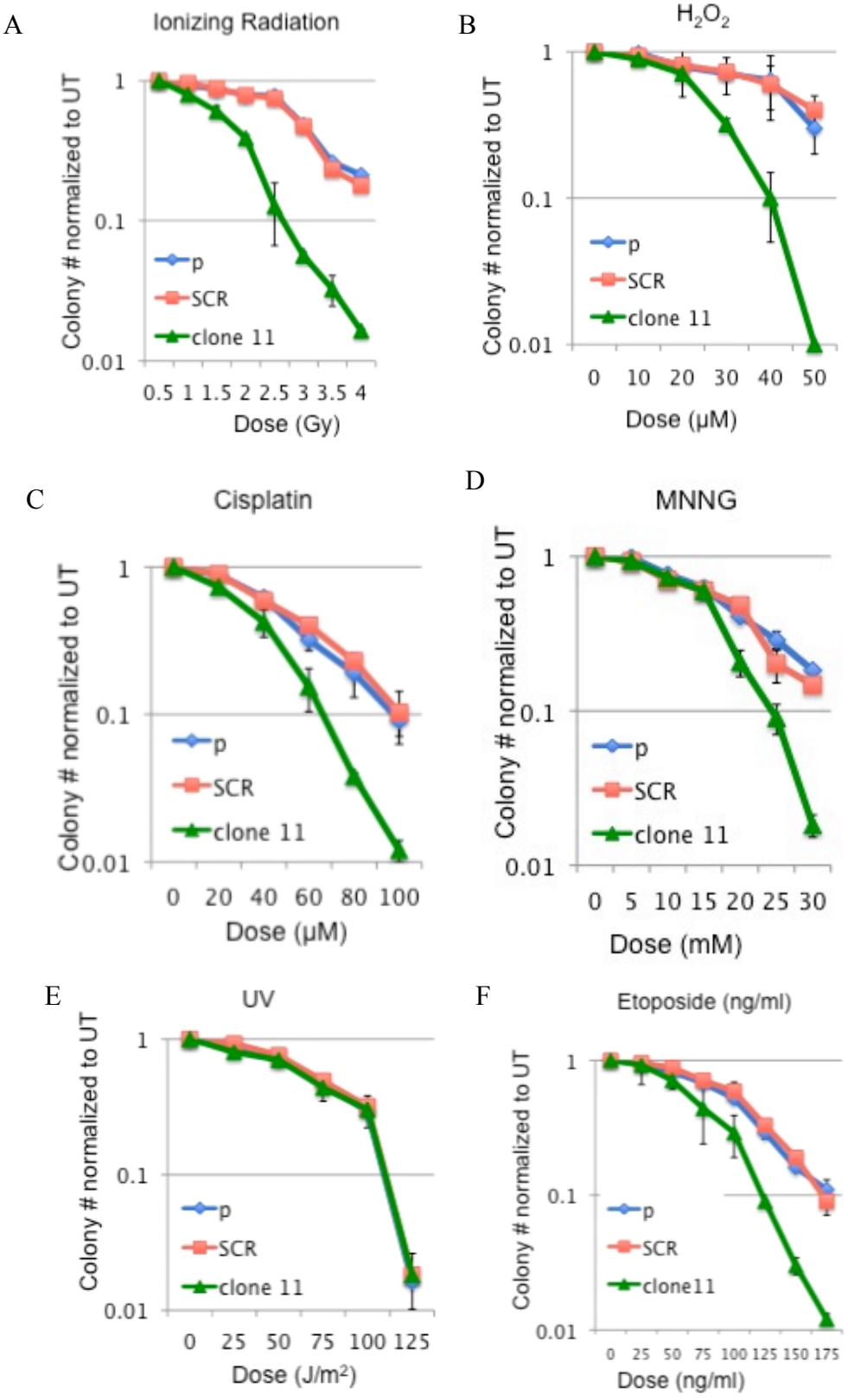
A
Ionizing Radiation
Colony # normalized to UT
1
0.1
0.01
p
SCR
clone 11
0.5 1 1.5 2 2.5 3 3.5 4
Dose (Gy)
B
H_2O_2
Colony # normalized to UT
1
0.1
0.01
p
SCR
clone 11
0 10 20 30 40 50
Dose (μM)
C
Cisplatin
Colony # normalized to UT
1
0.1
0.01
p
SCR
clone 11
0 20 40 60 80 100
Dose (μM)
D
MNNG
Colony # normalized to UT
1
0.1
0.01
p
SCR
clone 11
0 5 10 15 20 25 30
Dose (mM)
E
UV
Colony # normalized to UT
1
0.1
0.01
p
SCR
clone 11
0 25 50 75 100 125
Dose (J/m²)
F
Etoposide (ng/ml)
Colony # normalized to UT
1
0.1
0.01
p
SCR
clone11
0 25 50 75 100 125 150 175
Dose (ng/ml)

Figure 5.6 - **KUB5 loss affects the survival of cells upon treatment with several different types of DNA damage agents.** In A), cells were treated with doses of IR ranging from 0, 0.1, 1, 1.5, 2, 2.5, 3, 3.5 and 4 Gy. Colony formation assays measured the ability of the cells to survive this damage. Results support previous data collected showing clone 11, where KUB5 expression is low, are more sensitive to IR than parental and SCR cells. In B), cells were treated with H2O2 at doses 0, 10, 20, 30, 40, and 50 μM. In C), cells were treated with Cisplatin at doses 0, 20, 40, 60, 80, and 100 μM. In D), cells were treated with MNNG at doses 0, 5, 10, 15, 20, 25 and 30 mM. In E), cells were treated with UV at doses 0, 25, 50, 75, 100 and 125 J/m^2. In F), cells were treated with etoposide at doses 0, 25, 50, 75, 100, 125, 150, 175 ng/ml. Each colony forming experiment was performed in triplicate. The experiment was repeated at least 3 times, and in the case of MNNG treatment was repeated 5 times.

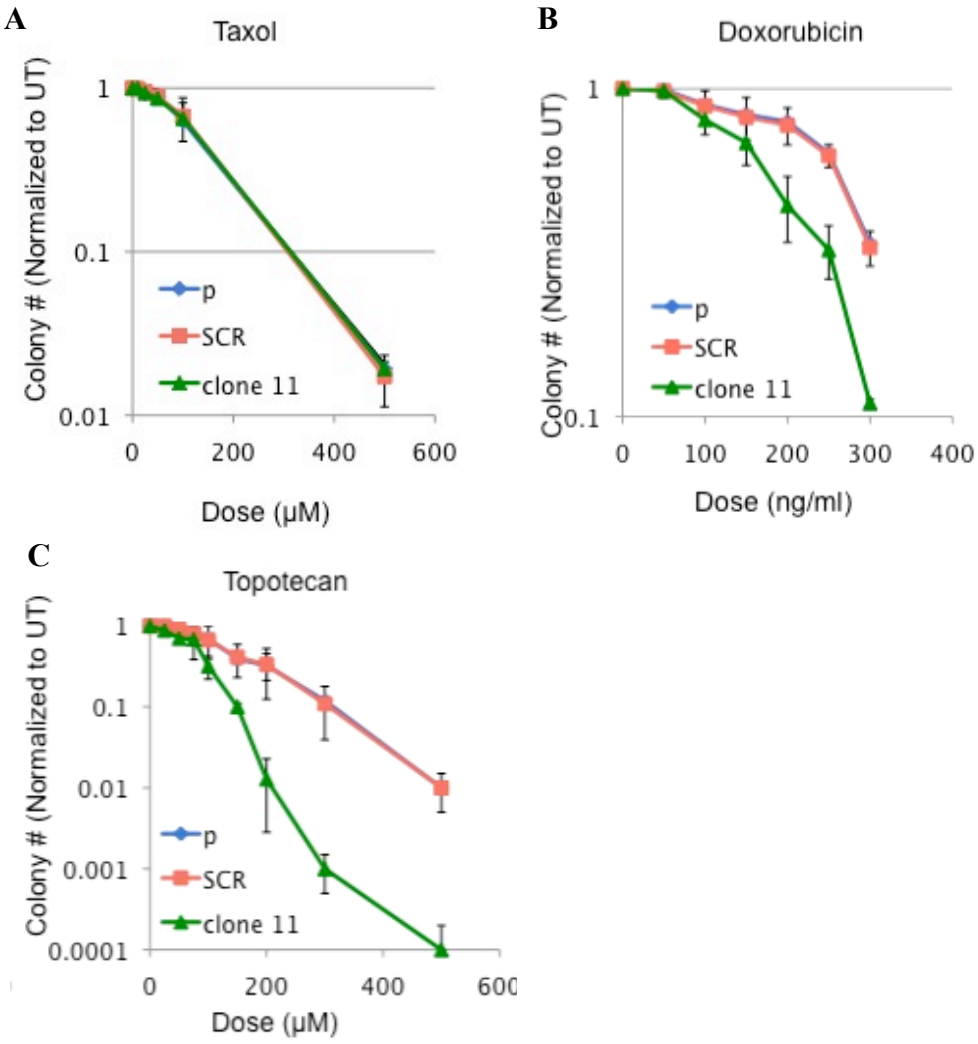

Figure 5.7 – **KUB5 deficient cells are sensitive to some common chemotherapeutic agents.** In A), cells were treated with TAXOL at doses 0, 10, 25, 50, 100 and 500 μM and colony formation assay performed. There appeared to be no difference in KUB5 knockdown cells and parental and SCR in sensitivity to this agent. In B), cells were treated with Doxorubicin at doses 0, 50, 100, 150, 200, 250 and 300 ng/ml. KUB5 knockdown cells appeared to be more sensitive to Doxorubicin with an LD_{50} of 250 ng/ml where parental LD_{50} was 300 ng/ml. In C), cells were treated with Topotecan at doses 0, 25, 50, 75, 100, 150, 200, 300 and 500 μM. KUB5 knockdown cells appeared to be more sensitive to topotecan with an LD_{50} of 150 μM whereas parental cells had an LD_{50} of 200 μM.

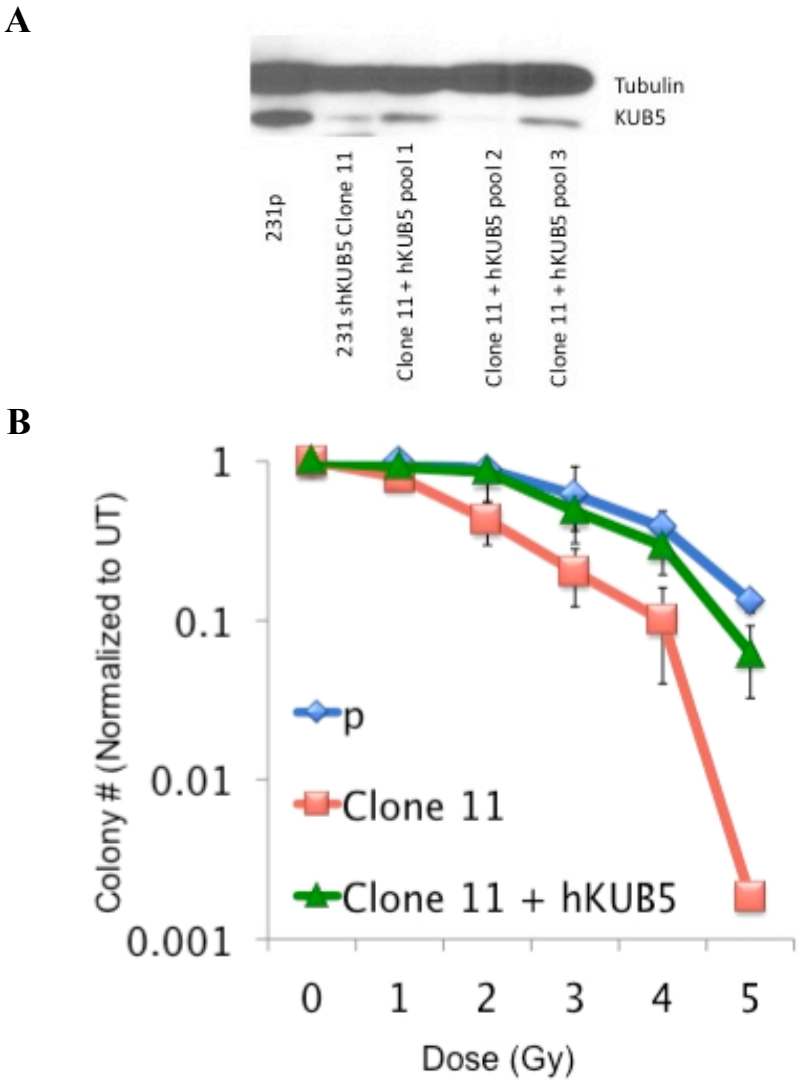

Figure 5.8 – **hKUB5 transfected into shKUB5 231 cells resulted in rescue of IR sensitivity.** In A), western blot shows pooled population isolated after several weeks on Neomycin selection. hKUB5 rescue pool 1 and 3 showed re-expression of KUB5 protein whereas pool 2 did not. In B), Colony formation assay was performed using clone 11 + pool 1. Results indicate rescue of IR sensitivity seen in KUB5 knockdown cells.

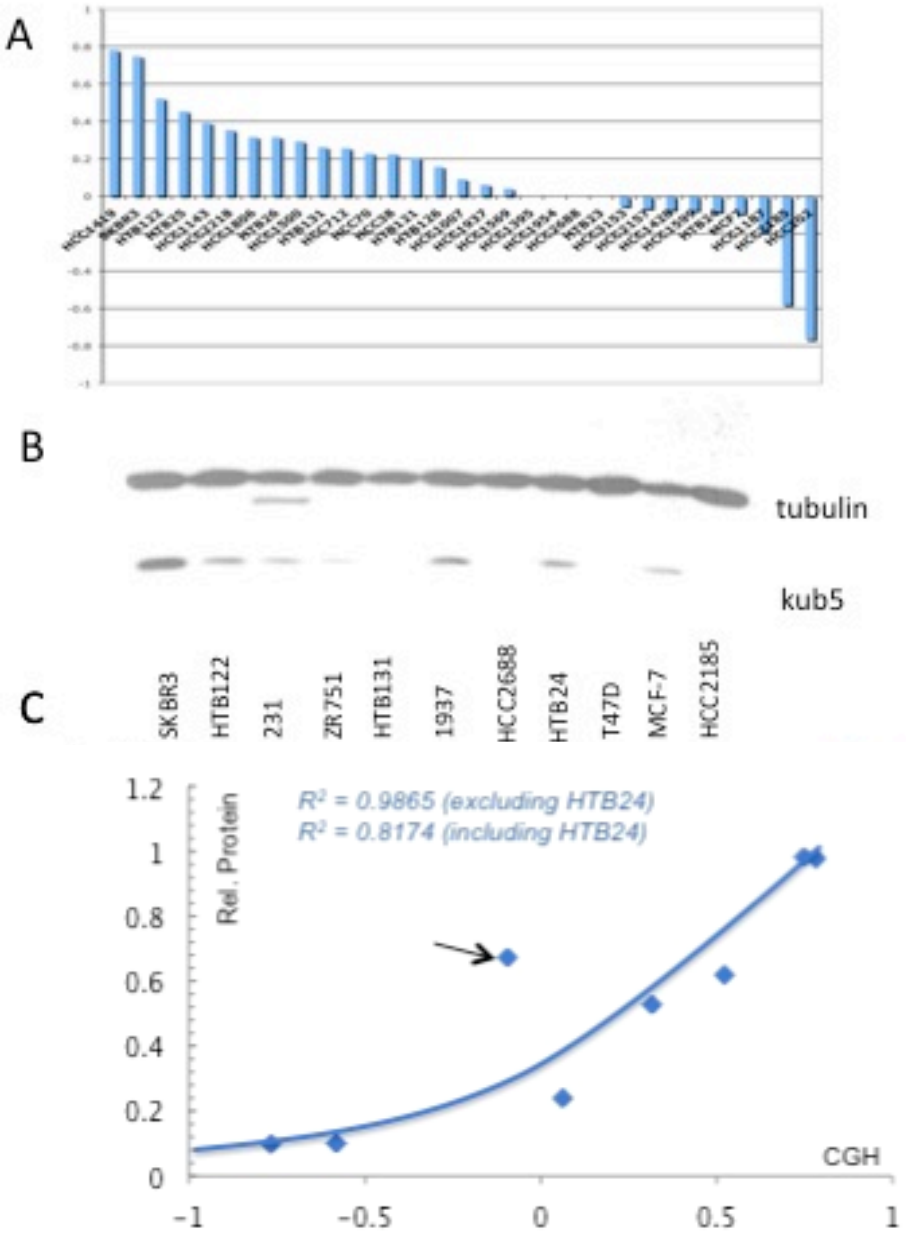

Figure 5.9 – **Comparative Genomic Hybridization Analysis and Western blot protein analysis illustrate endogenous KUB5 levels in Breast Cancer Cell Lines.** In A), CGH analysis performed by Dr. John Minna Laboratory show copy number loss or gain in 31 breast cancer cell lines. An amplification of 0.5 or above indicates over 1 copy number amplificaton. In B) Western blot analysis of whole cell lysates indicates endogenous protein levels in breast cancer cell lines

studied. In C), A strong correlation between copy number gain/loss and relative protein amount in cells is noted. Statistics results yield an R^2 value of 0.7452 and a p-value = 0.0013.

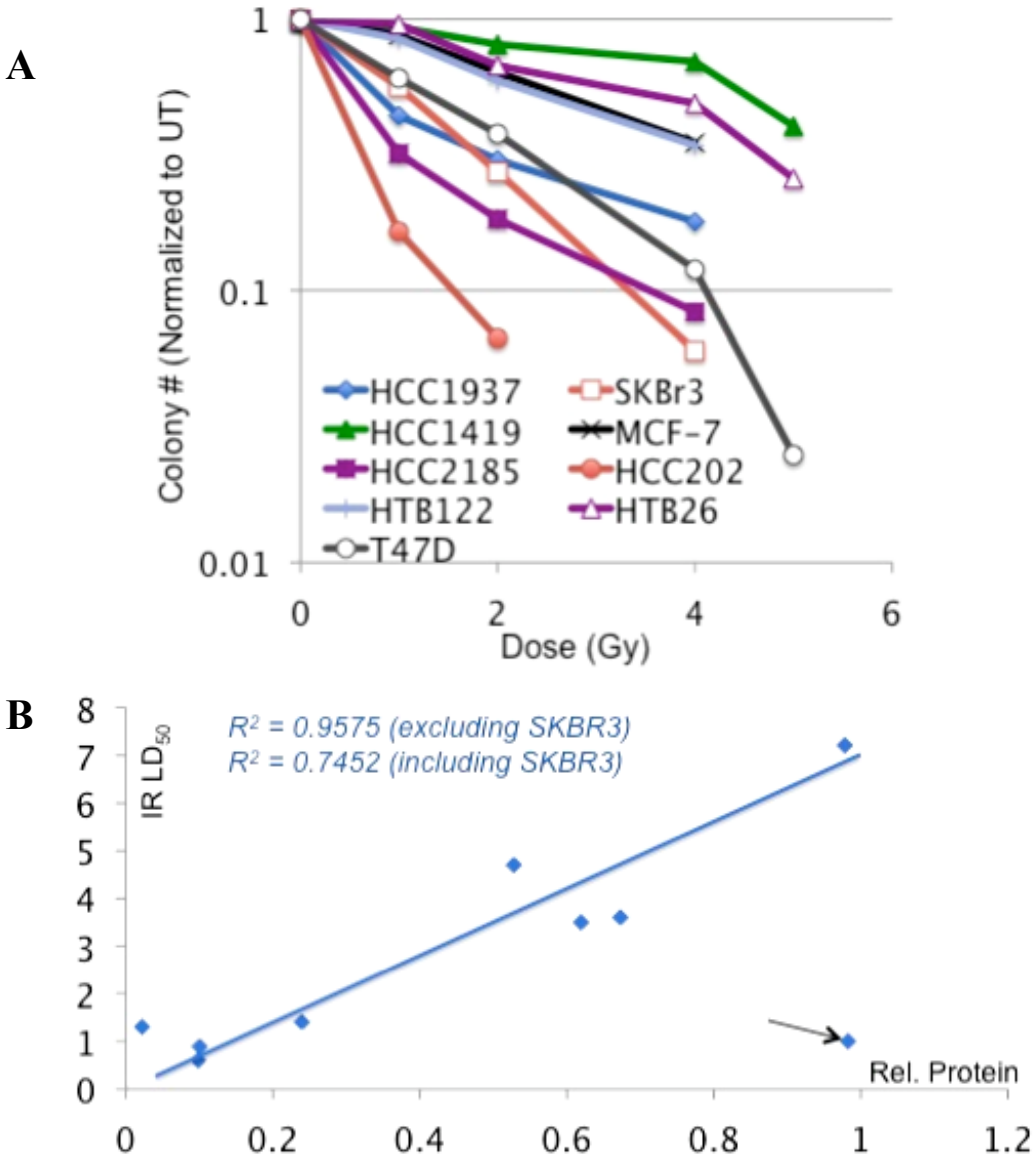

Figure 5.10 – **A strong correlation exists between relative protein level in breast cancer cell lines and radiation sensitivity.** In A), Colony formation studies were performed on several of the breast cancer cell lines after increasing doses of IR. Nine of the cells lines were able to form colonies and are summarized in the graph. HCC202 appeared to be the most sensitive to IR, and HCC1419 appeared to be the most resistant. In B), relative protein levels determined by western blot are plotted against LD50 values for IR. The outlier SKBR3 was excluded from the graph and calculations yielding a p-value < 0.0001.

Cell Line	CGH	IR LD50	p53	HER2	ER/PR	BRCA 1
HCC 1143	0.391	4.8	R248Q	-	-/-	wt
HCC1419	0.782	4.8	Y220C	+	-/-	wt
HTB25	0.454	4.5	WT	?	?	wt
MDA-231	0.165	3.7	Mt	-	-/-	wt
HTB122	0.522	3.4	WT	-	-/-	wt
MCF-7	-0.095	2.9	Gain o/f	N	+/+	wt
SKBR3	0.748	2.2	R175H	+	?	wt
HCC1937	0.062	2	loss	-	-/-	Loss
HCC2185	-0.582	1.9	Gain o/f	+	-/-	wt
HCC202	-0.768	1.6	loss	+	-/-	wt
T47D	?	1.6	L194P	?	+/+	wt

Table 5.1 – **KUB5 loss and radiation sensitivity does not seem to correlate with HER2, ER, PR or BRCA1 status of the cells.** Eleven cell lines are represented with their corresponding CGH level of KUB5 and IR LD_{50}. The cell lines are ranked from most resistant to IR down to most sensitive to IR. p53 mutations are listed for each cell line. HER2, ER/PR and BRCA1 loss or gains are summarized in the last 3 columns. Data used for this table was extracted from the SPORE database from Dr. John Minna's laboratory.

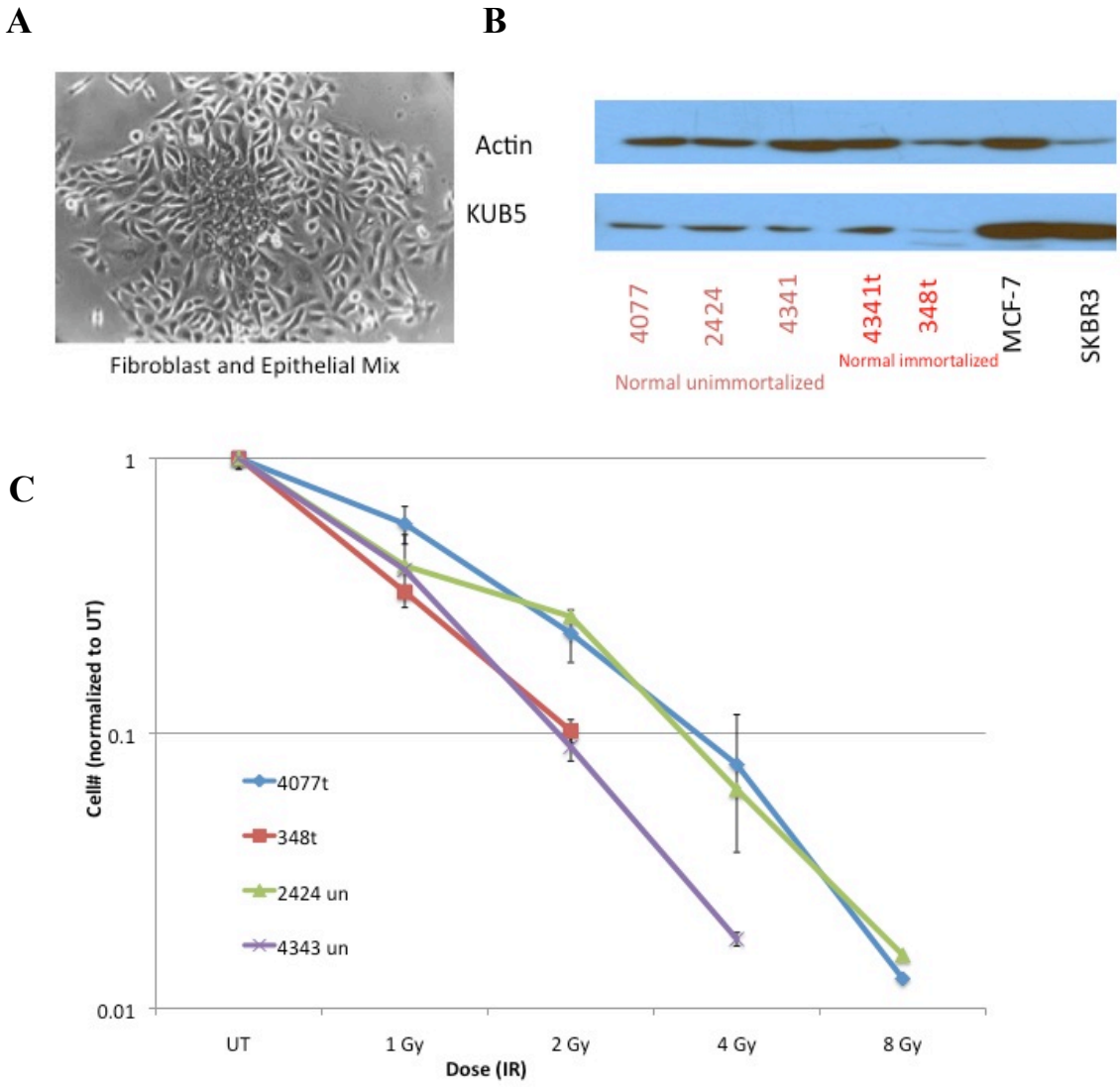

Figure 5.11 – **Analysis of primary HMECs both un-imortalized and immortalized shows low basal KUB5 expression level.** In A), microscope photo represents the distinction of epithelial cells from fibroblast cells from the initial isolate from a non-cancerous human breast mass. Here epithelial cells were distinguished as tightly clustered spherical cells. Fibroblasts can be differentiated

from epithelial cells by their characteristic long extended cellular bodies and their inability to form tight colonies. In B), Western blot analysis shows normal un-imortalized HMECs in lanes 1, 2 and 3 and normal immortalized HMECs in lanes 4 and 5. The final two lanes are loaded with two breast cancer cell lines MCF-7 in lane 6 and SKBR3 in lane 7. Overall KUB5 expression level in normal HMECs is considerably lower than that seen in most breast cancer cell lines. In C), the IR sensitivity of the HMECs is shown. Here all the HMECs are considerably more sensitive to IR than the breast cancer cell lines from figure 4.10.

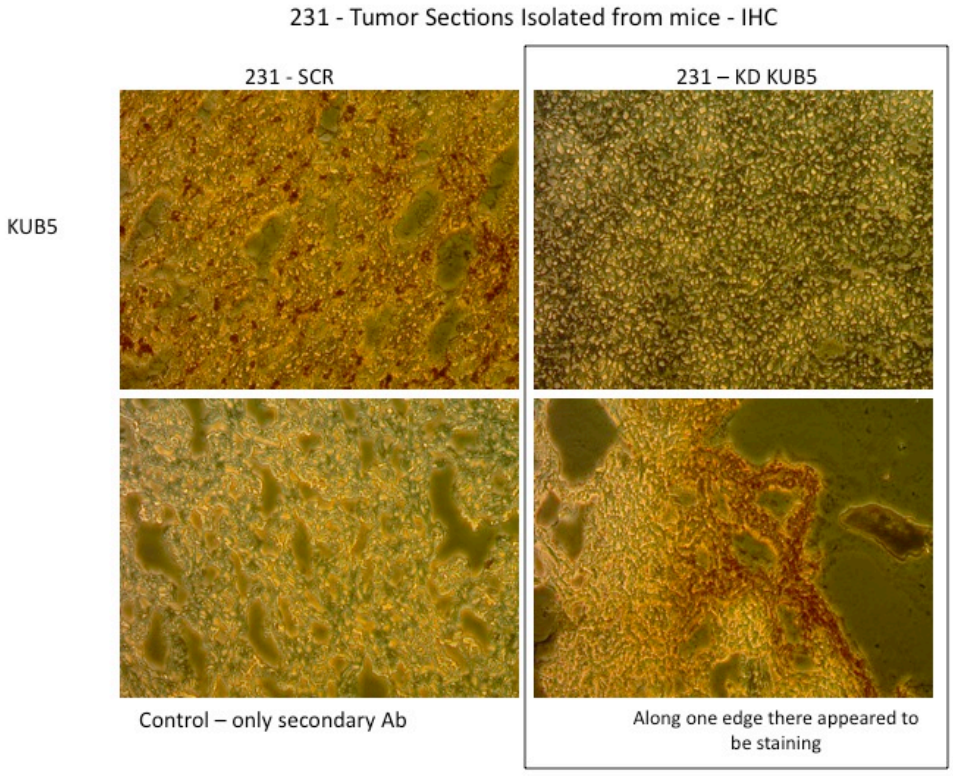

Figure 5.12 – **Immunohistochemistry of 231 subcutaneous tumor specimens showed decreased KUB5 expression in knockdown cells.** MDA-231-Luciferase SCR and shKUB5 cells were implanted subcutaneously at density 10^6 cells per injection site. Tumor formation was monitored by bioluminescence imaging. Mice were sacrificed when tumors reached 10 cm^3 and tumors extracted and frozen. Frozen tissue was sectioned and probed for KUB5 expression with KUB5 monoclonal antibody. 231 SCR cells showed highest KUB5 expression, though non-uniformly likely due to permeabilization procedure of tissue. In KUB5 knockdown tumor tissue KUB5 expression levels were not detected in central tumor slice, however along the edges of the tumor there appeared to be KUB5 expression, likely due to mouse tissue contamination.

CHAPTER VI

CONCLUSIONS AND FUTURE DIRECTIONS

The central hypothesis of this thesis is that KUB5/HERA is a novel factor involved in DSB repair. Cells hyper-sensitive to DNA damage agents creating DSBs show increased death as observed in rtt103-/- yeast, KUB5/HERA deficient mice as well as mouse or human KUB5/HERA knockdown cell lines. More specifically and importantly, G_1 arrested haploid yeast, that were forced to undergo NHEJ for survival, were hypersensitive to these agents, whereas log-phase yeast that prefer HR showed no significant increase in sensitivity to any DNA damaging agents. These data were strongly supported by plasmid re-ligation results showing that RTT103 loss in yeast results in the specific inability to repair blunt and non-compatible DNA ends. These data strongly suggest that KUB5/HERA is specifically involved in NHEJ.

Although these data are extremely supportive of a role for RTT103 in NHEJ in yeast, data in support of a specific involvement of human KUB5/HERA in NHEJ are not as strong, simply because direct experiments in human cells have not been performed. Data that appear to support an involvement of human KUB5/HERA in the NHEJ system, include hypersensitivities to DNA damage agents, resulting in delayed foci formation and an increase in DSBs. The data showing association with Artemis and Ku70 further support this theory. It will be important to perform similar studies, as performed in yeast, with plasmid re-ligation assays, in mammalian systems to confirm KUB5/HERA's involvement in

mammalian NHEJ. Studies using G0 arrested cells should also be performed since these cells would not have the capacity to perform HR. If mammalian cells lacking KUB5/HERA also show a deficiency in their ability to repair blunt and non-compatible DNA ends, evidence would strongly support a unique KUB5/HERA function in NHEJ. Our data, however, do suggest that KUB5/HERA functions are fairly well conserved, since re-expression of KUB5/HERA cDNA in yeast resulted in almost complete rescue of IR sensitivity and restoration in the capacity to re-ligate complex DSB ends, These findings support KUB5/HERA's role in NHEJ, yet they are difficult to explain if one proposes KUB5/HERA is only involved in termination of transcription.

Some of the data presented in this thesis does not fit the classical model of characteristics of a NHEJ protein. One example, of a characteristic not usual for proteins involved in NHEJ, is the early embryonic lethality upon homozygous KUB5 loss. Typically, loss of classical DNA repair proteins, e.g., Ku70, Ku80, DNAPKcs, and Artemis, do not result in early embryonic lethality. Ku70 and Ku80(Ku86) deficient mice display premature ageing and low neuronal apoptosis (150, 151). DNAPKcs and Artemis deficient mice have no obvious abnormalities (152, 153). The only case where a known NHEJ protein is early embryonic lethal is for DNA Ligase IV (150). This is interesting in the respect that DNA Ligase IV is involved in an end joining event, much like KUB5 is expected to be in reference to plasmid re-ligation assays. Based on data suggesting that the half-life

of artemis was affected by KUB5/HERA knockdown and IP data showing KUB5 binding in complex with Artemis, Dr. Julio Morales proposed that KUB5/HERA may be responsible for Artemis' recruitment to the site of DNA damage in order for end processing to take place. His data showed that upon KUB5/HERA loss, Artemis disappears, or is de-localized in cells lacking KUB5 (data not shown, western blot and fluorescence microscopy); perhaps indicating that KUB5/HERA was necessary to bring this factor to DNA damage, or important in Artemis transcription (data unpublished). If the sole function for KUB5/HERA was to recruit Artemis to the site of damage in order for end processing to take place for NHEJ, it would be expected that since Artemis deficient mice survive, so too would KUB5/HERA deficient mice. To complicate matters more, our NHEJ data showing that RTT103 was necessary for resealing blunt and non-compatible DNA ends, and specifically for NHEJ, was only confirmed in yeast, a repair system notably different than that of mammalian NHEJ (Table 2.1). If RTT103 is functioning in yeast as KUB5/HERA would in mammalian cells, then one would expect a loss of RTT103 to be lethal in yeast, contrary to this hypothesis the RTT103 deficient yeast survive.

It is possible that KUB5/HERA's main function in cells could be as a transcription termination factor. Several yeast papers have been published showing the role of RTT103 in RNA transcription termination, including an in-depth domain analysis showing direct interaction with the phosphorylated C-

terminal domain of RNA polymerase II (70). In addition to published work by other labs supporting RTT103 involvement in transcription termination, this thesis shows RTT103 and KUB5/HERA loss resulted in hypersensitivity to DNA damage agents, and I report the observation that Kub5/Hera-/- knockout mice exhibit early embryonic lethality. All these responses are typical of cells defective in transcription termination. One model for how KUB5/HERA could be functioning within this pathway could involve transcription termination, as suggested for RTT103 function (70-73). Transcription of a gene by RNA polymerase results in creation of mRNAs with a 7-methyl-guanosine cap (m_7G) at one end and a polyadenosine (poly(A)) tail at the other (Figure 6.1). The carboxy-terminal domain (CTD) of RNA polymerase II, which is known to interact directly with RTT103 carrying the serine 2 phosphorylation, moves along the mRNA until it associates with the Rat1 (Xrn2 in humans) and Rai1. The poly(A) site undergoes cleavage where Rat1 binds and eats away the free end of RNA, until it reaches polymerase (eta), where transcription is then halted(70-73). If RTT103 is lost, the Rat1 cannot bind and carry out its function, creating an R-loop, DNA/RNA hybrid, which remains attached. Transcription cannot be properly terminated, and therefore, may result in DNA damage as it collides with other replication or DNA repair machinery. The general idea would be that more DSBs are being formed in the absence of KUB5/HERA than can be repaired due to R-loop-mediated genomic instability.

Some of my data shown in this thesis do not, however, seem to support such a model. One example is the inability of RTT103-/- yeast to specifically repair blunt and non-compatible ends, and the specificity of the yeast being in a growth arrested haploid state that forces them into NHEJ in order for increased IR hypersensitivity. Also, KUB5/HERA loss resulted in specific hypersensitivity to DSB-inducing agents, whereas it would be expected that a deficiency in transcription termination would result in sensitivity to all agents causing DNA damage. Finally, KUB5/HERA direct interaction with Ku70 does not fit the model, as Ku70 is not implicated in transcription termination. That is, unless KUB5/HERA complex formation has a separate function when interacting with Artemis versus RNA polymerase.

Another possible role for KUB5/HERA could more global and I hypothesize that KUB5/HERA may have the ability to act as a molecular matchmaker. Traditionally the definition of a molecular matchmaker is that which increases the affinity of two or more molecules for each other. Supporting this idea is are the data and observations that KUB5/HERA and Ku70 appear to be tightly interacting. Given Ku70 involvement in several cellular processes, KUB5 acting in unison with Ku70 as a matchmaker could aid in efficient Ku70 processes by aiding in Ku70 affinity. KUB5/HERA could act to stabilize Ku70 interactions with other proteins, such as those involved in NHEJ and/or DNA repair. Another theory, closely related to KUB5 function as a

molecular matchmaker, is that of a role of KUB5/HERA in stabilizing Ku70 when not interacting with Ku80. Co-IP data supports this theory due to Ku80 being absent from all IPs showing Ku70 and KUB5/HERA interaction. Since Ku70 is known to have a highly unstable C-terminal region, perhaps when Ku70 is free, it needs to associate with KUB5/HERA in order to be stabilized, or possibly KUB5/HERA helps Artemis bind and stabilize Ku70. These data are supported by the biochemical domain analyses showing KUB5/HERA interacting with Ku70 C-terminal domain. Finally, KUB5/HERA could also have a possible dual role in both DNA repair and transcription termination. Though there have not been any previous reports of such a bi-functional protein, combined data from RTT103 and KUB5/HERA studies support this hypothesis. The fact that gel filtration indicated separate higher molecular weight complexes containing KUB5/HERA, associated with KU70 and separate complexes that are consistent with association with RNA polymerase (and that co-IPs have indicated associated of KUB5/HERA with xrn2 and pms (two RNA termination factors), strongly suggests that KUB5/HERA may form separate complexes with separate functions.

Biochemical and functional analyses of both RTT103 and KUB5/HERA have generated more questions than answers on the specific function of this novel protein. Results obtained from cells where KUB5/HERA was knocked down, showed hypersensitivity to a wide range of DNA damage agents and suggested that KUB5/HERA could be used as a marker for DNA damage responses.

Clinically, this could be incredibly important as KUB5 expression level in tumors could be indicative of amount of DNA damage agent needed to effectively kill the tumor. For example, a tumor with very low KUB5 protein expression, could be treated with the smallest dose of radiation or DNA damage agent; whereas a tumor showing higher or normal KUB5 expression would need to be treated with much higher doses in order to obtain efficient killing of the cancer. Results summarized in figure 4.10, support the possibility of KUB5 being used clinically in this way. Though these data are preliminary, a much larger screen would need to be performed both in cancer cell lines as well as patient tumor samples, in order to push this finding into a position where it could be used to clinically improve the treatment of cancer. Another important step in making this a functional testing system for doctors and patients, would be continued testing of the KUB5 antibody. It would be necessary to determine the best conditions for immunohistochemistry (IHC) so pathologists could have an easily re-producible system of screening patient samples for KUB5 expression levels. This would require not only perfecting the conditions for KUB5 antibody use in IHC, but would also require a standardized method of grading KUB5 expression and correlating that expression level to radiation or DNA damage agent responsiveness of the tumor.

In summary, the data presented in this thesis begin to outline the importance of KUB5/HERA in not only embryonic development, but also maintenance of

genomic stability. KUB5/HERA could be functioning in several different pathways, such as embryonic development, Transcription Termination, NHEJ and genomic stability. The unifying evidence suggests that KUB5/HERA is necessary for efficient DNA DSB repair. Without this factor the cells repair DNA damage inefficiently or not at all and cannot survive, unless p53 is mutant. Interestingly, the majority of breast cancers are mutant for p53, allowing them to accumulate genomic instability and survive when KUB5 is lost. KUB5/HERA has proven more complex than originally thought, and understanding its complex function(s) in cells will prove increasingly more important with each new discovery along the way.

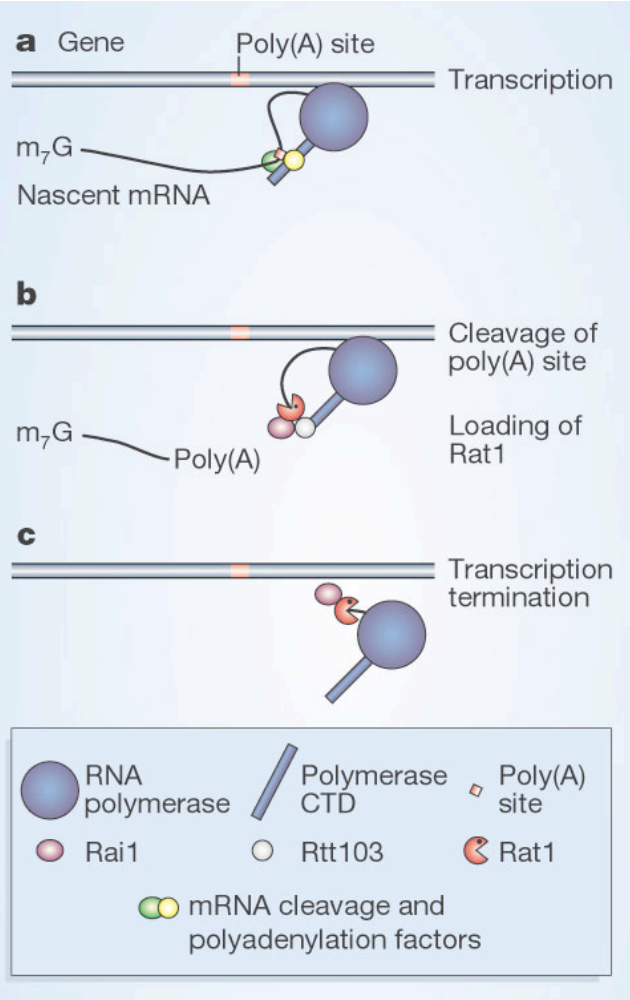

Figure 6.1: ***Published model of transcription termination in yeast*** (154). Here Transcription of a gene by RNA polymerase results in creation of mRNAs with a 7-methyl-guanosine cap (m_7G) at one end and a polyadenosine (poly(A)) tail at the other. The carboxy-terminal domain (CTD) of RNA polymerase II, which is known to interact directly with RTT103 carrying the serine 2 phosphorylation, moves along the mRNA until it associates with the Rat1 (Xrn2 in humans) and Rai1. The poly(A) site undergoes cleavage where Rat1 binds and eats away the free end of RNA, until it reaches polymerase (eta), where transcription is then halted.

REFERENCES

1. Elledge SJ. Cell cycle checkpoints: preventing an identity crisis. Science. 1996;274(5293):1664-72.

2. Keith CT, Schreiber SL. PIK-related kinases: DNA repair, recombination, and cell cycle checkpoints. Science. 1995;270(5233):50-1.

3. Manning G, Whyte DB, Martinez R, Hunter T, Sudarsanam S. The protein kinase complement of the human genome. Science. 2002;298(5600):1912-34.

4. Savitsky K, Sfez S, Tagle DA, Ziv Y, Sartiel A, Collins FS, et al. The complete sequence of the coding region of the ATM gene reveals similarity to cell cycle regulators in different species. Hum Mol Genet. 1995;4(11):2025-32.

5. Shiloh Y. ATM and related protein kinases: safeguarding genome integrity. Nat Rev Cancer. 2003;3(3):155-68.

6. Keegan KS, Holtzman DA, Plug AW, Christenson ER, Brainerd EE, Flaggs G, et al. The Atr and Atm protein kinases associate with different sites along meiotically pairing chromosomes. Genes Dev. 1996;10(19):2423-37.

7. Wright JA, Keegan KS, Herendeen DR, Bentley NJ, Carr AM, Hoekstra MF, et al. Protein kinase mutants of human ATR increase sensitivity to UV and ionizing radiation and abrogate cell cycle checkpoint control. Proc Natl Acad Sci U S A. 1998;95(13):7445-50. PMCID: 22645.

8. Cliby WA, Roberts CJ, Cimprich KA, Stringer CM, Lamb JR, Schreiber SL, et al. Overexpression of a kinase-inactive ATR protein causes sensitivity to

DNA-damaging agents and defects in cell cycle checkpoints. EMBO J. 1998;17(1):159-69. PMCID: 1170367.

9. Bakkenist CJ, Kastan MB. DNA damage activates ATM through intermolecular autophosphorylation and dimer dissociation. Nature. 2003;421(6922):499-506.

10. Tibbetts RS, Brumbaugh KM, Williams JM, Sarkaria JN, Cliby WA, Shieh SY, et al. A role for ATR in the DNA damage-induced phosphorylation of p53. Genes Dev. 1999;13(2):152-7. PMCID: 316393.

11. Khosravi R, Maya R, Gottlieb T, Oren M, Shiloh Y, Shkedy D. Rapid ATM-dependent phosphorylation of MDM2 precedes p53 accumulation in response to DNA damage. Proc Natl Acad Sci U S A. 1999;96(26):14973-7. PMCID: 24757.

12. Serrano M, Hannon GJ, Beach D. A new regulatory motif in cell-cycle control causing specific inhibition of cyclin D/CDK4. Nature. 1993;366(6456):704-7.

13. Matsuoka S, Huang M, Elledge SJ. Linkage of ATM to cell cycle regulation by the Chk2 protein kinase. Science. 1998;282(5395):1893-7.

14. You YH, Pfeifer GP. Similarities in sunlight-induced mutational spectra of CpG-methylated transgenes and the p53 gene in skin cancer point to an important role of 5-methylcytosine residues in solar UV mutagenesis. J Mol Biol. 2001;305(3):389-99.

15. Kraemer KH, Lee MM, Scotto J. Xeroderma pigmentosum. Cutaneous, ocular, and neurologic abnormalities in 830 published cases. Arch Dermatol. 1987;123(2):241-50.

16. de Vries A, van Oostrom CT, Hofhuis FM, Dortant PM, Berg RJ, de Gruijl FR, et al. Increased susceptibility to ultraviolet-B and carcinogens of mice lacking the DNA excision repair gene XPA. Nature. 1995;377(6545):169-73.

17. Sands AT, Abuin A, Sanchez A, Conti CJ, Bradley A. High susceptibility to ultraviolet-induced carcinogenesis in mice lacking XPC. Nature. 1995;377(6545):162-5.

18. Bebenek K, Matsuda T, Masutani C, Hanaoka F, Kunkel TA. Proofreading of DNA polymerase eta-dependent replication errors. J Biol Chem. 2001;276(4):2317-20.

19. Feuerhahn S, Egly JM. Tools to study DNA repair: what's in the box? Trends Genet. 2008;24(9):467-74.

20. Berg RJ, Rebel H, van der Horst GT, van Kranen HJ, Mullenders LH, van Vloten WA, et al. Impact of global genome repair versus transcription-coupled repair on ultraviolet carcinogenesis in hairless mice. Cancer Res. 2000;60(11):2858-63.

21. Bohr VA, Smith CA, Okumoto DS, Hanawalt PC. DNA repair in an active gene: removal of pyrimidine dimers from the DHFR gene of CHO cells is much more efficient than in the genome overall. Cell. 1985;40(2):359-69.

22. Ma L, Hoeijmakers JH, van der Eb AJ. Mammalian nucleotide excision repair. Biochim Biophys Acta. 1995;1242(2):137-63.

23. Lindahl T, Wood RD. Quality control by DNA repair. Science. 1999;286(5446):1897-905.

24. Masutani C, Sugasawa K, Yanagisawa J, Sonoyama T, Ui M, Enomoto T, et al. Purification and cloning of a nucleotide excision repair complex involving the xeroderma pigmentosum group C protein and a human homologue of yeast RAD23. EMBO J. 1994;13(8):1831-43. PMCID: 395023.

25. Winkler GS, Sugasawa K, Eker AP, de Laat WL, Hoeijmakers JH. Novel functional interactions between nucleotide excision DNA repair proteins influencing the enzymatic activities of TFIIH, XPG, and ERCC1-XPF. Biochemistry. 2001;40(1):160-5.

26. O'Donovan A, Davies AA, Moggs JG, West SC, Wood RD. XPG endonuclease makes the 3' incision in human DNA nucleotide excision repair. Nature. 1994;371(6496):432-5.

27. Yokoi M, Masutani C, Maekawa T, Sugasawa K, Ohkuma Y, Hanaoka F. The xeroderma pigmentosum group C protein complex XPC-HR23B plays an important role in the recruitment of transcription factor IIH to damaged DNA. J Biol Chem. 2000;275(13):9870-5.

28. Park CH, Mu D, Reardon JT, Sancar A. The general transcription-repair factor TFIIH is recruited to the excision repair complex by the XPA protein

independent of the TFIIE transcription factor. J Biol Chem. 1995;270(9):4896-902.

29. Araujo SJ, Nigg EA, Wood RD. Strong functional interactions of TFIIH with XPC and XPG in human DNA nucleotide excision repair, without a preassembled repairosome. Mol Cell Biol. 2001;21(7):2281-91. PMCID: 86862.

30. Wakasugi M, Shimizu M, Morioka H, Linn S, Nikaido O, Matsunaga T. Damaged DNA-binding protein DDB stimulates the excision of cyclobutane pyrimidine dimers in vitro in concert with XPA and replication protein A. J Biol Chem. 2001;276(18):15434-40.

31. Khan AU, Kasha M. Singlet molecular oxygen in the Haber-Weiss reaction. Proc Natl Acad Sci U S A. 1994;91(26):12365-7. PMCID: 45438.

32. Goldstein S, Meyerstein D, Czapski G. The Fenton reagents. Free Radic Biol Med. 1993;15(4):435-45.

33. Lingens F, Haerlin R, Sussmuth R. Mechanism of mutagenesis by N-methyl-N'-nitro-N-nitrosoguanidine (MNNG). Methylation of nucleic acids by N-trideuteriomethyl-N'-nitro-N-nitrosoguanidine (D3-MNNG) in the presence of cysteine and in cells of Escherichia coli. FEBS Lett. 1971;13(4):241-2.

34. Berardini M, Mazurek A, Fishel R. The effect of O6-methylguanine DNA adducts on the adenosine nucleotide switch functions of hMSH2-hMSH6 and hMSH2-hMSH3. J Biol Chem. 2000;275(36):27851-7.

35. Kunkel TA, Erie DA. DNA mismatch repair. Annu Rev Biochem. 2005;74:681-710.

36. Hsieh P. Molecular mechanisms of DNA mismatch repair. Mutat Res. 2001;486(2):71-87.

37. Seeberg E, Eide L, Bjoras M. The base excision repair pathway. Trends Biochem Sci. 1995;20(10):391-7.

38. Barnes DE, Lindahl T. Repair and genetic consequences of endogenous DNA base damage in mammalian cells. Annu Rev Genet. 2004;38:445-76.

39. Robertson AB, Klungland A, Rognes T, Leiros I. DNA repair in mammalian cells: Base excision repair: the long and short of it. Cell Mol Life Sci. 2009;66(6):981-93.

40. Williams SD, David SS. Evidence that MutY is a monofunctional glycosylase capable of forming a covalent Schiff base intermediate with substrate DNA. Nucleic Acids Res. 1998;26(22):5123-33. PMCID: 147954.

41. Bailly V, Verly WG. AP endonucleases and AP lyases. Nucleic Acids Res. 1989;17(9):3617-8. PMCID: 317828.

42. Howell WM, Grundberg I, Faryna M, Landegren U, Nilsson M. Glycosylases and AP-cleaving enzymes as a general tool for probe-directed cleavage of ssDNA targets. Nucleic Acids Res. 2010;38(7):e99. PMCID: 2853139.

43. Ward JF. Mechanisms of DNA repair and their potential modification for radiotherapy. Int J Radiat Oncol Biol Phys. 1986;12(7):1027-32.

44. San Filippo J, Sung P, Klein H. Mechanism of eukaryotic homologous recombination. Annu Rev Biochem. 2008;77:229-57.

45. Shrivastav M, De Haro LP, Nickoloff JA. Regulation of DNA double-strand break repair pathway choice. Cell Res. 2008;18(1):134-47.

46. Fu YP, Yu JC, Cheng TC, Lou MA, Hsu GC, Wu CY, et al. Breast cancer risk associated with genotypic polymorphism of the nonhomologous end-joining genes: a multigenic study on cancer susceptibility. Cancer Res. 2003;63(10):2440-6.

47. Mimori T, Hardin JA. Mechanism of interaction between Ku protein and DNA. J Biol Chem. 1986;261(22):10375-9.

48. Scully R, Chen J, Plug A, Xiao Y, Weaver D, Feunteun J, et al. Association of BRCA1 with Rad51 in mitotic and meiotic cells. Cell. 1997;88(2):265-75.

49. Baumann P, Benson FE, West SC. Human Rad51 protein promotes ATP-dependent homologous pairing and strand transfer reactions in vitro. Cell. 1996;87(4):757-66.

50. Gupta RC, Bazemore LR, Golub EI, Radding CM. Activities of human recombination protein Rad51. Proc Natl Acad Sci U S A. 1997;94(2):463-8. PMCID: 19535.

51. Paull TT, Gellert M. Nbs1 potentiates ATP-driven DNA unwinding and endonuclease cleavage by the Mre11/Rad50 complex. Genes Dev. 1999;13(10):1276-88. PMCID: 316715.

52. Dronkert ML, Beverloo HB, Johnson RD, Hoeijmakers JH, Jasin M, Kanaar R. Mouse RAD54 affects DNA double-strand break repair and sister chromatid exchange. Mol Cell Biol. 2000;20(9):3147-56. PMCID: 85609.

53. Johnson RD, Jasin M. Sister chromatid gene conversion is a prominent double-strand break repair pathway in mammalian cells. EMBO J. 2000;19(13):3398-407. PMCID: 313931.

54. Paillard S, Strauss F. Analysis of the mechanism of interaction of simian Ku protein with DNA. Nucleic Acids Res. 1991;19(20):5619-24. PMCID: 328966.

55. Hammarsten O, Chu G. DNA-dependent protein kinase: DNA binding and activation in the absence of Ku. Proc Natl Acad Sci U S A. 1998;95(2):525-30. PMCID: 18453.

56. Smith GC, Jackson SP. The DNA-dependent protein kinase. Genes Dev. 1999;13(8):916-34.

57. Anderson CW, Lees-Miller SP. The nuclear serine/threonine protein kinase DNA-PK. Crit Rev Eukaryot Gene Expr. 1992;2(4):283-314.

58. Leber R, Wise TW, Mizuta R, Meek K. The XRCC4 gene product is a target for and interacts with the DNA-dependent protein kinase. J Biol Chem. 1998;273(3):1794-801.

59. Ma Y, Pannicke U, Schwarz K, Lieber MR. Hairpin opening and overhang processing by an Artemis/DNA-dependent protein kinase complex in nonhomologous end joining and V(D)J recombination. Cell. 2002;108(6):781-94.

60. Chan DW, Chen BP, Prithivirajsingh S, Kurimasa A, Story MD, Qin J, et al. Autophosphorylation of the DNA-dependent protein kinase catalytic subunit is required for rejoining of DNA double-strand breaks. Genes Dev. 2002;16(18):2333-8. PMCID: 187438.

61. Lee KJ, Huang J, Takeda Y, Dynan WS. DNA ligase IV and XRCC4 form a stable mixed tetramer that functions synergistically with other repair factors in a cell-free end-joining system. J Biol Chem. 2000;275(44):34787-96.

62. Hsu HL, Yannone SM, Chen DJ. Defining interactions between DNA-PK and ligase IV/XRCC4. DNA Repair (Amst). 2002;1(3):225-35.

63. DeFazio LG, Stansel RM, Griffith JD, Chu G. Synapsis of DNA ends by DNA-dependent protein kinase. EMBO J. 2002;21(12):3192-200. PMCID: 126055.

64. Chan DW, Lees-Miller SP. The DNA-dependent protein kinase is inactivated by autophosphorylation of the catalytic subunit. J Biol Chem. 1996;271(15):8936-41.

65. Yang CR, Yeh S, Leskov K, Odegaard E, Hsu HL, Chang C, et al. Isolation of Ku70-binding proteins (KUBs). Nucleic Acids Res. 1999;27(10):2165-74. PMCID: 148436.

66. Yang CR, Leskov K, Hosley-Eberlein K, Criswell T, Pink JJ, Kinsella TJ, et al. Nuclear clusterin/XIP8, an x-ray-induced Ku70-binding protein that signals cell death. Proc Natl Acad Sci U S A. 2000;97(11):5907-12. PMCID: 18532.

67. Leskov KS, Klokov DY, Li J, Kinsella TJ, Boothman DA. Synthesis and functional analyses of nuclear clusterin, a cell death protein. J Biol Chem. 2003;278(13):11590-600.

68. Fischer U, Hemmer D, Heckel D, Michel A, Feiden W, Steudel WI, et al. KUB3 amplification and overexpression in human gliomas. Glia. 2001;36(1):1-10.

69. Kelly DE, Lamb DC, Kelly SL. Genome-wide generation of yeast gene deletion strains. Comp Funct Genomics. 2001;2(4):236-42. PMCID: 2447215.

70. Lunde BM, Reichow SL, Kim M, Suh H, Leeper TC, Yang F, et al. Cooperative interaction of transcription termination factors with the RNA polymerase II C-terminal domain. Nat Struct Mol Biol. 2010;17(10):1195-201. PMCID: 2950884.

71. Dengl S, Cramer P. Torpedo nuclease Rat1 is insufficient to terminate RNA polymerase II in vitro. J Biol Chem. 2009;284(32):21270-9. PMCID: 2755851.

72. Vasiljeva L, Kim M, Mutschler H, Buratowski S, Meinhart A. The Nrd1-Nab3-Sen1 termination complex interacts with the Ser5-phosphorylated RNA polymerase II C-terminal domain. Nat Struct Mol Biol. 2008;15(8):795-804. PMCID: 2597375.

73. Kim M, Krogan NJ, Vasiljeva L, Rando OJ, Nedea E, Greenblatt JF, et al. The yeast Rat1 exonuclease promotes transcription termination by RNA polymerase II. Nature. 2004;432(7016):517-22.

74. Wilkinson LE, Pringle JR. Transient G1 arrest of S. cerevisiae cells of mating type alpha by a factor produced by cells of mating type a. Exp Cell Res. 1974;89(1):175-87.

75. Day A, Schneider C, Schneider BL. Yeast cell synchronization. Methods Mol Biol. 2004;241:55-76.

76. Breeden LL. Alpha-factor synchronization of budding yeast. Methods Enzymol. 1997;283:332-41.

77. Pieper AA, Verma A, Zhang J, Snyder SH. Poly (ADP-ribose) polymerase, nitric oxide and cell death. Trends Pharmacol Sci. 1999;20(4):171-81.

78. Helleday T, Bryant HE, Schultz N. Poly(ADP-ribose) polymerase (PARP-1) in homologous recombination and as a target for cancer therapy. Cell Cycle. 2005;4(9):1176-8.

79. Gottipati P, Vischioni B, Schultz N, Solomons J, Bryant HE, Djureinovic T, et al. Poly(ADP-ribose) polymerase is hyperactivated in homologous recombination-defective cells. Cancer Res. 2010;70(13):5389-98.

80. Siede W, Friedl AA, Dianova I, Eckardt-Schupp F, Friedberg EC. The Saccharomyces cerevisiae Ku autoantigen homologue affects radiosensitivity only in the absence of homologous recombination. Genetics. 1996;142(1):91-102. PMCID: 1206967.

81. Tsukamoto Y, Kato J, Ikeda H. Silencing factors participate in DNA repair and recombination in Saccharomyces cerevisiae. Nature. 1997;388(6645):900-3.

82. Laroche T, Martin SG, Gotta M, Gorham HC, Pryde FE, Louis EJ, et al. Mutation of yeast Ku genes disrupts the subnuclear organization of telomeres. Curr Biol. 1998;8(11):653-6.

83. Fernandez-Capetillo O, Celeste A, Nussenzweig A. Focusing on foci: H2AX and the recruitment of DNA-damage response factors. Cell Cycle. 2003;2(5):426-7.

84. Anderson L, Henderson C, Adachi Y. Phosphorylation and rapid relocalization of 53BP1 to nuclear foci upon DNA damage. Mol Cell Biol. 2001;21(5):1719-29. PMCID: 86718.

85. Zou Y, Lim S, Lee K, Deng X, Friedman E. Serine/threonine kinase Mirk/Dyrk1B is an inhibitor of epithelial cell migration and is negatively

regulated by the Met adaptor Ran-binding protein M. J Biol Chem. 2003;278(49):49573-81.

86. Ho SN, Hunt HD, Horton RM, Pullen JK, Pease LR. Site-directed mutagenesis by overlap extension using the polymerase chain reaction. Gene. 1989;77(1):51-9.

87. Horton RM, Hunt HD, Ho SN, Pullen JK, Pease LR. Engineering hybrid genes without the use of restriction enzymes: gene splicing by overlap extension. Gene. 1989;77(1):61-8.

88. Li CJ, Li YZ, Pinto AV, Pardee AB. Potent inhibition of tumor survival in vivo by beta-lapachone plus taxol: combining drugs imposes different artificial checkpoints. Proc Natl Acad Sci U S A. 1999;96(23):13369-74. PMCID: 23954.

89. Koike M, Koike A. Accumulation of Ku80 proteins at DNA double-strand breaks in living cells. Exp Cell Res. 2008;314(5):1061-70.

90. Mari PO, Florea BI, Persengiev SP, Verkaik NS, Bruggenwirth HT, Modesti M, et al. Dynamic assembly of end-joining complexes requires interaction between Ku70/80 and XRCC4. Proc Natl Acad Sci U S A. 2006;103(49):18597-602. PMCID: 1693708.

91. Vazquez A, Bond EE, Levine AJ, Bond GL. The genetics of the p53 pathway, apoptosis and cancer therapy. Nat Rev Drug Discov. 2008;7(12):979-87.

92. Levine AJ. p53, the cellular gatekeeper for growth and division. Cell. 1997;88(3):323-31.

93. Riley T, Sontag E, Chen P, Levine A. Transcriptional control of human p53-regulated genes. Nat Rev Mol Cell Biol. 2008;9(5):402-12.

94. Iwakuma T, Lozano G. Crippling p53 activities via knock-in mutations in mouse models. Oncogene. 2007;26(15):2177-84.

95. Lozano G, Zambetti GP. What have animal models taught us about the p53 pathway? J Pathol. 2005;205(2):206-20.

96. Yonish-Rouach E, Resnitzky D, Lotem J, Sachs L, Kimchi A, Oren M. Wild-type p53 induces apoptosis of myeloid leukaemic cells that is inhibited by interleukin-6. Nature. 1991;352(6333):345-7.

97. Hakem R, de la Pompa JL, Elia A, Potter J, Mak TW. Partial rescue of Brca1 (5-6) early embryonic lethality by p53 or p21 null mutation. Nat Genet. 1997;16(3):298-302.

98. Vogelstein B, Lane D, Levine AJ. Surfing the p53 network. Nature. 2000;408(6810):307-10.

99. Bode AM, Dong Z. Post-translational modification of p53 in tumorigenesis. Nat Rev Cancer. 2004;4(10):793-805.

100. El-Deiry WS. The role of p53 in chemosensitivity and radiosensitivity. Oncogene. 2003;22(47):7486-95.

101. Sax JK, El-Deiry WS. p53 downstream targets and chemosensitivity. Cell Death Differ. 2003;10(4):413-7.

102. el-Deiry WS, Tokino T, Velculescu VE, Levy DB, Parsons R, Trent JM, et al. WAF1, a potential mediator of p53 tumor suppression. Cell. 1993;75(4):817-25.

103. vom Brocke J, Schmeiser HH, Reinbold M, Hollstein M. MEF immortalization to investigate the ins and outs of mutagenesis. Carcinogenesis. 2006;27(11):2141-7.

104. Hahn WC, Weinberg RA. Modelling the molecular circuitry of cancer. Nat Rev Cancer. 2002;2(5):331-41.

105. Zindy F, Eischen CM, Randle DH, Kamijo T, Cleveland JL, Sherr CJ, et al. Myc signaling via the ARF tumor suppressor regulates p53-dependent apoptosis and immortalization. Genes Dev. 1998;12(15):2424-33. PMCID: 317045.

106. Morrison C, Sonoda E, Takao N, Shinohara A, Yamamoto K, Takeda S. The controlling role of ATM in homologous recombinational repair of DNA damage. EMBO J. 2000;19(3):463-71. PMCID: 305583.

107. Wang H, Perrault AR, Takeda Y, Qin W, Iliakis G. Biochemical evidence for Ku-independent backup pathways of NHEJ. Nucleic Acids Res. 2003;31(18):5377-88. PMCID: 203313.

108. Lavin MF. The Mre11 complex and ATM: a two-way functional interaction in recognising and signaling DNA double strand breaks. DNA Repair (Amst). 2004;3(11):1515-20.

109. Jeggo PA. Identification of genes involved in repair of DNA double-strand breaks in mammalian cells. Radiat Res. 1998;150(5 Suppl):S80-91.

110. Tanner MM, Tirkkonen M, Kallioniemi A, Collins C, Stokke T, Karhu R, et al. Increased copy number at 20q13 in breast cancer: defining the critical region and exclusion of candidate genes. Cancer Res. 1994;54(16):4257-60.

111. Tanner MM, Tirkkonen M, Kallioniemi A, Holli K, Collins C, Kowbel D, et al. Amplification of chromosomal region 20q13 in invasive breast cancer: prognostic implications. Clin Cancer Res. 1995;1(12):1455-61.

112. Fojo T, Coley HM. The role of efflux pumps in drug-resistant metastatic breast cancer: new insights and treatment strategies. Clin Breast Cancer. 2007;7(10):749-56.

113. Zhou BB, Elledge SJ. The DNA damage response: putting checkpoints in perspective. Nature. 2000;408(6811):433-9.

114. Zheng L, Li S, Boyer TG, Lee WH. Lessons learned from BRCA1 and BRCA2. Oncogene. 2000;19(53):6159-75.

115. Welcsh PL, Owens KN, King MC. Insights into the functions of BRCA1 and BRCA2. Trends Genet. 2000;16(2):69-74.

116. Chen Y, Lee WH, Chew HK. Emerging roles of BRCA1 in transcriptional regulation and DNA repair. J Cell Physiol. 1999;181(3):385-92.

117. Baldeyron C, Jacquemin E, Smith J, Jacquemont C, De Oliveira I, Gad S, et al. A single mutated BRCA1 allele leads to impaired fidelity of double strand break end-joining. Oncogene. 2002;21(9):1401-10.

118. Merel P, Prieur A, Pfeiffer P, Delattre O. Absence of major defects in non-homologous DNA end joining in human breast cancer cell lines. Oncogene. 2002;21(36):5654-9.

119. Moynahan ME, Chiu JW, Koller BH, Jasin M. Brca1 controls homology-directed DNA repair. Mol Cell. 1999;4(4):511-8.

120. Snouwaert JN, Gowen LC, Latour AM, Mohn AR, Xiao A, DiBiase L, et al. BRCA1 deficient embryonic stem cells display a decreased homologous recombination frequency and an increased frequency of non-homologous recombination that is corrected by expression of a brca1 transgene. Oncogene. 1999;18(55):7900-7.

121. Wang H, Zeng ZC, Bui TA, DiBiase SJ, Qin W, Xia F, et al. Nonhomologous end-joining of ionizing radiation-induced DNA double-stranded breaks in human tumor cells deficient in BRCA1 or BRCA2. Cancer Res. 2001;61(1):270-7.

122. Zhang J, Willers H, Feng Z, Ghosh JC, Kim S, Weaver DT, et al. Chk2 phosphorylation of BRCA1 regulates DNA double-strand break repair. Mol Cell Biol. 2004;24(2):708-18. PMCID: 343805.

123. Zhong Q, Boyer TG, Chen PL, Lee WH. Deficient nonhomologous end-joining activity in cell-free extracts from Brca1-null fibroblasts. Cancer Res. 2002;62(14):3966-70.

124. Zhong Q, Chen CF, Chen PL, Lee WH. BRCA1 facilitates microhomology-mediated end joining of DNA double strand breaks. J Biol Chem. 2002;277(32):28641-7.

125. Davis TW, Wilson-Van Patten C, Meyers M, Kunugi KA, Cuthill S, Reznikoff C, et al. Defective expression of the DNA mismatch repair protein, MLH1, alters G2-M cell cycle checkpoint arrest following ionizing radiation. Cancer Res. 1998;58(4):767-78.

126. Konstantinidou G, Bey EA, Rabellino A, Schuster K, Maira MS, Gazdar AF, et al. Dual phosphoinositide 3-kinase/mammalian target of rapamycin blockade is an effective radiosensitizing strategy for the treatment of non-small cell lung cancer harboring K-RAS mutations. Cancer Res. 2009;69(19):7644-52. PMCID: 2760010.

127. Jenkins DE, Oei Y, Hornig YS, Yu SF, Dusich J, Purchio T, et al. Bioluminescent imaging (BLI) to improve and refine traditional murine models of tumor growth and metastasis. Clin Exp Metastasis. 2003;20(8):733-44.

128. Kang J, Ferguson D, Song H, Bassing C, Eckersdorff M, Alt FW, et al. Functional interaction of H2AX, NBS1, and p53 in ATM-dependent DNA

damage responses and tumor suppression. Mol Cell Biol. 2005;25(2):661-70. PMCID: 543410.

129. Horvathova E, Dusinska M, Shaposhnikov S, Collins AR. DNA damage and repair measured in different genomic regions using the comet assay with fluorescent in situ hybridization. Mutagenesis. 2004;19(4):269-76.

130. Collins AR. The comet assay for DNA damage and repair: principles, applications, and limitations. Mol Biotechnol. 2004;26(3):249-61.

131. Ostling O, Johanson KJ. Microelectrophoretic study of radiation-induced DNA damages in individual mammalian cells. Biochem Biophys Res Commun. 1984;123(1):291-8.

132. Nakada S, Katsuki Y, Imoto I, Yokoyama T, Nagasawa M, Inazawa J, et al. Early G2/M checkpoint failure as a molecular mechanism underlying etoposide-induced chromosomal aberrations. J Clin Invest. 2006;116(1):80-9. PMCID: 1312016.

133. Sung PA, Libura J, Richardson C. Etoposide and illegitimate DNA double-strand break repair in the generation of MLL translocations: new insights and new questions. DNA Repair (Amst). 2006;5(9-10):1109-18.

134. Imlay JA, Chin SM, Linn S. Toxic DNA damage by hydrogen peroxide through the Fenton reaction in vivo and in vitro. Science. 1988;240(4852):640-2.

135. Imlay JA, Linn S. DNA damage and oxygen radical toxicity. Science. 1988;240(4857):1302-9.

136. Acharya S, Foster PL, Brooks P, Fishel R. The coordinated functions of the E. coli MutS and MutL proteins in mismatch repair. Mol Cell. 2003;12(1):233-46.

137. Friedberg EC. Relationships between DNA repair and transcription. Annu Rev Biochem. 1996;65:15-42.

138. Whitmore SE, Potten CS, Chadwick CA, Strickland PT, Morison WL. Effect of photoreactivating light on UV radiation-induced alterations in human skin. Photodermatol Photoimmunol Photomed. 2001;17(5):213-7.

139. Manfredi JJ, Parness J, Horwitz SB. Taxol binds to cellular microtubules. J Cell Biol. 1982;94(3):688-96. PMCID: 2112233.

140. Horwitz SB, Parness J, Schiff PB, Manfredi JJ. Taxol: a new probe for studying the structure and function of microtubules. Cold Spring Harb Symp Quant Biol. 1982;46 Pt 1:219-26.

141. Branham MT, Nadin SB, Vargas-Roig LM, Ciocca DR. DNA damage induced by paclitaxel and DNA repair capability of peripheral blood lymphocytes as evaluated by the alkaline comet assay. Mutat Res. 2004;560(1):11-7.

142. Ollikainen T, Knuuttila A, Suhonen S, Taavitsainen M, Jekunen A, Mattson K, et al. In vitro sensitivity of normal human mesothelial and malignant mesothelioma cell lines to four new chemotherapeutic agents. Anticancer Drugs. 2000;11(2):93-9.

143. Digue L, Orsiere T, De Meo M, Mattei MG, Depetris D, Duffaud F, et al. Evaluation of the genotoxic activity of paclitaxel by the in vitro micronucleus test in combination with fluorescent in situ hybridization of a DNA centromeric probe and the alkaline single cell gel electrophoresis technique (comet assay) in human T-lymphocytes. Environ Mol Mutagen. 1999;34(4):269-78.

144. Fornari FA, Randolph JK, Yalowich JC, Ritke MK, Gewirtz DA. Interference by doxorubicin with DNA unwinding in MCF-7 breast tumor cells. Mol Pharmacol. 1994;45(4):649-56.

145. Momparler RL, Karon M, Siegel SE, Avila F. Effect of adriamycin on DNA, RNA, and protein synthesis in cell-free systems and intact cells. Cancer Res. 1976;36(8):2891-5.

146. Cutts SM, Nudelman A, Rephaeli A, Phillips DR. The power and potential of doxorubicin-DNA adducts. IUBMB Life. 2005;57(2):73-81.

147. Liu X, Lin J, Bao Y, Lin X, An L. Camptothecin-mediated apoptosis and antiproliferation effect is accompanied by down-regulation of telomerase activity in HaCaT cells. J Dermatol Sci. 2006;42(3):262-4.

148. Jia P, Wu S, Li F, Xu Q, Wu M, Chen G, et al. Breast cancer resistance protein-mediated topotecan resistance in ovarian cancer cells. Int J Gynecol Cancer. 2005;15(6):1042-8.

149. Rice RH, Steinmann KE, deGraffenried LA, Qin Q, Taylor N, Schlegel R. Elevation of cell cycle control proteins during spontaneous immortalization of human keratinocytes. Mol Biol Cell. 1993;4(2):185-94. PMCID: 300914.

150. Gao Y, Sun Y, Frank KM, Dikkes P, Fujiwara Y, Seidl KJ, et al. A critical role for DNA end-joining proteins in both lymphogenesis and neurogenesis. Cell. 1998;95(7):891-902.

151. Barnes DE, Stamp G, Rosewell I, Denzel A, Lindahl T. Targeted disruption of the gene encoding DNA ligase IV leads to lethality in embryonic mice. Curr Biol. 1998;8(25):1395-8.

152. Gu Y, Sekiguchi J, Gao Y, Dikkes P, Frank K, Ferguson D, et al. Defective embryonic neurogenesis in Ku-deficient but not DNA-dependent protein kinase catalytic subunit-deficient mice. Proc Natl Acad Sci U S A. 2000;97(6):2668-73. PMCID: 15987.

153. Moshous D, Callebaut I, de Chasseval R, Corneo B, Cavazzana-Calvo M, Le Deist F, et al. Artemis, a novel DNA double-strand break repair/V(D)J recombination protein, is mutated in human severe combined immune deficiency. Cell. 2001;105(2):177-86.

154. Tollervey D. Molecular biology: termination by torpedo. Nature. 2004;432(7016):456-7.